University of Nebraska - Lincoln

DigitalCommons@University of Nebraska - Lincoln

Construction Systems -- Dissertations & Theses   Construction Systems

12-5-2008

Development of High Performance Precast/Prestressed Bridge Girders

Amin K. Akhnoukh
University of Nebraska, aakhnoukh@mail.unomaha.edu

Follow this and additional works at: https://digitalcommons.unl.edu/constructiondiss

Part of the Construction Engineering and Management Commons

DEVELOPMENT OF HIGH PERFORMANCE

PRECAST/PRESTRESSED BRIDGE GIRDERS

By

Amin K Akhnoukh

A Dissertation

Presented to the Faculty of

The Graduate College at the University of Nebraska

In Partial Fulfillment of Requirements

For the Degree of Doctor of Philosophy

Major: Construction Engineering

Under the Supervision of Professors:

George Morcous

Maher Tadros

Lincoln, Nebraska

December, 2008

TABLE OF CONTENTS

LIST OF TABLES

LIST OF FIGURES

ACKNOWLEDGEMENTS

DEDICATION

To The Glory of the LORD

Jesus Christ

To the One Flowing in My Blood

Egypt

DEVELOPMENT OF HIGH Performance

PRECAST/PRESTRESSED BRIDGE GIRDERS

Amin K. Akhnoukh

University of Nebraska-Lincoln, 2008

Advisors: George Morcous, Maher Tadros

Demand continues to increase for bridges with long spans and shallow depths. Due to safety concerns, four-span overpasses are being replaced with two span overpasses to avoid placement of piers near the highway shoulders. In the meantime, the bridge profile is restricted due to existing businesses nearby. Thus, nearly the same superstructure depth must be used for double the span length. This dissertation focuses on topics aiming at providing precast prestressed concrete girders with the shallowest possible depth for a given span. It forms parts of larger projects conducted by the University of Nebraska for the Nebraska Department of Roads and for the Wire Reinforcement Institute. Specifically, the following issues were researched:

(1) Use of 0.7 in. diameter Grade 270 ksi strands for pretensioning of precast concrete girders at a strand spacing of 2 inches by 2 inches. This arrangement gives nearly 190 percent of the prestressing with 0.5 in. diameter strands and nearly 135 percent with 0.6 in. strands. The research focuses on the required confinement steel to allow determination of transfer and development lengths according to current procedures in the AASHTO LRFD Bridge Design Specifications for smaller strands.

(2) Develop a self consolidating concrete (SCC) mix, using Nebraska aggregates that will allow for a specified design strength at service of 15 ksi and a minimum strength at one day of 10 ksi, representing the demand at the time of release of the prestress to the concrete member.   Prior to this study, standard concrete strength prevailing in Nebraska has been 8 ksi at service and 6.5 ksi at release. It was the goal of the research to keep the cost of materials as low as possible but not exceeding $250 per cubic yard, compared to the proprietary mixes that cost approximately four times this amount.

(3) Use of 80 ksi welded wire reinforcement (WWR) as the auxiliary reinforcement for shear, web end splitting and flange confinement. This would result in higher quality product, less reinforcement congestion, about 25 percent savings in the steel materials, and considerable savings in girder fabrication costs.

A combination of theoretical and experimental work has resulted in the following findings:

(1) A shear friction model can be used to estimate the required amount of confinement of the bottom flange.

(2) A reasonable reinforcement detail is needed, even with very heavily prestressed NU I girder bottom flange, to allow use of the current methods of estimating strands transfer and development lengths.

(3) Two SCC mixes with materials costs less that $200 dollars per cubic yard and with the required strengths were able to be developed. The mixes exhibited excellent flowability and predictable engineering properties.

(4) Grade 80 WWR was successfully used.   Its shear resistance was theoretically predictable. It produced higher capacity than the Ultra High Performance steel fiber concrete demonstrated by the Federal Highway Administration, with much lower costs and conventionally predicable design strength.

Chapter 1

Introduction

1.1 Introduction

High strength materials are improves the design of new girder bridges, with large span-to-depth ratios (greater than 30) and results in labor and material savings. In addition, they reduces the number of intermediate supports and increase the vertical clearance underneath the bridge. Examples of these materials are 0.7 in. prestressing strands, high strength concrete (HSC), and Grade 80 welded wire reinforcement (WWR). The main impediments of wide spread use of these materials for girder bridges include the following:

1. Unknown transfer and development length of 0.7 in. strands.

2. High material cost of fiber-reinforced proprietary UHPC mixes.

3. The absence of production and quality control procedures of fiber-reinforced concrete, and excessive mixing time.

The main objectives of this research are:

1. Investigate the effect of confinement on the transfer and development length of prestressing strands.

2. Develop economical self-consolidating high strength concrete with minimum 24-hour strength of 10 ksi and minimum 28-day strength of 15 ksi.

3. Investigate the performance and economical feasibility of using Grade 80 WWR compared to the random steel fibers in girders shear reinforcement.

1.2 Research Outlines

According to the specified objectives, the research is divided into three correlated topics large diameter strands, high strength concrete mix development, the use of grade 80 WWR instead of random steel fibers in I-girders shear reinforcement.

1.2.1 Large Diameter (0.7 in) Strands

Large diameter strands are used in cable-stayed bridges and mining applications in the United States and post-tensioning tendons in Europe and Japan. Seven-wire prestressing strands of 0.7 in. diameter were introduced for the first time in pretension application in North America on the Pacific Street and I-680 bridge in Omaha, Nebraska, as shown in Figure 1.1.

Figure 1.1: Pacific Street and I-680 Bridge, Omaha, Nebraska

In this research, the effect of confinement on transfer and development length is investigated. The transfer length is important in girder design. An over-estimated transfer length results in a conservative shear design, but may lead to crack development at the girder's top fibers upon strands release. An under-estimated transfer length results in excessive shear design, despite of having fewer top cracks upon strand release. Similarly, the correct estimation of the development length is important for bridge girders. An under-estimated development length results in a lower girder capacity resulting in a premature structural failure.

The cross-section area of this type of strands is 0.294 in^2. Thirty five percent more prestressing force is achieved when 0.7 in. strands are used to replace 0.6 in. strands, and 92% more when used to replace 0.5 in. strands. Additional advantages are associated with the incorporation of large strands in precast/prestressed concrete girders. First, the use of fewer strands for a certain application results in significant labor savings. Second, fewer number of chucks are used to perform the pretension process. These advantages increase the turnaround of the prestressing beds.

The significant advantages of 0.7 in. strands are exploited when HSC is used in girder fabrication. Figure 1.2 shows the increase in the positive moment capacity of NU1100 girder with 7.5 in. deck with the increase in girder strength. (deck strength is kept constant at 4.0 ksi) when 0.5 in., 0.6 in., and 0.7 in. strands are used. This is because the ultimate tensile force in the strands must be balanced by the compressive force in the girder/deck at the top of the member. When the compression block depth exceeds the

deck thickness, as it is the case with 0.7 in. strands, the girder strength becomes an effective factor in determining the girder flexure capacity.
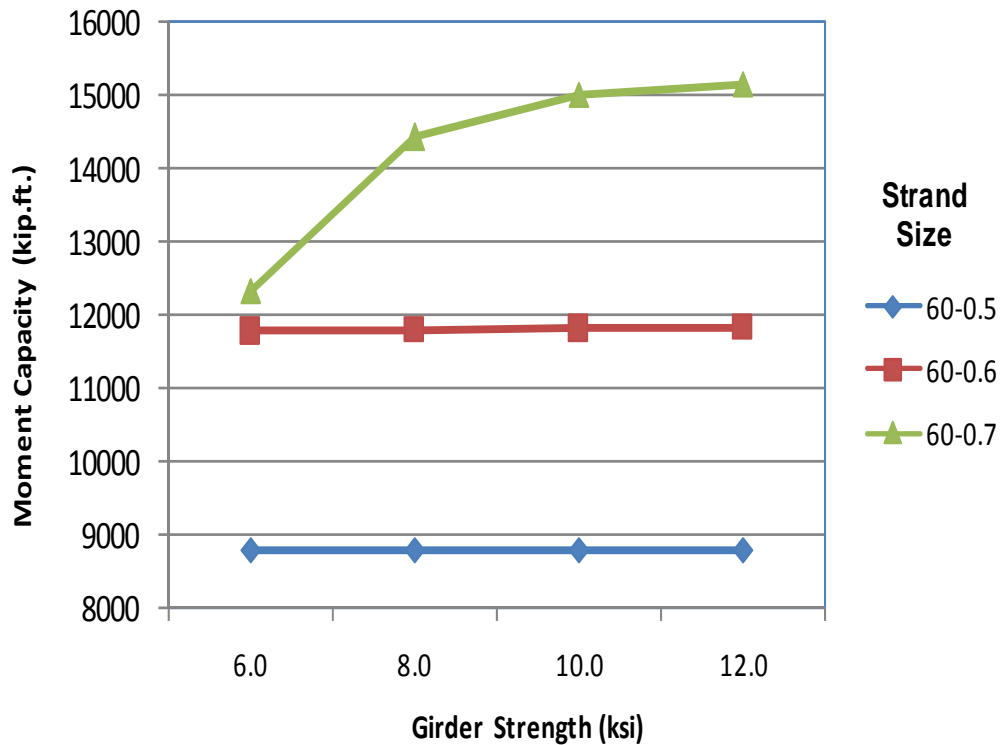
Figure 1.2: Moment capacity versus girder strength at variable strand size and 4 ksi deck
`

1.2.2 High Strength Concrete

High strength concrete is advantageous in precast/prestressed concrete industry when larger 0.7 in. strands are used (refer to Figure 1.2). The following criteria are specified for high strength concrete definition, according to a Strategic Highway Research Program (SHRP) study by Zia et al. (1991):

1. A maximum water-to-powder ratio of 0.35.

2. Strength criteria of:

   A. 3000 psi at age of 4 hours.

B.   5000 psi at age of 24 hours.

C.   10,000 psi at age of 28 days.

The main properties for HSC mix developed in this research are specified according to precasters requirements, as follows:

1. Minimum 24-hour strength of 10 ksi for early strand release, which increases precaster's efficiency.

2. Maximum 28-day strength of 15 ksi to be used with current AASHTO LRFD equations and design charts.

3. Mixing time should not exceed 20 minutes according to current practice to avoid the formation of cold joints.

1.2.3 The performance of Grade 80 WWR Compared to Random Steel Fibers in Girders Shear Performance

The performance and economical feasibility of Grade 80 WWR used in shear reinforcement of I-girders precast with HSC mix is compared to the random steel fibers. In general, WWR is characterized by ease of construction, labor and time saving in precast yards. In addition, the elimination of random steel fibers reduces concrete mixing time and saves $400 per cubic yard of the mix final material cost. In this research, the structural performance and economical feasibility of the tested girders are compared with similar type of I-girders fabricated using Ductal and tested in the Federal Highway Administration Turner Fairbank Highway Research Center in McLean, Virginia.

1.3 Research Significance

The use of 0.7 in. strands and HSC in fabricating bridge girders results in high span-to-depth ratio. Shallower girders results in higher vertical clearances and larger spans help reducing the number of intermediate bridge supports (piers). Smaller sections and/or lesser number of girders used in bridge construction due to using high strength materials results in significant labor and material savings, expedites the construction process, and requires construction equipments of lower capacities. For research purpose, a 46.67 ft. wide two-span bridge constructed with 15 ksi HSC and 0.7 in. strands I-girders was compared to a similar bridge designed using 8 ksi concrete and 0.6 in. strands. The designed bridge(s) included the following parameters:

- Two-span girder-bridge, girders are continuous for live load.
- NU900 I-girders are used, fabricated with HSC of 15 ksi final strength, and containing 60-0.7 in. strands at bottom flange.
- 4 girders are at 12 ft. spacing were used for HSC and 0.7 in. strands girders.
- 7.5 in. deck and a 1 in. thick haunch were cast in place using 5 ksi concrete.

The afore-mentioned bridge specifications were successfully used to design a 105 ft. span bridge. For comparison sake, similar bridge was designed using 8 ksi concrete and 0.6 in. strands. The design required the use of 6 girders spaced at 8 ft. spacing. Detailed designs of both girder types are shown in Appendix A. Material quantities and production prices of the two girder types are shown in Table 1.1. The pricing of bridges included $850 per cubic yard for 8 ksi concrete girders, $950 per cubic yard for HSC girders, $450 per cubic yard for cast-in-place haunch and slab, $0.85 per pound for prestressing strands, and $0.75 per pound for reinforcing steel.

Table 1.1: HSC girder cost analysis vs. regular concrete girders

	Girder Concrete (yd³)	Slab Concrete (yd³)	Huanch Concrete (yd³)	Strands weight (lbs)	Slab steel (lbs)
0.7 in. + HSC Girders	142	245	10.6	51,000	68,000
Cost (USD)	135,000	110,000	5,000	43,350	51,000
Total Cost (USD)	344,350				
0.6 in. + 8 ksi Girders	213	245	15.9	56,000	68,000
Cost (USD)	181,000	110,000	7,000	47,600	51,000
Total Cost (USD)	396,600				

8 ksi and 0.6 in. strands bridge section

HSC and 0.7 in. strands bridge section
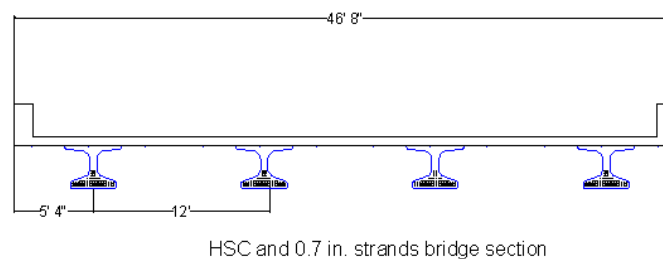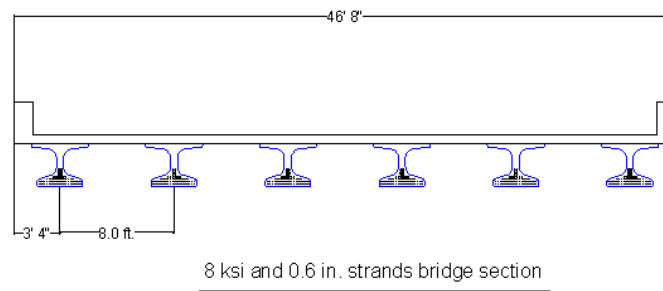
Figure 1.3: Alternative Bridge Designs

By comparing the production cost of both design alternatives for the bridge superstructure, a direct saving of 14% is achieved when bridge girders are fabricated using HSC and 0.7 in. prestressing strands compared to the current practice, where 8 ksi and 0.6 in. prestressing strands are used.

1.4 Outlines of the Report

This report is divided into 6 chapters. Chapter 1 provides an introduction, research significance, objectives, and report outlines. Chapter 2 presents a literature review for transfer and development length, in addition, to the factors affecting strands transfer and development length, and review of current pullout tests used in investigating strand-concrete bond quality. Chapter 3 presents the derivation of the equation to calculate the required confinement to contain the 0.7 in. strands used in girders construction, and experimental investigation using pullout tests. Chapter 4 includes the previous research done on Ultra-high performance concrete and high strength concrete, the development of economical self-consolidating HSC mixes, and testing their material properties. Chapter 5 includes the use of WWR in shear reinforcement of I-girders fabricated with developed HSC mix. Conclusions and suggestions for future research are included in Chapter 6.

Chapter 2

Literature Review

2.1 Transfer Length

Transfer length, denoted as L_t, is the length of the strand measured from the end of the prestressed member over which the effective prestress is transferred to the concrete. The transferred force along the transfer length varies linearly from a value of zero at the member's end to the value of the effective prestress at the point of transfer.

Prestressing force is transmitted to the concrete through different mechanisms. These are: 1) Adhesion, 2) Wedging (Hoyer) effect, and 3) Mechanical interlock. The adhesion between the concrete and prestressing strands is assumed to be effective till slippage is initiated. The magnitude of the bond resulting from the adhesion is hard to be quantified as it is highly sensitive to the strand surface condition. The effect of the adhesion on the bond between strands and concrete is shown in Figure 2.1.
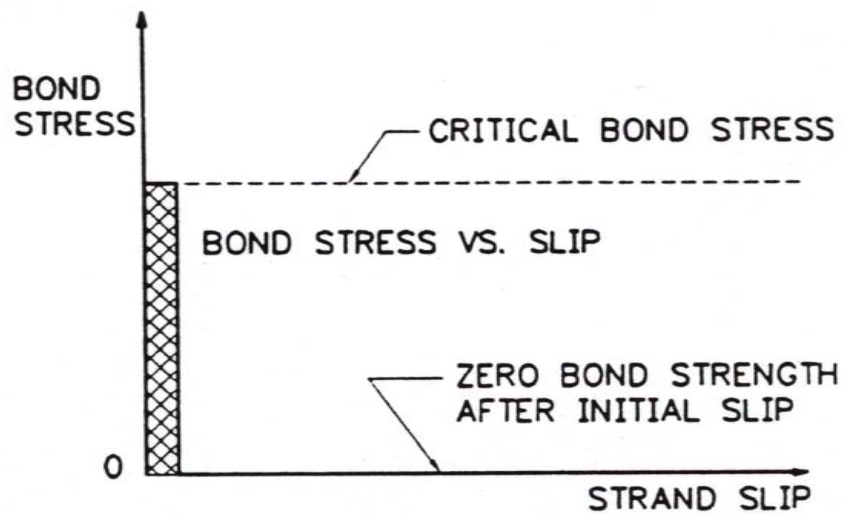
Figure 2.1: Adhesion between prestressing strands and concrete (Russell and Burns, 1996)

The other mean of providing a bond between concrete and prestressed strands is the wedging effect, commonly known as "Hoyer" effect, after the engineer who explained the effect. Due to the prestressing (tensile) force applied to the strands in pretensioning applications, the cross section area of the strand is decreased (Poisson's ratio). When concrete hardens, and desired initial compressive strength is achieved, prestressing strands are released. The strand tries to restore its original section prior to pretensioning. At the end of the transfer length, the strand maintains its reduced section (achieved during strand pretensioning). The prestressing strand area is linearly shifted from the original strand size at the end of the member to its smallest size at a distance from the member's end equal to the transfer length. This linear transformation creates a wedge-like shape (at the girder two ends). This wedging (Hoyer) effect is shown in Figure 2.2.
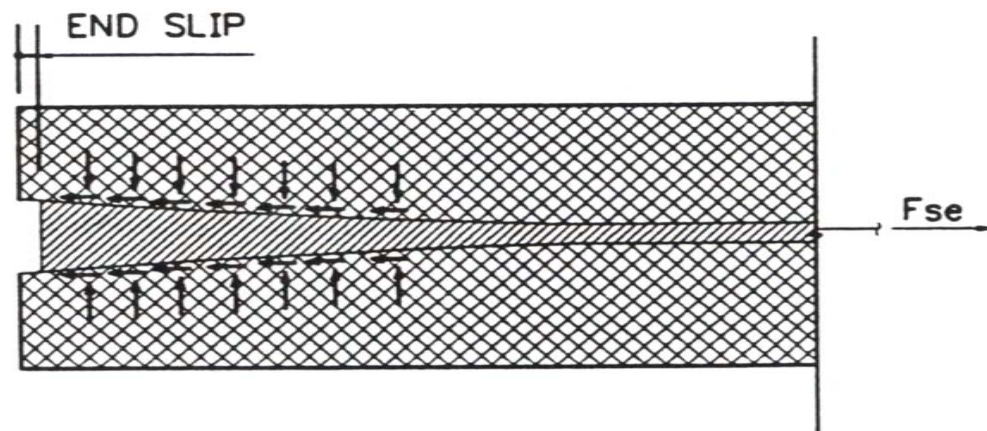
Figure 2.2: The wedging (Hoyer) effect (Russell and Burns, 1996)

The third factor in the strand-concrete bonding mechanism is the interlock between the strands wires and the concrete. Currently, the most common type of strands in the precast/prestressed concrete industry is the low-relaxation seven-wire strand, with a

helical shape. When concrete is poured, it starts to form around the strand, providing a bond that is commonly known as the mechanical interlocking mechanism. This mechanism is highly dependent on different factors and design parameters including the level of confinement at the girder end zone, concrete strength, strand surface condition, number and spacing of prestressing strands. The concrete stress distribution around the prestressing strands due to the mechanical interlock is not uniform. Figure 2.3 shows how the mechan
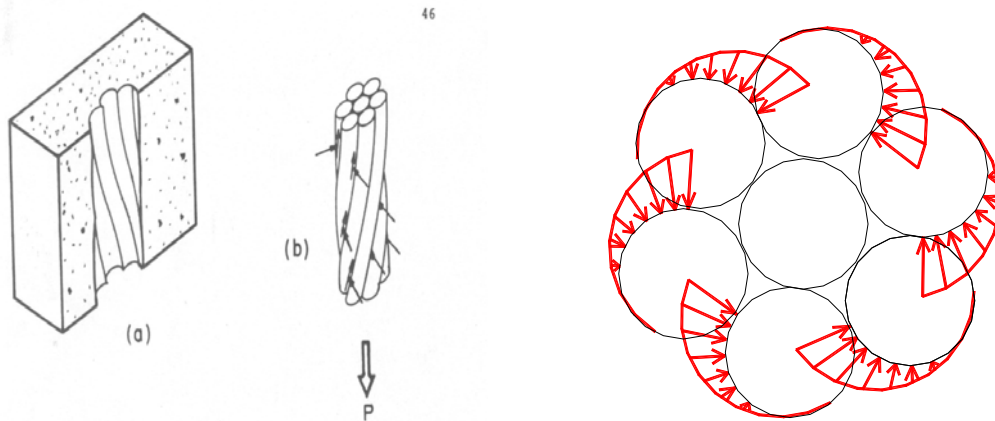
Figure 2.3: Mechanical interlock (Salmons and McCrate, 1973)

The approximate contribution of the three effects on the transfer length can be shown on a single chart to show the magnitude of their contribution. According to Russell and Burns (1996), the adhesion's contribution should be ignored at the point, where the strand starts to slip. Hence, the major contributors for strand-concrete bond mechanism will be the wedging (Hoyer) effect, followed by the mechanical interlocking mechanism, as shown in Figure 2.4.
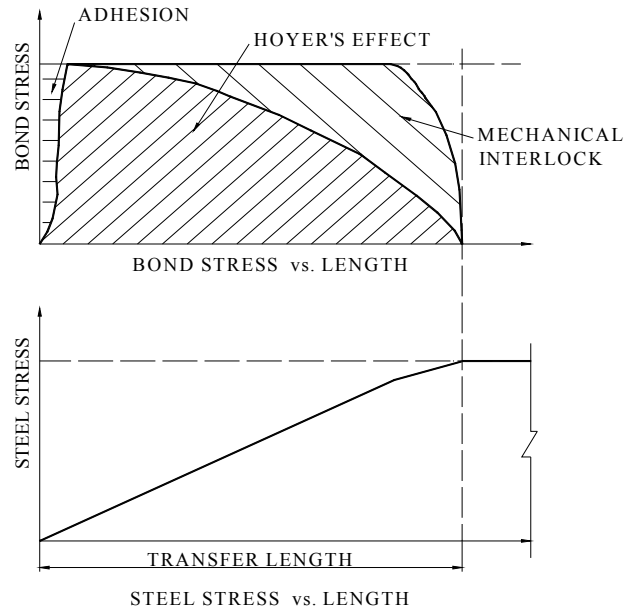
Figure 2.4: Interrelation between forces causing bond (Russell and Burns, 1996)

2.2 Development Length

The development length of prestressing strands, denoted as L_d, is defined as the minimum embedment needed to reach the section ultimate capacity without strand slippage. Thus, at the point of strand development, the strand stress could reach a maximum tensile stress (f_{ps}), without strand-concrete bond failure. The development length is measured from the member end to the point of maximum stress. The development length is composed of two main segments, as shown in Figure 2.5:

1- *The transfer length (L_t)*: where the pretension effective stress (f_{pe}) is transferred to the concrete.

2- *The flexure bond length (L_b):* where the stresses resulting from the bond (mechanical interlock) equilibrate the difference in stresses between the design (maximum) stress (f_{ps}) and the effective stress (f_{pe}).
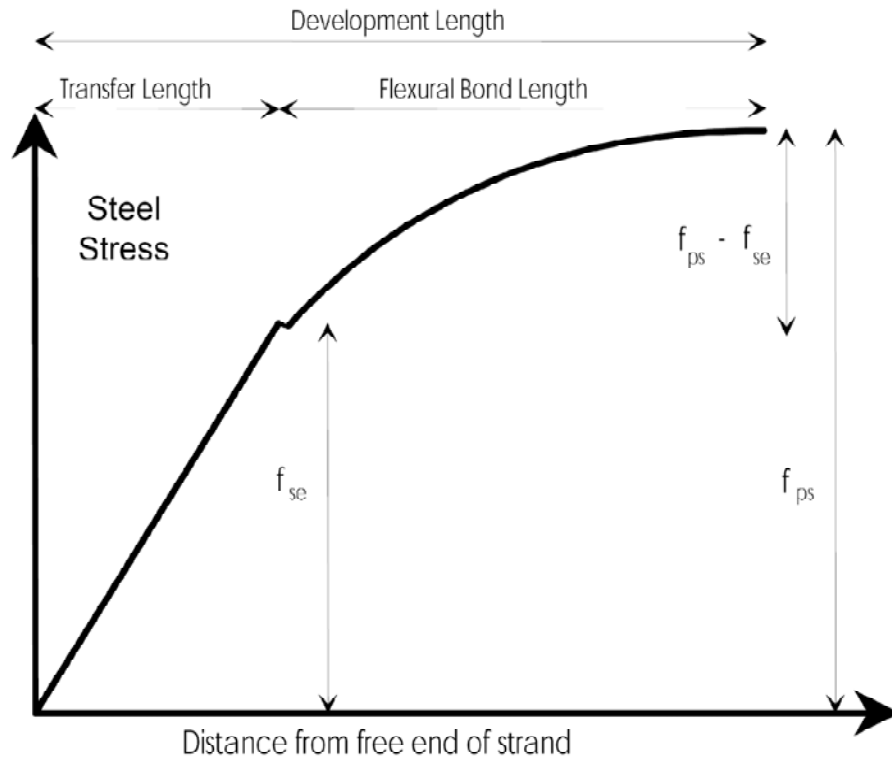
Figure 2.5: Variation of stress from the end of the strand (Gross and Burns, 1995)

2.3 History of Transfer and Development Length Formula

Prior to 1988, 0.5 in. prestressing strands were widely used in the precast/prestressed concrete industry in the United States. Minimum centerline spacing of strands was 2.0 in. Research engineers and strand manufacturers were interested in increasing the size of the strands to increase the prestressing force applied to the pretensioned member. In conjunction with their proposal to adopt the 0.6 in. strands, strand manufacturers and research engineers wanted to maintain the vertical and horizontal spacing between strands centerlines at 2.0 in. Despite of the expected benefits of increasing the efficiency of prestressing process, increasing the prestressed section capacity, and expected increase in prestressed member span-to-depth ratio, the additional prestressing force added to the

concrete section for using larger strands at similar spacing may increase the possibility of end zone cracking. Moreover, no previous experience was available for the bond behavior between the concrete and the larger strands.

The conventional strands spacing was calculated according to the "4x standard", which is known as the bond-development length equation. This equation states that the minimum spacing between strands should be kept at a distance equal to four times the strand diameter. Hence, it was acceptable to use 0.5 in. strands at 2.0 in. spacing, while a spacing of 2.4 in. was required to adopt the 0.6 in. strands in the precast/prestressed concrete industry.

In October 1988, The Federal Highway Administration issued a memorandum that forbade the use of 0.6 in. strands until further research is done to confirm the safety of its application. The FHWA was seeking for an answer to the following questions:

1- How safe are the 0.6 in. strands?

2- Can the conventional 2 in. spacing be used with the 0.6 in. strands?

3- How will the strand-concrete bond relation be affected by using the new strands at 2.0 in. spacing?

The FHWA contracted with Professor Dale Buckner from Virginia Military Institute (VMI) to gather data and perform research about the possibility of using the 0.6 in. strands at 2.0 in. spacing. In December 1994, Professor Buckner submitted his report confirming that the 0.6 in. strands are safe to be used in precast/prestressed applications

at 2.0 in. spacing. Furthermore, Professor Buckner suggested that the bond-development equation should be reassessed. In May 1996, the FHWA released a memorandum announcing that the 0.6 in. strands are safe to be used at 2.0 in. spacing. FHWA also stated that it is acceptable to use the 0.5 in. strands at a spacing of 1.75 in. In 1997, the AASHTO approved the usage of 0.6 in. strands at 2.0 in. spacing, and 0.5 in. strands at 1.75 in. spacing. The AASHTO specifications were promptly changed to reflect the new changes in strand sizes and spacing. The following section presents the research efforts and various proposed equations for transfer and development lengths, since 1949.

1949 Freyssinet

The influence of surrounding concrete on the transfer length of prestressing strands is well acknowledged. In 1949, Freyssinet wrote the following:

"Transfer bond stress can only attain a certain maximum value which depends on the friction and on the maximum pressure which the concrete can exert on the wire; this maximum pressure depends on the tensile strength and on the hardness of the concrete surrounding the wire. The performance of a bond anchorage therefore depends upon the quality of the concrete" (Guyon, 1953)

1954 Janney

Janney reported the results of experimental research program investigating the transfer and development of specimens prestressed using seven-wire strands. Janney reported that both transfer and flexure bond behavior will improve with the increase of strand

roughness. His report pointed out to the positive effect of concrete strength on transfer of prestress.

1959: Hanson and Kaar

Hanson and Kaar developed the original code expression for the calculation of transfer and development length from testing conducted in the late 1950s and early 1960s. Their research resulted in determining the minimum requirement for prestress strand embedment. Despite of having over conservative estimation for development length, their program provided a significant basis for future research.

1963: Kaar et al.

Kaar et al (1963) conducted a research to measure the strands transfer length. In this research, thirty six prestressed rectangular prisms were used. The concrete strength was up to 5000 psi, and the transfer length for strands of diameters 0.25, 0.375, 0.5, and 0.6 in. was measured. The transfer length showed no correlation between diameter and concrete strength for strands with diameter less than 0.6 in. However, the transfer length decreased with the increase in concrete strength for 0.6 in. strand diameter. The transfer length was roughly proportional to the strand diameters for strands up to 0.5 in. diameter. The 0.6 in. strand diameter exhibited shorter transfer length than its expected value if the transfer length were proportional to the diameter.

1977: Zia and Mostafa

Researchers at North Carolina State University conducted a research to investigate the parameters affecting the bond strength of prestressing strands embedded in a concrete

member. Researchers developed a formula to calculate the transfer length of strands. The proposed formula was:

$$L_t = \left[1.5 \left(f_{si} \Big/ f_{ci}' \right) d_b \right] - 4.6 \qquad (2.1)$$

1986: Cousins et al.

Cousins et al. (1986) studied the effect of epoxy coating on the transfer and development length of prestressing strands. Single strand rectangular prisms were investigated for the transfer and development length calculations. Tested strands had diameters of 0.375, 0.5, and 0.6 in. The tested strands had either uncoated or epoxy coated surfaces. The research results showed that the three different types of strands require a transfer length of 34, 50, and 56 in., and a development length of 57, 119, and 132 in. These values were higher than the estimated transfer and development length by either AASHTO or ACI code equations. These research findings lead to the issuance of the afore-mentioned FHWA 1988 memorandum regarding the transfer and development length. Based on Cousins et al research, the following equation was proposed to calculate the strands transfer length:

$$L_t = 0.5 \left(\frac{U_t}{B} \right) + \frac{f_{se} \cdot A_{ps}}{\pi \cdot d_b \cdot U_t} \qquad (2.2)$$

1991, 1992: Shahawy et al.

The Florida Department of Transportation (FDOT) conducted three separate research programs to investigate the transfer and development length of strands in different

prestress applications. These projects included the testing of seven voided slabs (Shahawy et al., 1991), 17 AASHTO Type II girders with composite slabs (Shahawy et al., 1992), and piles embedded in cast-in-place pile caps. Based on the research findings, the following equation for calculating strands transfer length was proposed:

$$L_t = \frac{f_{si} \cdot d_b}{3} \qquad (2.3)$$

The proposed equation introduced a conservative estimation of the transfer length as compared to the current AASHTO and ACI code equations, where the effective prestressing value currently utilized is replaced by the initial prestress value. In addition to the transfer length equation, FDOT submitted a proposal to the AASHTO committee T-10 to adopt a different equation for the development length calculation. FDOT proposed equation was as follows:

$$L_d = \left[\frac{\dfrac{f_{si} \cdot d_b}{3} + \left(f_{ps} - f_{se}\right) d_b}{K_b \cdot \mu_{ave}} \right] \qquad (2.4)$$

Where μ_{ave} equals 250 psi and k_b is a dimensionless constant, equals to 8 for piles embedded in pier caps (or concrete footings), and 4 for slabs and slender members. The major concerns about the FDOT development length equation was the conservative values achieved for deep members, which is about double the values using AASHTO and ACI equations, and the un-conservative value achieved for the embedded piles.

1993: Abdalla et al.

Researchers at Purdue University conducted a research to develop equations for strand development length (Abdalla et al., 1993). The experimental program at Purdue University included the testing of AASHTO bridge girders and box beams. The testing of the girders to failure was done by using point loads acting on the girders at a distance from the end equal to 1.2 times the development length calculated by the AASHTO equations. The girder failed before achieving the design ultimate load. Based on multiple experiments, Purdue University researchers proposed the following equation for the strand development length calculation:

$$L_d = \frac{f_{se}}{3} + 1.7\left(f_{ps} - f_{se}\right)d_b \qquad (2.5)$$

1993: Mitchell et al. (1993)

McGill University conducted an experimental research program to calculate the strand development length. Mitchell et al. (1993) expressed the development length as a function of concrete compressive strength. The development length equations used by the AASHTO and ACI codes was modified in two ways. First, the effective value of prestress was replaced by initial prestress. Second, both transfer length and flexure bond length were modified using a multiplier involving the concrete compressive strength. McGill University development length proposed equation was as follows:

$$L_d = 0.33 f_{si} \cdot d_b \cdot \sqrt{\frac{3}{f_{ci}'}} + \left(f_{ps} - f_{se}\right)d_b \cdot \sqrt{\frac{4.5}{f_c'}} \qquad (2.6)$$

The McGill University development length equation did not compare well with any of the studies available at that time. This was attributed to the following:

1- The gradual release method of the prestressing strands as compared to the sudden release employed in all other research programs.

2- The prestressing strands used in conducting the research at McGill University were described as a slightly rusted surface strands. Surface roughness due to rust is well-known to improve the bond conditions.

1993: Russell and Burns

Russell and Burns (1993) conducted an experimental research at the University of Texas at Austin concerning the strands transfer and development length. The University of Texas study concluded that the prevention of cracks at the transfer zone is the main factor behind the development of prestressed strands. Based on this approach, the flexural bond strength used in current codes was accepted. However, the following transfer length equation was proposed:

$$L_t = \frac{f_{se} \cdot d_b}{2} \qquad (2.7)$$

1994: Burdette et al.

Burdette et al. (1994) conducted an experimental program at the University of Tennessee at Knoxville using 20 full-size AASHTO Type II girders. The jacking stress of strands used in manufacturing these girders were 203 ksi, and the average prestress immediately after strand release was calculated to be 186 ksi. The release and initial prestressing

forces were used to develop an expression for the strand development length. The proposed equation for development length is as follows:

$$L_d = \frac{f_{si} \cdot d_b}{3} + 1.5\left(f_{ps} - f_{se}\right)d_b \qquad (2.8)$$

1995: Dale Buckner

Professor Buckner was contracted by the FHWA to study the variation in results obtained by different researchers concerning the transfer and development length of pretensioned members. In his study, presented to the FHWA, Buckner presented the following:

1- A review of the previous research regarding the transfer and development length.

2- Analysis of data from recent studies, conducted after the FHWA memorandum issued in 1988.

3- Recommend the equation to measure strand transfer and development length.

Based on Buckner research, the following equation for measuring development length was proposed:

$$L_d = \frac{f_{si} \cdot D}{3} + \lambda(f_{se}^* - f_{se}) \cdot D \qquad (2.9)$$

Buckner theory depended on correlating the flexure bond length to the strain in the strand at maximum load. According to the research findings, the constant term (λ) was calculated as follows:

$$\lambda = \left(0.6 + 40\,\varepsilon_{ps}\right) \qquad (2.10)$$

Dr. Buckner presented his report to the FHWA in December 1995. As a result, the FHWA released the 1996 memorandum allowing the use of 0.6 in. strands at 2.0 in. spacing, and 0.5 in. strands at 1.75 in. spacing. However, the FHWA retained the previously imposed multiplier (of value = 1.6) on the AASHTO code equation, till further research confirms otherwise.

1995: Gross and Burns

Gross and Burns (1997) conducted an experimental research to calculate both transfer and development length for prestressing strands. In this research, two 42 in. deep rectangular beams were fabricated, with 0.6 in. strands at 2.0 in. spacing (center-to-center). The concrete strength was 7040 psi at release and 13,160 psi at the time of development length testing. Based on their testing, an average transfer length of 14.3 in. was measured. This measured length was much less than the transfer length measured using either AASHTO provisions or ACI 318 code equations. Similarly, the development length for these strands was found less than 78 in. which is roughly equal to the development length calculated by the AASHTO provisions.

1998: Susan Lane

Susan Lane at the FHWA conducted an experimental research program to investigate the transfer and development length of prestressing strands. A number of parameters were investigated for possible use in the new transfer length equations. These included:

- Concrete compressive strength at transfer, and concrete compressive strength at 28 days.

- Concrete modulus of elasticity at 28 days.

- Concrete unit weight.

- Prestressing strand diameter.

- Stress in prestressing strands prior to transfer of prestress.

- Effective prestress (f_{se}).

Based on regression analysis, the following equation for transfer length of the prestressing strands was developed:

$$L_t = \left[\frac{4.f_{pi} \cdot d_b}{f_c'} - 5 \right] \qquad (2.11)$$

Researchers at the FHWA evaluated the flexural bond length needed beyond the transfer length to achieve the ultimate strength of the prestressed member. In their investigation, the following parameters are considered:

- Concrete compressive strength at transfer and 28 days.

- Depth of the concrete rectangular stress.

- Prestressing strand diameter and area.

- Effective prestress.

- Stress in prestressing strand at the ultimate strength of the member.

- Strain in prestressing strand at the ultimate strength of the member.

The new development length equation proposed by the FHWA research was:

$$L_d = \left[\frac{4.f_{pi}.D}{f_c'} - 5 \right] + \left[\frac{6.4(f_{ps}^* - f_{se})(D)}{f_c'} + 15 \right] \qquad (2.12)$$

1998: Cooke et al.

The State of Colorado sponsored a research program to evaluate both transfer and development length of 0.6 in. strands in high performance concrete (HPC) box beams. Prestressing strands were used at a spacing of 2.0 in. (center-to-center). The concrete strength was 7800 psi at release and 11000 psi at the time of development length measurement. The researchers reported an average transfer length of 23.4 in. and a development length of 60 in. Both results are less than that calculated by AASHTO and ACI code equations.

1999: Ozyildirim and Gomez

The State of Virginia supported an experimental project to measure the transfer length of 0.6 in. strands in HPC. Results reported by Ozyildirim and Gomez (1999) indicated that the transfer length of 0.6 in. strands was substantially less than the transfer length measured by the AASHTO and ACI code equations.

2000: Barnes and Burns

The University of Texas at Austin had a research project to measure the transfer length of 0.6 in. strands by testing 36 AASHTO Type I girders. Strands were spaced at 2 in. spacing (center-to-center) and the concrete compressive strength at release ranged from 3950 psi to 11000 psi. The results of transfer lengths measured showed a trend where the transfer lengths measured were inversely proportional to the square root of the concrete strength at release.

2001: Shahawy

Shahawy performed an experimental program, sponsored by the FDOT, to measure the development length of the strands. His approach depended on evaluating the effect of shear cracks on the bond mechanism. Shahawy performed extensive statistical analysis for the available data. The proposed development length expression was as follows:

$$L_d = \left[\frac{f_{si}}{3} d_b \right] + \left[\frac{(f_{ps} - f_{se}) d_b}{1.2} \right] + K \qquad (2.13)$$

The constant K has a value of 0 for embedded piles and flexural members with depth $\leq$ 24 in., and a value of 1.5h for members with depths > 24 in.

2002: Kahn et al.

Kahn et al. (2002) at Georgia Institute of Technology conducted an experimental research to verify that the transfer and development length of 15-mm (0.6 in.) diameter prestressing strands were less than calculated by the current AASHTO LRFD when high strength concrete is used. The research program included the testing of 4 AASHTO Type II girders, two made with 70 MPa concrete, and the other two were made with 100 MPa concrete. Transfer length was measured by calculating surface strain using Demec points. While development length was measured by conducting 8 flexural tests using different strand embedment lengths. The average measured transfer length was 17.6 in. and 14.6 in. for the 70 MPa, and 100 MPa concretes respectively. The development length was found to be 80 in. The measured values indicated that the current AASHTO and ACI code

provisions over-estimate the transfer and development length of the 0.6 in. diameter strands in high strength concrete.

2005: Kose and Burkett

Kose and Burkett (2005) conducted an experimental research to study the effect of concrete strength and strands surface conditions on transfer and development length of fully bonded strands, in addition to various combinations of bonded and debonded strands in AASHTO Type I I-beams. The experimental program included the testing of 6 AASHTO girders fabricated with low strength concrete and rusty 0.6 in. strands. The results of the research program indicated that the transfer length equations by ACI, AASHTO, and Buckner are conservative, but the Lane equation is very conservative. The development length results indicated that ACI and AASHTO are conservative for fully bonded strands and overly-conservative for the debonded strands, while Buckner and Lane equations are very conservative for fully-bonded strands, and decreasingly conservative for debonded strands. In a different research Kose (2007) was successfully able to accurately predict the effect of different parameters (strand condition, concrete strength, strand-to-concrete area) on the transfer length of prestressing strands.

2005: Kose and Burkett

Kose and Burkett (2005) gathered data from research programs done by different schools, and state DOTs considering both transfer and development lengths. The researchers were able, through regression analysis, to propose the following formula for transfer length measurement:

$$L_t = 95 \frac{f_{pi}(1-d_b)^2}{\sqrt{f_c^{'}}} \qquad (2.14)$$

Similarly, Kose and Burkett proposed an equation to calculate the development length of prestressing strands. Proposed equation was as follows:

$$L_d = 95 \frac{f_{pi}(1-d_b)^2}{\sqrt{f_c^{'}}} + \left[8 + 400 \frac{(f_{pu} - f_{pi})(1-d_b)^2}{\sqrt{f_c^{'}}} \right] \qquad (2.15)$$

2007: Ramirez and Russell

Ramirez and Russell (2007) conducted an experimental research to calculate the transfer, development and splice length of strands/reinforcement in HPC. In their report prepared for the National Cooperative Highway Research Program (NCHRP 12-60), different equations for the calculations of both transfer and development length were introduced. The proposed equations correlated the transfer and development length of prestressing strands with initial concrete compressive strength (in case of transfer length), and both initial and final compressive strength (in case of development length). The proposed equations are as follows:

Transfer Length – The proposed equation provides a transfer length of 60 strand diameter, similar to current AASHTO provisions for concrete with initial compressive strength of 4 ksi. The recommended limitation of a minimum of 40 strand diameter limits the advantage of using HPC to a concrete initial strength of 9 ksi. Proposed transfer length equation was as follows:

$$L_t = \left[\frac{120 d_b}{\sqrt{f'_{ci}}} \right] \geq 40 d_b \qquad (2.16)$$

Development Length – The proposed equation is easier in application compared to the current AASHTO and ACI code equations. Where development length is not correlated to the maximum or effective stress of strands within the member, which is highly dependent on the precision of immediate and long-term losses calculations. Proposed development length equation was as follows:

$$L_d = \left[\frac{120}{\sqrt{f'_{ci}}} + \frac{225}{\sqrt{f'_c}} \right] d_b \geq 100 d_b \qquad (2.17)$$

2.4 Current AASHTO LRFD Transfer and Development Length Equations

According to AASHTO LRFD provision (5.11.4.1) prestressing force is assumed to have a value of zero at the prestressed member end. The prestressing force may be assumed to vary linearly from zero at the point where bonding commences to a maximum at the transfer length. The distance on which the transfer occurs is estimated as:

$$L_t = 60 \times d_b \qquad (2.18)$$

Between the transfer and the development length, the strand force may be assumed to increase in a parabolic manner, reaching the tensile strength of the strand at the development length. According to AASHTO LRFD (5.11.4.2), pretensioning strands shall be bonded beyond the critical section for the development length L_d, where L_d shall satisfy:

$$L_d = 1.6 \left(f_{ps} - \frac{2}{3} f_{pe} \right) d_b \qquad (2.19)$$

Transfer and development length equations are shown in Tables 2.1, and 2.2

Table 2.1: Different proposed formulas for transfer length

ACI 318 and AASHTO STD	50 x strand diameter
AASHTO LRFD	60 x strand diameter
Zia and Mostafa (1977)	$L_t = \left[1.5 \left(\dfrac{f_{si}}{f'_{ci}} \right) d_b \right] - 4.6$
Cousins et al. (1986)	$L_t = 0.5 \left(\dfrac{U_t}{B} \right) + f_{se} A_{ps} / (\pi d_b U_t)$
Shahawy (1992)	$L_t = \left[\dfrac{f_{se}}{3} d_b \right]$
Russell and Burns (1993)	$L_t = \dfrac{f_{se} \cdot d_b}{2}$
Buckner (1995)	$L_t = \left[\dfrac{f_{si}}{3} d_b \right]$
Susan Lane (1998)	$L_t = \left[\dfrac{4 \cdot f_{pi} \cdot d_b}{f'_c} - 5 \right]$
Kose and Burkett (2005)	$L_t = 95 \dfrac{f_{pi} \cdot (1 - d_b)^2}{\sqrt{f'_c}}$
Ramirez and Russell (2007)	$L_t = \left[\dfrac{120 d_b}{\sqrt{f'_{ci}}} \right] \geq 40 d_b$

Table 2.2: Different proposed formulas for development length

AASHTO STD	$L_d = \left(f_{ps} - \dfrac{2}{3}f_{se}\right)d_b$
AASHTO LRFD	$L_d = 1.6\left(f_{ps} - \dfrac{2}{3}f_{se}\right)d_b$
Abdalla et al. (1993)	$L_d = \dfrac{f_{se}}{3} + 1.7\left(f_{ps} - f_{se}\right)d_b$
Mitchell et al. (1993)	$L_d = 0.33\, f_{si}\, d_b \sqrt{\dfrac{3}{f_{ci}'}} + \left(f_{ps} - f_{se}\right)d_b \sqrt{\dfrac{4.5}{f_c'}}$
Burdette et al. (1994)	$L_d = \dfrac{f_{si}d_b}{3} + 1.5(f_{ps} - f_{se})d_b$
Buckner (1995)	$L_d = \dfrac{f_{si}D}{3} + \lambda(f_{su}^{*} - f_{se})(D)$
Susan lane (1998)	$L_d = \left[\dfrac{4f_{pt}D}{f_c'} - 5\right] + \left[\dfrac{6.4(f_{su}^{*} - f_{se})(D)}{f_c'} + 15\right]$
Shahawy (2001)	$L_d = \left[\dfrac{f_{si}}{3}d_b\right] + \left[\dfrac{\left(f_{ps} - f_{se}\right)d_b}{1.2}\right] + K$
Ramirez and Russell (2007)	$L_d = \left[\dfrac{120}{\sqrt{f_{ci}'}} + \dfrac{225}{\sqrt{f_c'}}\right]d_b \geq 100d_b$

The afore-mentioned transfer and development length equations are dependent on several factors that include the concrete initial and final strength, initial, effective and maximum prestressing, and strand diameter. For comparison purpose, examples of transfer and development length estimates by different equations were plotted vs. concrete strength and strand diameter, as shown in the following Figures:
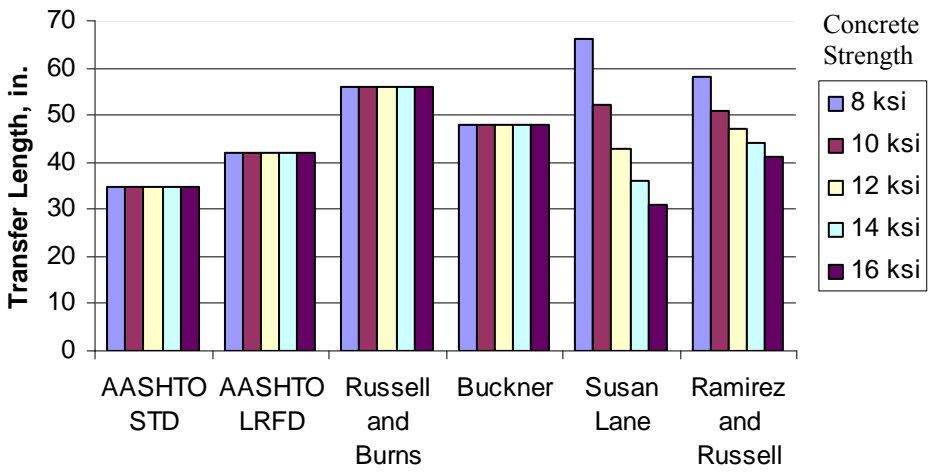
Figure 2.6: Transfer length vs. concrete final strength (0.7 in. strands)
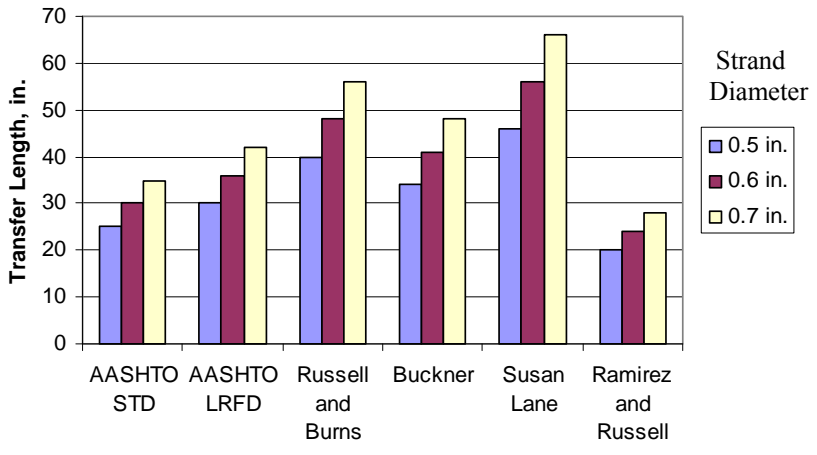
Figure 2.7: Transfer length vs. strand diameter (concrete final strength = 8 ksi)
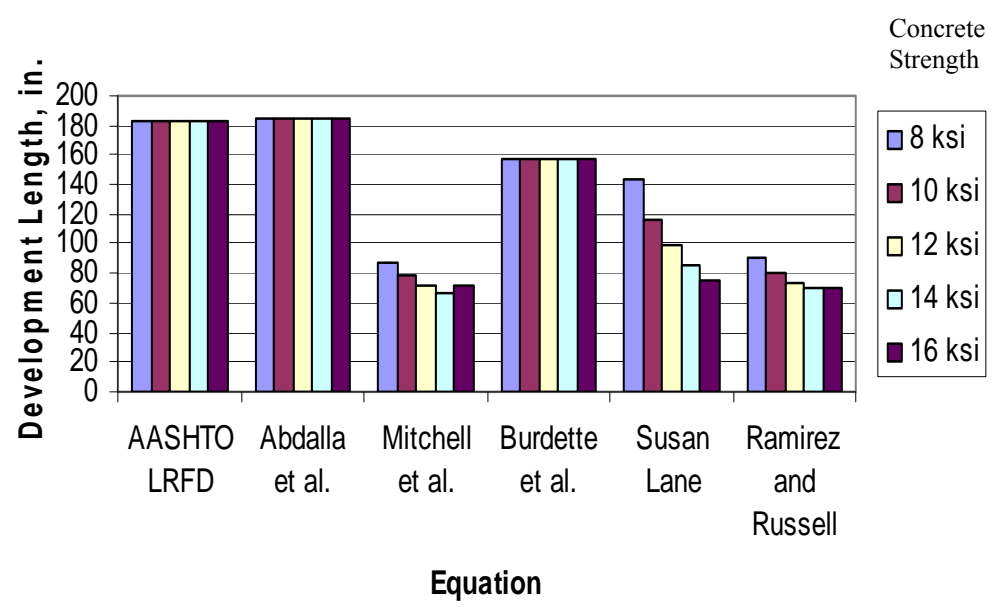
Figure 2.8: Development length vs. concrete final strength (0.7 in. strands)
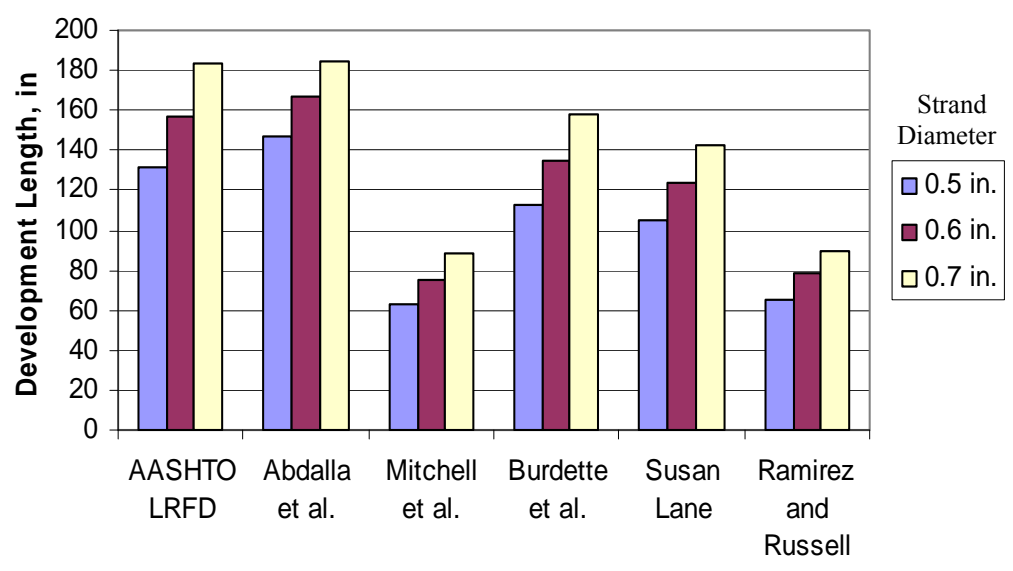
Figure 2.9: Development length vs. strand diameter (concrete final strength = 8 ksi)

Based on the transfer and development length calculations presented in the afore-mentioned figures, the following conclusions are achieved:

1. Both transfer and development length values are highly dependent on the used equation. The difference in results is attributed to the difference in parameters considered in every equation. Also, Transfer and development length equations are derived from experimental work, which is highly dependent on the test conditions and human errors.

2. Some equations results in a more conservative transfer and development length measurements as compared to current AASHTO LRFD equations. The AASHTO memorandum that delayed the use of 0.6 in. prestressing strands in precast/prestressed concrete industry resulted from similar research findings that resulted in greater transfer and development length values.

3. Important parameters such as strand confinement are not considered. Though, AASHTO LRFD provides an empirical equation to incorporate confining steel in I-girders bottom flange. Ignoring the confinement effect in experimental work contributes to the results variations.

2.5 Factors Affecting Transfer and Development Length

Several design and material factors affect both transfer and development lengths measured in pretension applications. Several research programs included thorough review and calculation for these different factors. As a result of the large variations among the values of the calculated transfer and development lengths using the proposed equations by different research programs, researchers at the FHWA decided to examine different

variables for their possible contribution to the measured transfer and development length (Susan Lane, 1998). A thorough review of past research on the transfer and development length was done by Reutlinger (1999), Jukarev (2004).The different factors can be explained as follows:

2.5.1 Design Parameters

1. Strands confinement. This includes the size of confining bars, their spacing, and their yielding strength.

2. Strand diameter.

3. Number of Strands.

4. Strand Spacing.

5. Strand stress level at member maximum capacity.

6. Compressive strength of concrete.

7. Location of prestressing strands.

2.5.2   Material and Production Parameters

1. Type of strands (single wire or seven-wire strands).

2. Strand manufacturers.

3. Strand surface conditions (Bright, weathered, or epoxy coated).

4. Consolidation of concrete and type of used admixtures.

5. Type of strand release.

6. Time factor.

The afore-mentioned factors are explained as follows*:*

Strand confinement – it is the most important factor affecting and controlling both transfer and development length values. Confinement parameters includes the size (diameter) of confining bars, its yield strength (for development length control), and modulus of elasticity (for transfer length control), in addition to the bars spacing. The effect of confining is presented in details in Chapter 3.

Strand spacing – The effect of strand spacing on the transfer and development length has been examined after the 1988 FHWA memorandum. Russell and Burns (1993) reported that there has been no difference for the transfer length of 0.6 in. strands at spacing of 2.0 and 2.25 in. (center-to-center). Cousins et al (1993) presented one of the most detailed studies about the effect of strand spacing on the transfer and development length of pretension girders. In their study, 0.5 in. strands were used at spacing of 1.75 in. and 2.0 in. in different sets of girders. The study reported that there is no significant effect for the difference in strand spacing on the behavior of strands. The main outcomes of this research are summarized in the following:

1. The reduction of strand spacing from 2.0 in. to 1.75 in. has no significant effect on the transfer length and did not result in splitting of the members at the transfer of prestressing force.

2. Similar strand spacing reduction had no effect on the development length of the prestressing strands.

The authors made the following the following statement regarding 0.6 in. strands "The reported herein for specimens prestressed with 0.6 in. diameter strand, the use of 0.6 in. diameter strand at a spacing of 2.0 in. does appear reasonable" Burdette et al. (1994) reported that the usage of 0.5 in. strands at a spacing of 1.75 in. and 2.0 in. resulted in similar transfer length. Further testing is required to test for the minimum spacing for applying larger strand diameters.

Strand stress level at member maximum capacity – higher effective prestressing force (f_{use}) results in increased transfer length, since a higher strand stress must be developed within the transfer zone. On the same time, the flexure bond will be decreased with the increase in effective prestress. However, the decrease in the flexure bond will be larger than the increase in transfer length. As a result, the development length decreases with increased effective prestress.

Compressive strength of concrete – Kara et al. (1963) reported little influence of concrete strength on transfer length up to 0.5 in. diameter. Recently, the relation between concrete strength and strand transfer and development length has been investigated for different concrete strengths, including both high and ultra-high performance concrete. Castro dale et al. (1988) investigated the effect of higher concrete strength (28-day strength of 9400 psi) on the transfer length. A 30% decrease in transfer length was reported for this concrete strength. Mitchell et al. (1993) conducted an experimental program on both transfer and development length for concretes with initial compressive strength ranging from 3050 to 7250 psi and final compressive strength ranging from 4500 to 12900 psi.

Their research concluded that both transfer and development length is reduced using higher strength concrete.

Type of prestressing strands and surface condition – It is generally accepted that the type and surface conditions of prestressing strands affects the bond behavior. For example, seven-wire strands exhibit significantly larger bond capacity than straight wires. In addition the surface conditions of the strands affect the concrete-to-strand bond. Ban et al. (1960) stated that transfer length of rusted strands is one-half to two-thirds of those of undusted strands. Hanson (1963) reported a 30 percent improvement for transfer length associated with rusted strands. Martin and Scott (1976) mentioned that although rust may result in a smaller transfer length value, designers will not be able to benefit from this. Simply, the degree of rust is hard to be quantified. The issue of strands accidental contamination with oil was discussed by Russell and Burns (1993). When strands are pretension, strands surface may be contaminated with form oil which degrades the strand-to-concrete bond. This will results in a significant higher values of transfer length.

Strands from different manufacturers – Death rage and Burdette (1994) reported the results of an experimental research that included the testing of transfer and development length of 0.5 in. strands supplied by different manufacturers. The inconsistency of results achieved for strands transfer and development length was clear. Transfer length for one of the suppliers ranged from 18 to 36 in. Other manufacturer had the transfer length ranging from 18 to 21 in.

Type of Admixtures – there is no comprehensive experimental program about the effect of different types of chemical admixtures as water reducers (WR), high range water reducer (HRWR), and air entrainment on the transfer and development length of prestressing strands. The fact that 95% of the prestressed concrete used in precast application in North America uses both WR and HRWR justifies all the effort to investigate the effect of admixtures on concrete.

Type of strand release – Several studies investigated the effect of prestress release method on the transfer length value. It was found that the sudden prestress release results in a longer transfer length compared to gradual release (Holmberg and Lindgren 1970, Rose and Russell 1997). Researchers attributed this phenomenon to the dynamic effect associated with the transfer of energy from prestressing strands to concrete members. Russell and Burns (1993) indicated that this phenomenon is obvious in small specimens. The CEB-FIP Model Code 1990 specifies an increase in transfer length of 25 percent for members subject to sudden release of strands.

Time factor – various research studies indicated that the transfer length increases with time. The increase of transfer length with respect to time is attributed to the inelastic behavior of concrete around the strands. Bruce et al. (1994) reported an increase of 10% over the first 28 days for full scale members precast by HPC. Lane (1992; 1998) reported that transfer length increases for 365 days. However, there is no pattern for the increase in transfer length. Oh and Kim (2000) reported an average increase of 5% in the transfer length after 90 days of measurements

2.6   Effect of Transverse Reinforcement on Development Length

Transverse reinforcement is used to improve the concrete-steel bond strength. At service loading, the lateral pressure introduced to the concrete due to lateral confinement reduces the tendency of the concrete to crack. Several research findings emphasized the importance of transverse confinement in reducing the splice length required for steel in tension and/or compression. Edina et al. (1999) conducted an experimental program that studied the contribution of the transverse confinement on reducing the lap splice of reinforcing steel bars. In this research, the transverse confinement introduced by spiral stirrups to three different patterns of lap splices, significantly reduced the lap length. Based on the research results, it was recommended to increase the maximum effect of transverse reinforcement, as compared to ACI 318-02 provisions. Tapers (1982) presented one of the first investigations to focus on the prediction of the bond strength for deformed bars. Tapers presented an analytical model, where the bond strength at steel-concrete interface is dependent on the capacity of the concrete surrounding the reinforcing bar to carry the hoop stresses.

There are two prevailing modes of steel-concrete bond failure. These can be explained as follows:

Mode 1 – The steel bars are near to the member face or when minimal transverse reinforcement is used. Concrete splitting is expected and steel-concrete bond failure occurs. This mode of failure is known as splitting-type bond failure.

Mode 2 - The steel bar is surrounded by an adequate concrete section. Or, sufficient confinement is utilized. A bond-shear of the rebar is expected to happen. This mode of failure is known as pullout bond failure.

The failure mechanism, in most cases, could be presented as a combination of the afore-mentioned modes. The steel-concrete bond slip is related to an increased circumferential stress within the transverse reinforcement, and a high level of radial stress within the concrete. There are two distinct types of confinement that affects the steel-concrete bond. These could be explained as follows:

Active Confinement - The active confinement is created through the application of a compression stress field that counteracts radial stress developed around reinforcing steel. Thus, reduce the formation and/or propagation of cracks. The active confinement is best represented by the reaction of the bearing on the end zone of a girder. This reaction creates a compression stress, which can be superimposed to the vertical radial stresses acting around the reinforcing steel. This compressive stresses help confine the girder end zone concrete and reduce cracking. Hence, it positively affects the development of rears.

Passive Confinement – The passive confinement is represented by transverse reinforcement, as stirrups, and spirals. The action of this confinement starts upon crossing internal cracks developed due to radial stresses. Because the action of this confinement system does not start except after the crack pattern is developed, it is so called "passive confinement". The efficiency of passive reinforcement is highly dependent on the

positioning of rears with respect to the extended crack pattern. The closer the confinement to the cracks, the higher is its efficiency.

Many experimental studies have been conducted to quantify the effect of both active and passive confinement on the bond strength between steel and concrete. In addition, different analytical models are available to describe the behavior of concrete structures under the effect of internal and external confinement. The following represents a background for the research efforts in this regards.

Untrue and Henry (1965)

Untrue and Henry studied the effect of active confinement on the bond strength. They conducted their research program by quantifying the effect of lateral pressure on 6 in. sided concrete cube, with #6 and #9 embedded rears. The lateral pressure imposed on the cube ranged from 0% to 50% of the concrete compressive strength. A slight increase in the bond strength was observed, which was numerically correlated to the square root of the concrete strength.

Oran gun Jars and Breen (1975, 1977)

Oran gun et al. (1975, 1977) tested the bond strength between rears and different types of concrete strength. In their research study, they developed and calibrated an expression correlating the bond strength with the concrete compressive strength. The calibrated equation was as follows:

$$\frac{u_{cal}}{\sqrt{f'_c}} = 1.2 + \frac{3C}{d_b} + \frac{50 d_b}{l_d} \qquad (2.20)$$

Where:

C = min of concrete cover or one half of the strand spacing.

Zia et al. (1991)

Research conducted by Zia et al. on the steel-concrete bond proved that higher rates of loading will cause a rapid deterioration on the bond. Hence requires longer development length for reinforcing steel. The same research proved that the bond strength is inversely proportional to the concrete age.

Giuliani et al (1991)

The research conducted by Giuliani et al investigated the effect of transverse (passive) confinement on the steel-concrete bond. In their research, they proved that the effect of confinement could be superimposed to external loading, and residual (tensile) strength of concrete, during its post-cracking non-linear behavior.

Azizinamini et al. (1992, 1993)

Azizinamini conducted an experimental research to investigate the tension splice of #8 and #11 bars within high performance concrete. The concrete specimens varied from 5 ksi to 15 ksi. The research findings showed that the stress distribution at ultimate stage might not be linear in case of high performance concrete. The research findings mentioned that in tension splice of rears in high performance concrete, it is not advisable

to utilize longer splice length. However, a minimum amount of transverse reinforcement may be needed to increase the bond strength.

Malvern (1992)

Malvern conducted an experimental research on the steel-concrete bond using steel bars embedded in concrete cylinders. Malvern reported that the bond strength vanishes when cracks due to radial stresses are formed, incase steel confinement is not available. Higher steel-concrete bond strength was achieved when steel bars were pushed into the concrete compared to the pullout test results. This is attributed to the Poisson's ratio effect.

The afore-mentioned studies are concerned with reinforcing steel-to-concrete bond. One study was completed on the prestressing strands-to-concrete bond strength. Russell and Burns (1993) investigated the effect of confinement on the prestressing strands-to-concrete bond. Mild steel hoops were used to contain all the strands used within prestressed concrete specimens. The research program concluded that strand confinement were efficient when designed to be near the prospective crack pattern location. The effect of confinement was decreased for specimens including large number of strands.

2.7   Strand Pullout Tests

Strand pullout testing was performed to assess the effect of confinement on the developed length of 0.7 in. prestressing strands. Several research programs considered pullout testing of strands as a direct method to assess the bond strength between different types of strands and concrete. Logan (1997) recommended that a unified testing technique

should be conducted to compare the bond strength resulting from the use of strands produced by different manufacturers in prestressing applications.

2.7.1 Mustafa Pullout Test (1974)

Mustafa (1974) developed a simple pullout procedure to test the bond strength between concrete and prestressing strands. The test method consisted of measuring the maximum pullout force resisted by unmentioned   prestressing strand embedded in a concrete block. The Mustafa pullout test was proposed as an initial attempt by researchers in the United States to calculate the bond strength between the unmentioned prestressing strands and concrete.

2.7.2   Concrete Technology Corporation (CTC) Pullout Tests (1992)

The precast/prestressed concrete institute (PCI) prestressing steel committee decided in 1992 to use the Mustafa pullout test to test lifting loops at the CTC in Tacoma, Washington. The test included the measuring of the maximum pullout force resisted by an unmentioned 0.5 in. prestressing strand embedded 18 in. within a concrete block (similar to Mustafa pullout test).

2.7.3 The University of Oklahoma Test Program (1997)

Some members of the PCI Prestressing Steel Committee objected to the use of simple pullout tests for prestressing strands. They assumed that the pullout of unmentioned strand may result in inaccurate measurement of strands development length. Researchers in the University of Oklahoma tried to assess the accuracy of various pullout test methods

for estimating strand bond quality. As-received strands from three different manufacturers were included in the test program (Rose and Russell 1997). Strands supplied from one of the manufacturers were tested with three different surface conditions: 1) cleaned with muriatic acid, 2) silage treated (simulating a slightly lubricated surface), and 3) weathered. The University of Oklahoma researchers reported that the pullout of pretension specimens is hard to perform. Due to this problem, they had inconsistent results. On the other hand, the pullout test of unpretensioned specimens was easy to perform. However, the results were highly dependent on the rate of pullout force. They recommended that future testing should be done using pullout of nonprestressed spans and Moustafa test loading rate.

2.7.4   Stresscon Test Program (1997)

Logan initiated a test program at Stresscon Corporation in Colorado to compare the development length results achieved by performing Moustafa pullout test and the development length of simply supported and cantilever beams (Logan 1997). The research program included the testing of five sets of "as received" strands supplied by five different strand manufacturers. A sixth set consisted of weathered strands supplied by one of the 5 manufacturers. Results of Moustafa pullout test for the six strand groups were compared with the development length tests for 10 beams. The results of the strand testing were as follows:

1. Four groups of strands had average bond capacity above 36 kips. Strands were ruptured corresponding to a slippage that ranged from 0.5 to 2.0 in. The

development length of these strand groups in flexure beam testing was less than
its estimated value according to the ACI 318 code equation.

2. Two groups of strands had an average pullout capacity of 11 kips. These strands
pulled out gradually while the test was ongoing. The peak resistance occurred
when the strands were pulled a distance of 6 to 8 in. The development length of
these strands in flexure testing was greater than the ACI 318 code estimation.

Based on the test results Logan suggested that the "good bond quality" of 0.5 in. strands
should attain an average capacity not be less than 36 kips, with a standard deviation less
than or equal 10%. Logan recommended that the Moustafa pullout test should be done
with different of concrete strengths ranging from 3500 and 5900 psi. In addition, Logan
recommended the usage of Moustafa pullout test for 0.6 in. prestressing strands.

2.7.5   Barnes et al. (1999)

As recommended by Logan, Researchers at the University of Texas at Austin conducted a
research to assess the development length of 0.6 in. prestressing strands in standard I-
shape concrete beams (Barnes et al. 1999). The research included the pullout testing of
0.6 in strands embedded in concrete blocks as a companion to beam specimens. The
pullout test blocks were made from similar concrete, as used in beam fabrication. Each
block had 6 strand specimens with a total embedment length of 18 in. Strands had a side
cover of 6 in. and a center-to-center spacing of 12 in. The ends of the six strands were
supported 4 in. above the bottom of the block. The pullout test block details are shown in
Figure 2.10
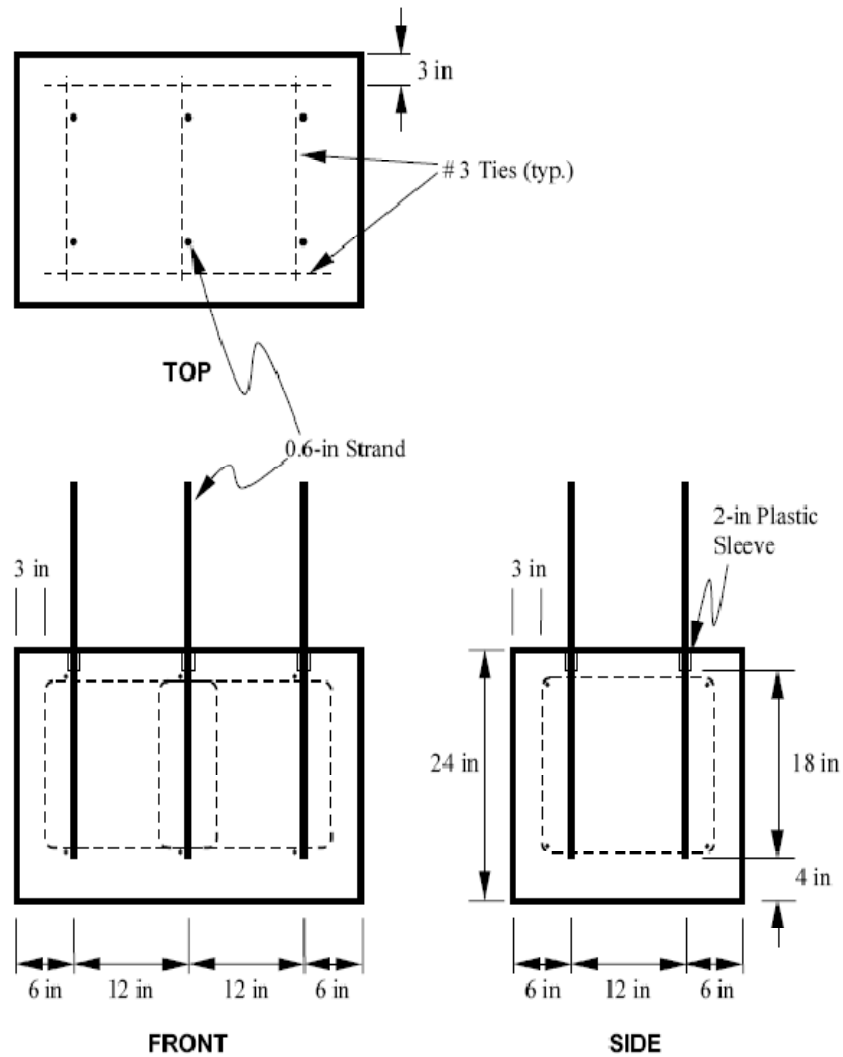
Figure 2.10: Pullout test block details (Barnes et al., 1999)

In this research programs, the actual beam specimen concrete mixes was used to pour the pullout blocks. These mixes contained high range water reducers, and its final compressive strength at pullout testing ranged from 4400 to 11710 psi. Finished pullout test block is shown in Figure 2.11.

Figure 2.11: Finished pullout test block (Barnes et al. 1999)

Strands pullout testing was done two to three days after concrete casting. The pullout test setup is shown in Figure 2.12. First, a bridging device was slipped over the strand, followed by a hollow load cell with 100 kip capacity. A 50 ton hydraulic cylinder was mounted on the load cell. A plate and a chuck were anchored on the top of the strand, against the piston of the hydraulic jack. A manually-controlled, variable speed, air-powered pump was used to apply the load at a rate of 20 kip per minute until the maximum load was reached.

Figure 2.12: Pullout test setup (Barnes et al. 1999)

According to Barnes et al. (1999), four types of failures were expected to exist. *Fracture* where one or more wire(s) of the strand are broken prior to test completion. *Abrupt slippage* where a sudden loss of resistance happens due to abrupt strand slip. *Gradual slippage* where the resistance reaches a peak value, then gradually diminishes as gradual slippage is initiated. *Test halted* where the pullout test is stopped after reaching a load higher than the strand ultimate capacity (58.6 kips for 0.6 in. strands). Based on Logan benchmark (36 kips for 0.5 in. strands), Barnes et al. considered a pullout capacity of 43.2 kips to be adequate for "good bond quality" of the 0.6 in. prestressing strands. This value is calculated based on proportioning the pullout force to the diameter of the prestressing strand (for 0.6 in. strands, pullout capacity $= 36 \times \dfrac{0.6in}{0.5in} = 43.2kips$).

The results of strand pullout test indicated that all strands (rusted and bright) used in this research program displayed a "high bond quality" according to the modified Logan benchmark. These results indicated that the bond quality of the tested 0.6 in. prestressing strands is adequate to satisfy the development length equation proposed by ACI code.

Chapter 3

Transfer and Development Length of 0.7 in Strands

3.1 Proposed Confinement Equation for Prestressing Strands

The shear-friction concept can be used to evaluate the effect of confinement on the development length of prestressing strands. By considering the equilibrium of forces in the axial direction of the bottom row of prestressing strands in a precast/prestressed concrete girder, as shown in Figure 3.1:

$$\text{Total force due to pretension} = F = A_{ps} \cdot f_{ps} \qquad (3.1)$$

Where:

F : Pullout force at failure.

A_{ps} : Total area of prestressing strands.

f_{ps} : Maximum prestressing stress at section ultimate capacity.
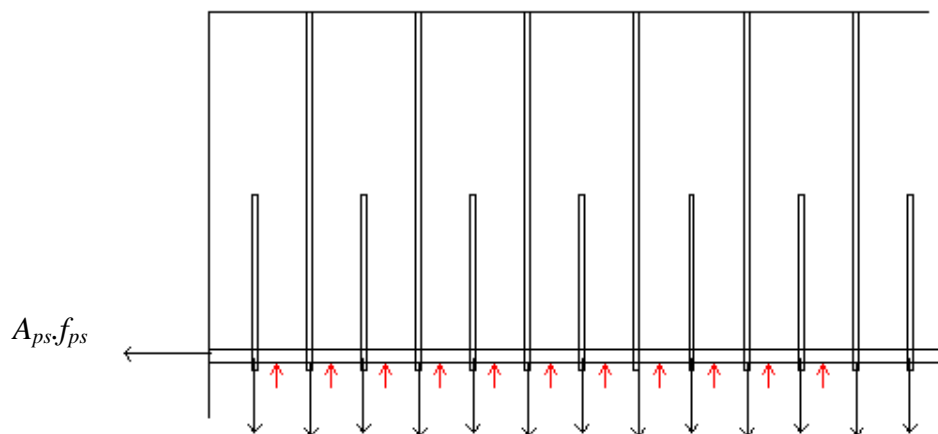
Figure 3.1: Pullout force acting on strands bottom row at section ultimate capacity

At ultimate load, prior to strand slippage, a lateral crack is assumed to develop through the bottom strand row. The resistance to strand pullout force is in effect through the transverse steel, as shown in Figure 3.2. Using the AASHTO LRFD shear-friction equation (5.8.4.1-1) for evaluating nominal pullout resistance:

$$V_n = c\,A_{cv} + \mu\left[A_{vf}\,f_y + P_c\right] \le 0.2\,f_c'\,A_c \qquad (3.2)$$

where:

V_n : Nominal shear resistance (kip).

A_{cv} : Area of concrete engaged in shear transfer (in^2).

A_{vf} : Area of shear reinforcement crossing the shear plane.

f_y : Yield strength of confining steel (ksi).

c   : Cohesion factor (AASHTO LRFD article 5.8.4.2, ksi).

μ   : Friction factor (AASHTO LRFD article 5.8.4.2).

P_c : Permanent net compressive strength (kip).

f_c' : Concrete compressive strength (ksi).
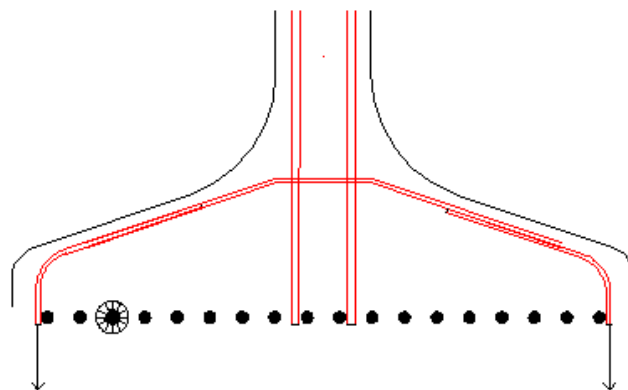
Figure 3.2: Vertical force applied by transverse steel

The cohesion between strands and concrete is assumed as zero (different materials), and no permanent compressive force is acting on the strands. Equation (3.2) can be rewritten as:

$$V_n = \mu \left[A_{vf} f_y \right] = \mu . A_{ts} . f_{tsy} \qquad (3.3)$$

where:

A_{ts} : Area of transverse reinforcement crossing the crack

f_{tsy} : Yield strength of transverse reinforcement

From equilibrium of forces, acting on the strand row in the axial direction:

$$A_{ps} . f_{ps} = \mu . A_{ts} . f_{tsy} \qquad (3.4)$$

Thus, the required area of transverse reinforcement along the developed length can be calculated as:

$$A_{ts} = \frac{A_{ps} . f_{ps}}{\mu . f_{tsy}} \qquad (3.5)$$

By considering the bearing pressure on the concrete around the strands along the horizontal crack line:

$$P_{bearing} = \frac{A_{ts} . f_{tsy}}{A_{bearing}} \qquad (3.6)$$

where:

$A_{bearing}$: Horizontal projection of bearing area.

$P_{bearing}$: Bearing pressure.

Forces are in equilibrium in the vertical direction, as shown in Figure 3.1. The area of bearing is considered as the horizontal projection of the circumferential area of strands. Thus:

$$A_{bearing} = n_{ps} \cdot L_d \cdot d_{ps} \qquad (3.7)$$

Where:

n_{ps} : Number of prestressing strands in one row.

L_d : Development length.

d_{ps} : Prestressing strand diameter.

The concrete bearing capacity can be calculated according to the AASHTO LRFD provisions as:

$$P_{bearing} \cdot A_{bearing} = A_{ts} \cdot f_{tsy} = 0.2 f_c' \cdot A_c \qquad (3.8)$$

Equation (3.8) can be rewritten as:

$$\frac{A_{ts} \cdot f_{tsy}}{n_{ps} \cdot d_{ps} \cdot L_d} \le 0.2 f_c' \qquad (3.9)$$

\

3.2   Theoretical Validation of Strands Confinement Equation

3.2.1   NU Girders Using 0.6 in. Strands

The NU girders have a bottom flange width of 38.3 in. The maximum number of prestressing strands contained at one row within the NU girder bottom flange is 18 strands (spaced at 2.0 in. centerline spacing). NU girders bottom flange are subjected to different cracking patterns upon reaching their ultimate capacity. The most critical crack

is developed horizontally through the 18 strands at the bottom row. This is attributed to the following reasons:

1. The largest stress within the prestressing strands is developed in the bottom row strands, which results in the maximum pullout force.

2. In order to achieve maximum section capacity, designers places the maximum possible amount of strands in the bottom row (18 strands).

At the ultimate section capacity, the section remains intact through the action of reinforcing steel crossing the crack. This reinforcing steel includes: 1) End zone reinforcement, 2) Shear reinforcement, and 3) Confining (transverse) reinforcement.

By considering an NU900 girder precast using 8000 psi concrete, and contains $18 - 0.6$ in. prestressing strands at the bottom row. The amount of transverse steel required is calculated according to Equation (3.5), as follows:

$$\text{Transverse steel required} = A_{ts} = \frac{18 \times 0.217 x 270}{1.4 \times 60} = 12.55 in^2$$

Where:

f_{ps} = maximum strand stress at section capacity = 270 ksi.

μ = 1.4 = coefficient of shear friction in monolithically cast concrete.

The calculated reinforcement is to be placed at a distance from the girder ends not to exceed the development length.

According to AASHTO LRFD specifications, the development length is calculated as:

$$L_d = 1.6\left(f_{ps} - \frac{2}{3}f_{pe}\right)d_{ps} = 1.6\left(270 - \frac{2}{3}.160\right) \times 0.6 = 156.8 in \qquad (3.10)$$

According to current AASHTO LRFD specifications, the following steel bars are calculated to cross the crack developed through the bottom strand row:

1. **End Zone Reinforcement**

$$P_o = 18 \times 0.217 \times 202.5 = 790.9 kips \qquad (3.11)$$

$$P_f = 0.04\, P_0 = 0.04 \times 790.9 = 31.6 kips \qquad (3.12)$$

$$A_s = \frac{P_f}{20ksi} = \frac{31.6}{20} = 1.58 in^2 \qquad (3.13)$$

According to AASHTO LRFD provision (5.10.10.1-1), the end zone reinforcement should be placed at a distance of H/4 from the girder end (where H is the girder total height).

2. **Shear Reinforcement**

From practice, 2#4 shear rebars are placed at 6 in. spacing along the girder total length (after the end of end zone reinforcement).

$$\text{Area of shear reinforcement} = \left(\frac{156.8 - 15}{6} + 1\right) \times 2 \times 0.2 = 9.8 in^2 \qquad (3.14)$$

3. **Confinement Reinforcement**

According to AASHTO LRFD provision (5.10.10.2), minimum confining of #3 reinforcing bars are placed at 6 in. spacing for a distance = 1.5H from the girder end.

$$\text{Number of confining bars} = \left(\frac{1.5H}{6}+1\right) = \left(\frac{1.5\times35}{6}+1\right) = 10 \qquad (3.15)$$

$$\text{Area of confining rebars} = 10\times2\times0.11 = 2.2in^2 \qquad (3.16)$$

The total area of transverse steel bars calculated = 1.58 + 9.8 + 2.2 = 13.58 in^2, this calculated amount is greater than the required transverse steel according to equation (3.5). Thus, the developed equation could be used in transverse steel calculations.

3.2.2 Full-Scale Testing of NU Girders Fabricated with 0.7 in. Strands

Two full-scale girder testing was done in the University of Nebraska-Lincoln using NU girders fabricated with 0.7 in. prestressing strands. First girder, denoted as girder A, represents the first precast/prestressed girder fabricated using 0.7 in. strands at a centerline spacing of 2.0 in. in North America. The second girder, denoted as girder B, was tested in flexure, and reported by Reiser (2007). The following represents the girder design and testing results.

3.2.2.1   Girder A – First I-Girder Fabricated with 0.7 in. Strands in North America

The first precast/prestressed I-girder fabricated with 0.7 in. prestressing strands at centerline spacing of 2.0 in. was made in Coreslab, Omaha, Inc. The girder was NU900, with a 1 in. thick haunch, and a 7.5 in. deck. Its bottom flange contained 30-0.7 in. straight prestressing strands. Welded wire fabric (WWR) was used for girder shear reinforcement.   2 meshes of 6x6 – D31xD31 meshes were used. The girder end zone reinforcement contained 4#6 bars at 2 in. spacing. Strands at the bottom flange were confined by D11 WWR at 6 in. spacing. Additional confinement of #3 bars was placed at

6 in. spacing for 36 in. at each girder end. The section details of the NU900 girder are shown in Figure 3.3
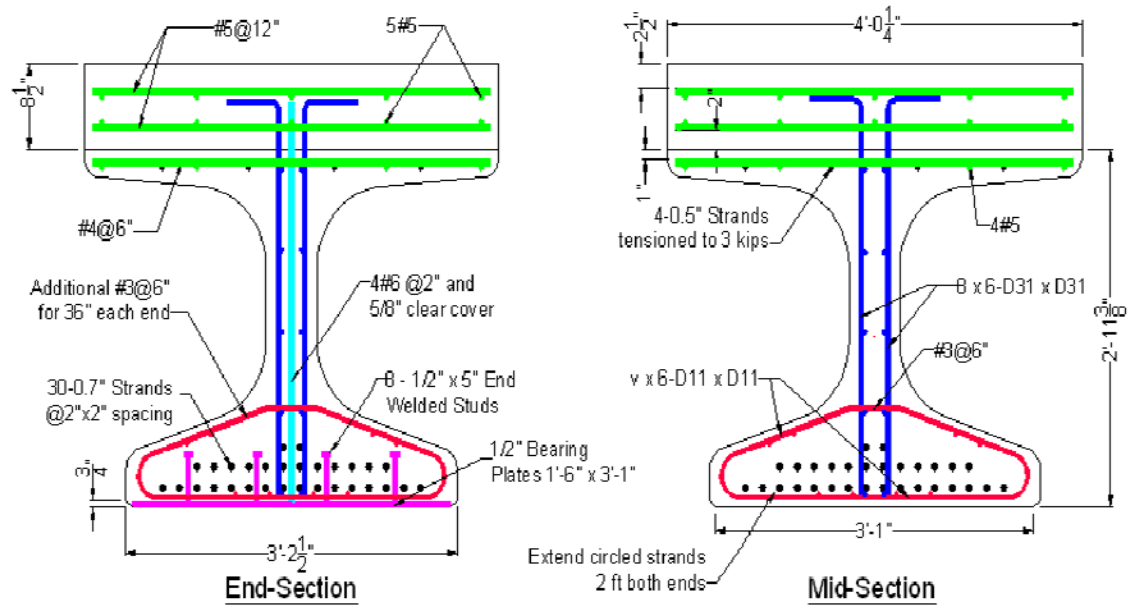
Figure 3.3: NU900 section details – girder A

According to the current AASHTO LRFD equation for development length estimation:

$$L_d = 1.6 \times \left(f_{ps} - \frac{2}{3} f_{pe} \right) \cdot d_b = 1.6 \times \left(270 - \frac{2}{3}.160 \right).0.7 = 183 in.$$

The girder was tested to its ultimate capacity with a point load acting on 15 ft (180 in.) from its end, as shown in Figure 3.4. The load point of action existed at a distance from the girder end equal to the development length, and no slippage was noticed on the strands. According to equation 3.5, the amount of steel required for full development of the strands is:

$$A_{ts} = \frac{A_{ps} \cdot f_{ps}}{\mu \cdot f_{tsy}} = \frac{16 \times 0.294 \times 270}{1.4 \times 80} = 11.34 in^2$$

Transverse reinforcement in the first 10 ft. of the girder includes the following:

- Shear Reinforcement:

$$A_{ts} = 0.31 \times 2 \times 27 = 16.74 in^2$$

- Confinement rebars:

$$A_{ts} = 19 \times 2 \times 0.11 = 4.18 in^2$$

The area of confinement resulting from the confinement and shear reinforcement is greater than the required area for girder development. Thus, strands are fully developed at a distance less than that estimated by AASHTO LRFD development length equation.
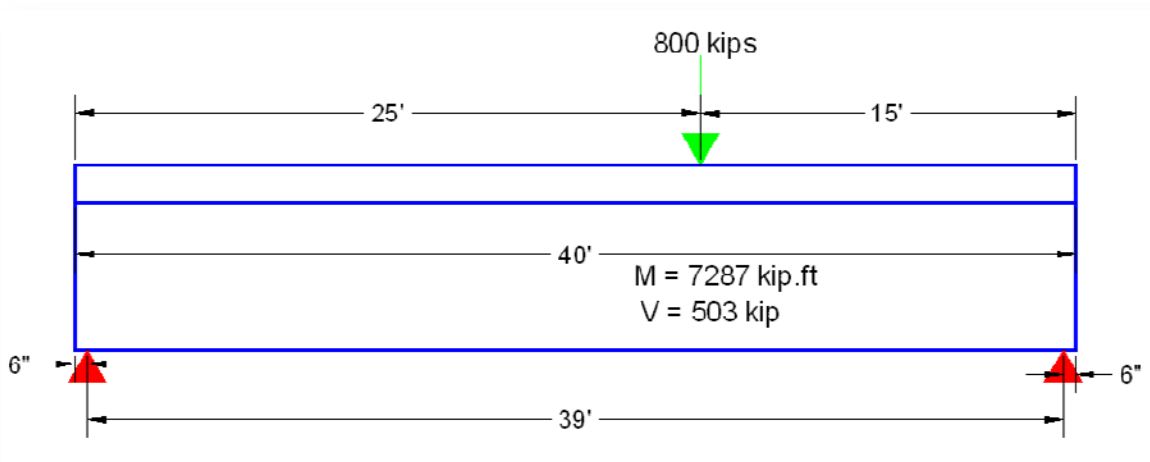
Figure 3.4: NU900 loading (flexure testing)

3.2.2.2   Girder B - Pacific St. Bridge Project NU900 I-Girder

NU900 girder was designed and tested in the preparation for the pacific street bridge project. According to Reiser (2007), the girder contained 24-0.7 in. prestressing strands in

the bottom flange, 4-0.5 in. partially stressed strands in the top flange. The girder transverse reinforcement included the following:

- 4 #6 bars for end zone reinforcement.

- 2 #4 @ 3 in. spacing for shear reinforcement.

- 15 # 3 hairpins for strand confinement at the bottom flange (first 45 in. of the girder ends). The cross-section of the girder is shown in Figure 3.5
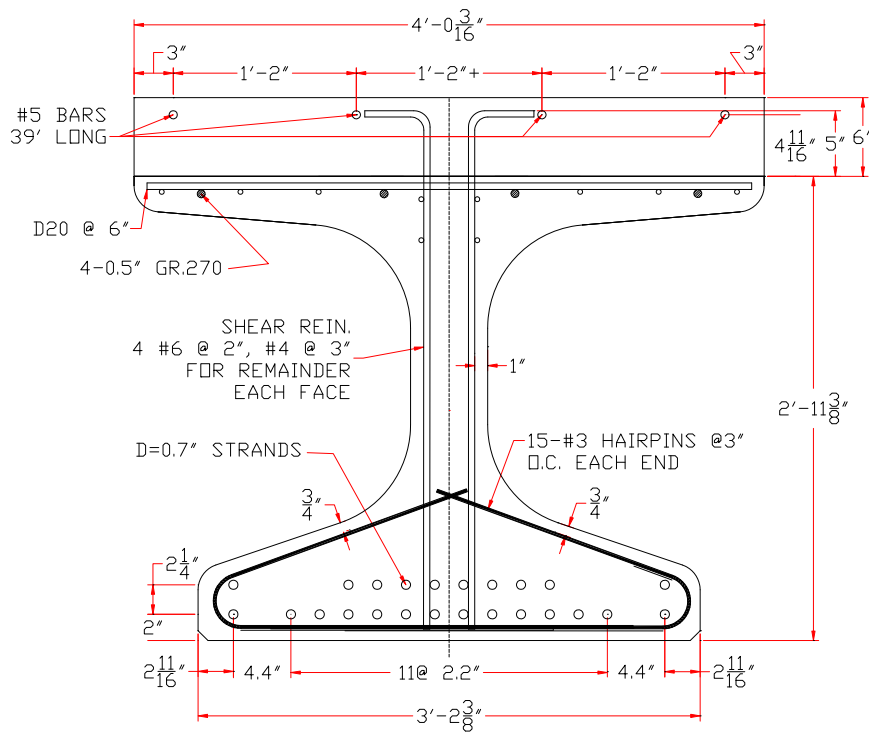
Figure 3.5: NU900 girder (Pacific St. Project, Reiser 2007).

According to equation 3.5, the amount of transverse reinforcement required for strand development is:

$$A_{ts} = \frac{A_{ps} \cdot f_{ps}}{\mu \cdot f_{tsy}} = \frac{14 \times 0.294 \times 270}{1.4 \times 60} = 13.23 in^2$$

The quantity of transverse reinforcement is calculated as follows:

- End zone reinforcement = 8#6 bars = 2.31 in^2

- Area of hairpins used in confinement = $15 \times 2 \times 0.11 = 3.3 in^2$

- Area of shear reinforcement = 0.4 in^2 @ 3 in.

Required area of shear reinforcement to be used in developing the strands = 13.23-2.31-3.3 = 7.62 in^2

Number of shear reinforcement lines = 7.62/0.4= 20 lines.

Shear reinforcement was placed after the end zone reinforcement was placed. Thus, the required shear reinforcement lines existed at distance $= 4 \times 2 + 20 \times 3 = 68 in.$ from the girder end. (Refer to Figure 3.6)
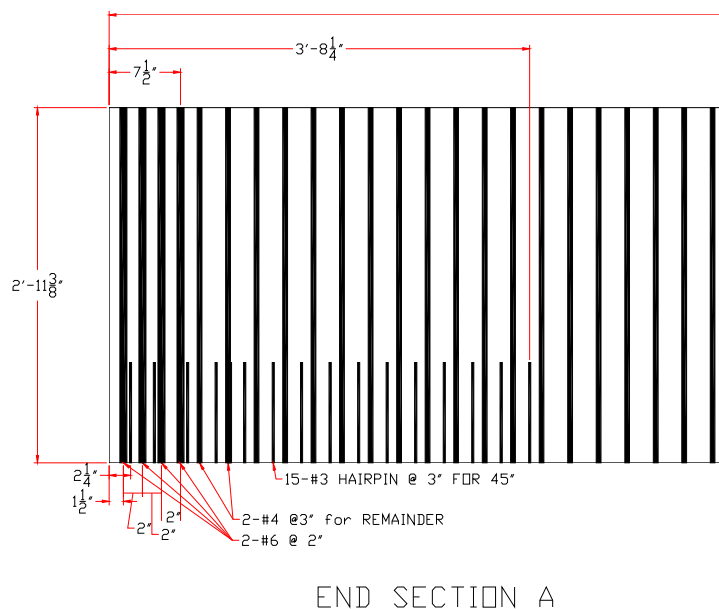
Figure 3.6: Transverse reinforcement at girder ends (Reiser, 2007)

The girder was tested by a point load at a distance of 14 ft (from the centerline of the end bearing). Thus, no strand slippage was observed.

3.3 Pullout Test of 0.7 in. Strands

In order to validate the use of shear friction theory in calculating the amount of confinement required for development of 0.7 in. diameter prestressing strands without violating the current AASHTO LRFD equations, pullout test program for prestressed specimens is conducted at the University of Nebraska. In this research program prestressed specimens was designed, and pullout testing was performed to assess the bond quality of confined prestressed strands. It was predetermined to continue the test until one of the following modes of failure is achieved:

1. Strand slippage: where strand starts to slip prior to its rupture. This slippage could be an abrupt or gradual slippage. Slippage prior to strand rupture is considered as an indication of confinement inadequacy.

2. Strand rupture: where strand is broken at a load greater than its ultimate capacity of 79.4 kips (equivalent to tensile strength of 270 ksi). Rupture of strands indicates its full development under the existing amount of confining steel.

3.3.1 Specimens Design and Fabrication

Square prisms with 7 in. side dimension were used to perform the pullout testing of 0.7 in. strands. Required confinement for strand development was calculated according to equation 3.5 as follows:

$$A_{ts} = \frac{A_{ps} \cdot f_{ps}}{\mu \cdot f_{tsy}} = \frac{0.294 \times 270}{1.4 \times 60} = 0.95 in^2$$

Grade 60 square ties were used for strand confinement. Ties had a side dimension of 5 in., and a diameter of 0.375 in^2. The minimum number of ties required for strand development was:

$$N_{ties} = \frac{0.95}{2 \times 0.11} = 5 \text{ ties.}$$

The stress developed in confining steel upon reaching ultimate pullout force, considering the use of 5 ties as confining steel bars is:

$$f_{tsy} = \frac{A_{ps} \cdot f_{ps}}{A_{ts} \cdot \mu} = \frac{0.294 \times 270}{2 \times 0.11 \times 5 \times 1.4} = 51.5ksi$$

The minimum length of concrete specimen was calculated according to equation 3.9 as follows:

$$\frac{A_{ts} \cdot f_{tsy}}{n_{ps} \cdot d_{ps} \cdot L_d} \leq 0.2 f_c'$$

Thus:

$$L_d = \frac{A_{ts} \cdot f_{tsy}}{n_{ps} \cdot d_{ps} \cdot 0.2 \cdot f_c'} = \frac{5 \times 2 \times 0.11 \times 51.5}{1 \times 0.7 \times 0.2 \times 8} = 50in.$$

A minimum specimen length of 4 ft. (48 in.) was considered for the pullout test.

Wooden forms were fabricated and confining steel ties were fixed to 1 in. side and bottom chairs attached to the form maintain there upright position when concrete is poured. Forms were placed in series within the 60 ft. prestressing bed available in the

structural testing lab at the University of Nebraska. Ties and formwork are shown in Figure 3.7.

Figure 3.7: Pretension specimen rows (form work and confining)

Prestressing strands of 0.7 in. strand was pretensioned to a jacking stress of 202.5 ksi (total force = 59.5 kips) using a mono-strand jacking device. The total length of prestressing strand between the prestressing bed two ends was 65 ft.. The strand was marked at its live end prior to pretensioning to measure the strand elongation after prestressing is completed to check the level of prestressing. When strand was tensioned, the displacement of the mark was measured, and compared to the calculated elongation (refer to Figure 3.8). The calculated (theoretical) elongation was as follows:

$$\text{Elongation} = \frac{\sigma}{E}.L = \frac{202.5 \times 65 \times 12}{28500} = 5.54 in. \quad (3.17)$$

Where:

σ : jacking stress (202.5 ksi).

E : strands modulus of elasticity (28500 ksi).

L : total strand length (65 ft.)

The actual measured elongation upon applying jacking prestress was 5.75 in, which was almost equal to the theoretical calculations. This step was done as a mean of quality control to ensure the accuracy of jacking prestress of strands.

Figure 3.8: Marking and measuring the strand elongation

Self-consolidating 8000 psi concrete mix was used in pouring specimens. The 8000 psi concrete strength represents the minimum concrete strength according to precast/prestressed concrete industry common practice in the State of Nebraska. The concrete mix was ordered and poured the same day of tensioning the strands. Figure 3.9

shows the concrete pouring. The mix design is shown in Table 3.1. Strands were released

24 hours after the concrete was poured. Concrete strength is shown in Figure 3.10

Figure 3.9: Specimens pouring

Table 3.1: Concrete mix design used in fabricating pullout specimens

Material	Quantity / cubic yard
Cement, Type I/II	705 lbs
Fly ash, class C	378 lbs
Water-cement ratio	0.24 lb/lb
Fine sand	420 lbs
Sand-gravel	980 lbs
½" BRS Limestone	1340 lbs
Pozzolith 322-N	3 oz. / 100 lbs
Glenium 3030	8-12 oz./ 100 lbs
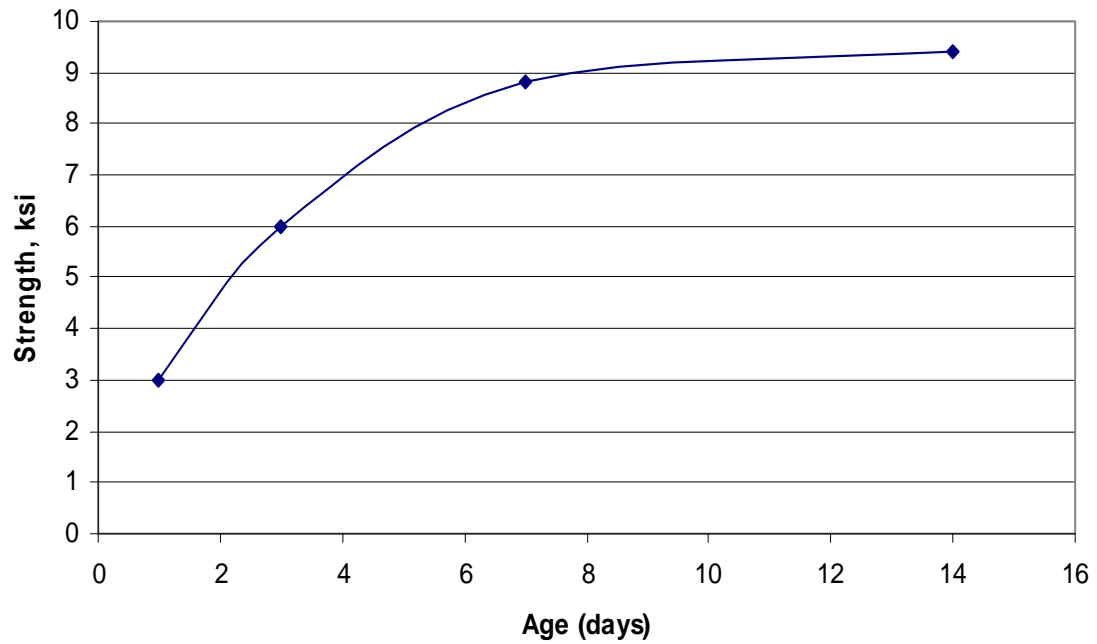
Figure 3.10: Pullout specimen concrete strength vs. time

3.3.2   Pullout Test Setup

Pullout testing of pretensioned specimens was designed to be done horizontally for safety purposes. First, a 5 in. square plate was slipped over the strand to be tested. This was followed by a 100 ton hydraulic jack with 2.5 in. cylindrical hole. Next, a loading cell was placed, such that the strand extends through the load cell center hole. Additional plate was slipped on top of the loading cell to be acted upon by the pushing forces. The main challenge was to design the strand gripping so that either strand slippage occurs or rupture is achieved at a load greater than strand ultimate strength (79.4 kips). A set of specimens were fabricated for trial purpose, all specimens were designed to fail in rupture. The following griping techniques were tried:

3.3.2.1   0.7 in. Chucks

Two types of chucks are available for use with 0.7 in. prestressing strands. A one time use and reusable chucks. Both have an outer diameter of 2.0 in. The total length of the reusable chuck is 4.5 in., while the one time use chuck has a length of 2.125 in. In the first test setup, a reusable chuck was used to grip the strands at pullout trials, complete test setup is shown in Figure 3.11

Figure 3.11: Pullout test setup (gripping technique #1)

Two pullout tests were conducted using the afore-mentioned gripping technique. The test was halted as wires of the prestressing strands were broken at the chuck location, and strand full rupture was achieved at a maximum load of 74300 lbs, and 61700 lbs. This is equivalent to a strand stress of 252.7 ksi, 209.9 ksi respectively. The premature rupture of strands was attributed to the stress concentration created at the chuck-strand interaction.

Due to this premature failure, it was not possible to decide whether or not the strands are fully developed. Strand failure is shown in Figure 3.12.

Figure 3.12: Strand failure at the chuck location

3.3.2.2   Using Grip Insert and 0.7 in. Chuck

A 5 in. long grip insert was attached to the prestressing strands before the chuck. It was hypothesized that a grip insert will increase the length of strand gripping, hence reduce the stress concentration that led to premature failure. The new gripping technique is shown in Figure 3.13

Figure 3.13: Pullout test setup (gripping technique #2)

Two pullout tests were conducted using gripping technique #2. Strand rupture occurred at a maximum load of 71600 lbs, and 78200 lbs. This is equivalent to strand stress of 243.5 ksi, and 265.9 ksi respectively. Despite of the better results of this technique, the maximum load at strand rupture was still below the required benchmark (79400 lbs), which is equivalent to a strand stress of 270 ksi. A longer grip insert was required for achieving the required failure load.

3.3.2.3   Using Hydraulic Jack, 9 in. Long Grip Insert, and 0.7 in. Chuck

A longer 9 in. grip insert was fabricated. The 2 grip halves were placed around the strand, confined by a metal frame, and firmly griped to the strand by a 30 ton load applied by using a hydraulic jack. A 0.7 in. chuck was directly seated at the end of the grip insert to

prevent any slippage. The evenly distributed jack loading acting on the grip, and the grip length were enough to eliminate the stress concentration resulting in premature strand failure. This test setup is shown in Figure 3.14, and Figure 3.15. Gripping technique is shown in Figure 3.16.
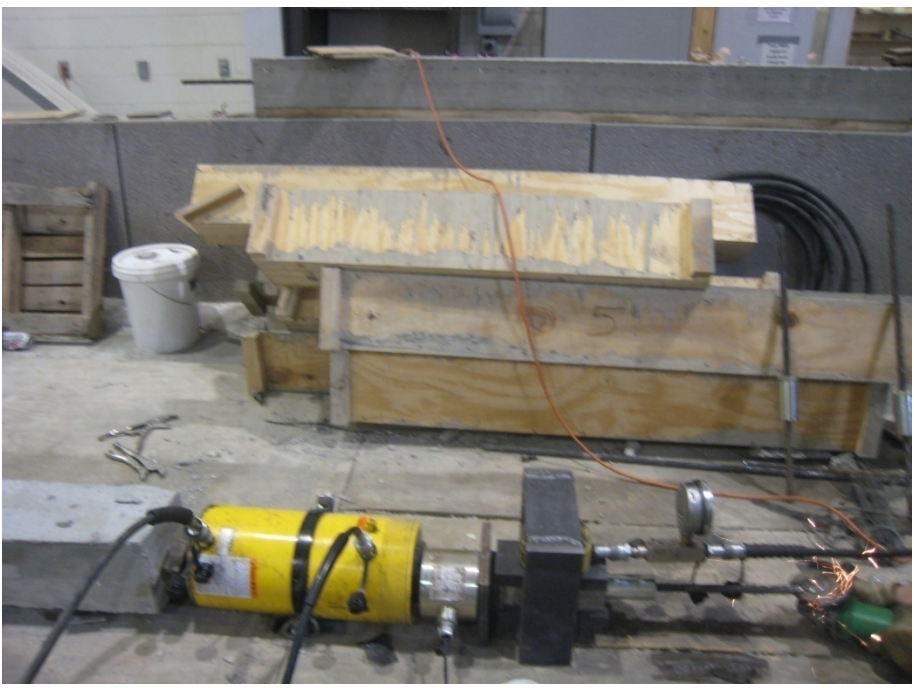
Figure 3.14: Pullout test setup (gripping technique #3)
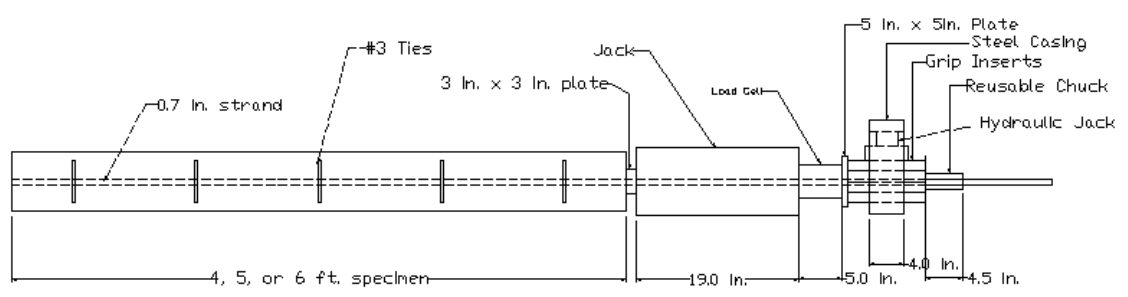
Figure 3.15: Pullout test setup (successful gripping technique)
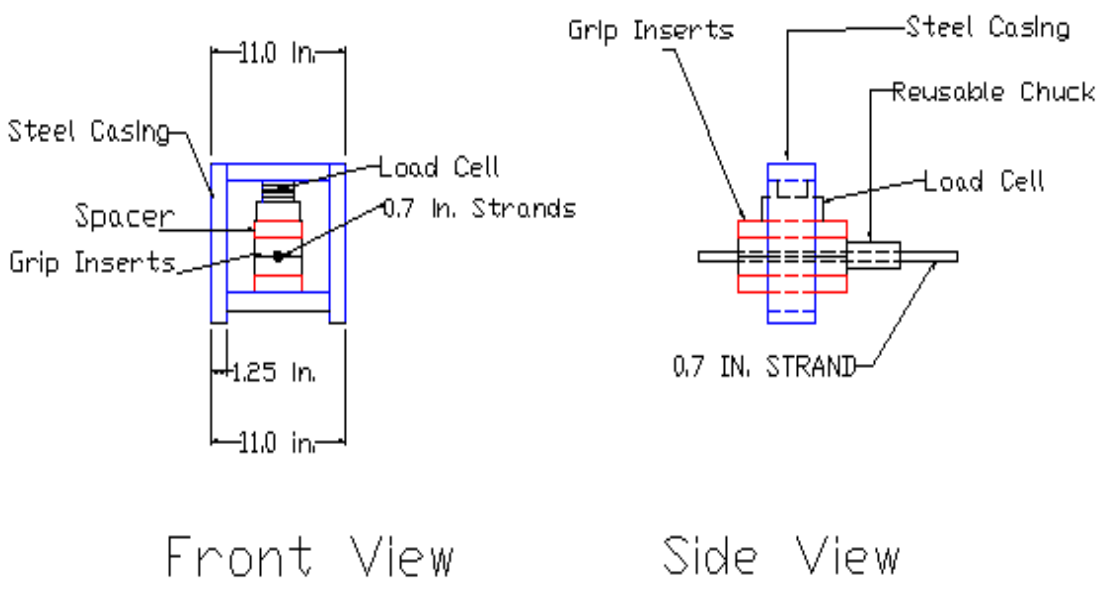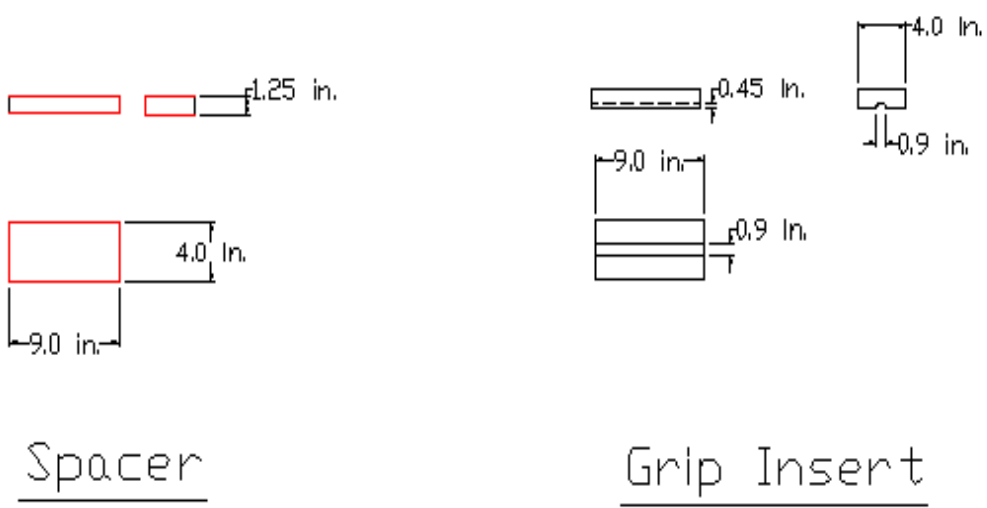
Figure 3.16: Gripping Technique

3.3.3 Results of Strands Pullout Tests

3.3.3.1 Pretensioned Specimens Set #1

First set of specimens were designed to conduct pullout test. Specimen lengths were 4 ft,

5 ft, and 6 ft. Minimum reinforcement of 5#3 ties were used as transverse reinforcement

of specimens. All specimens were designed to fail by strand rupture. Similar concrete

mix, as shown in Table 3.1 was used in strand pouring. Strands were released at concrete

strength of 6 ksi, and pullout tests were conducted when concrete strength reached to 8

ksi. A deflection gage was attached to the tested specimens to measure any strand

slippage. Specimen details are shown in Figure 3.17
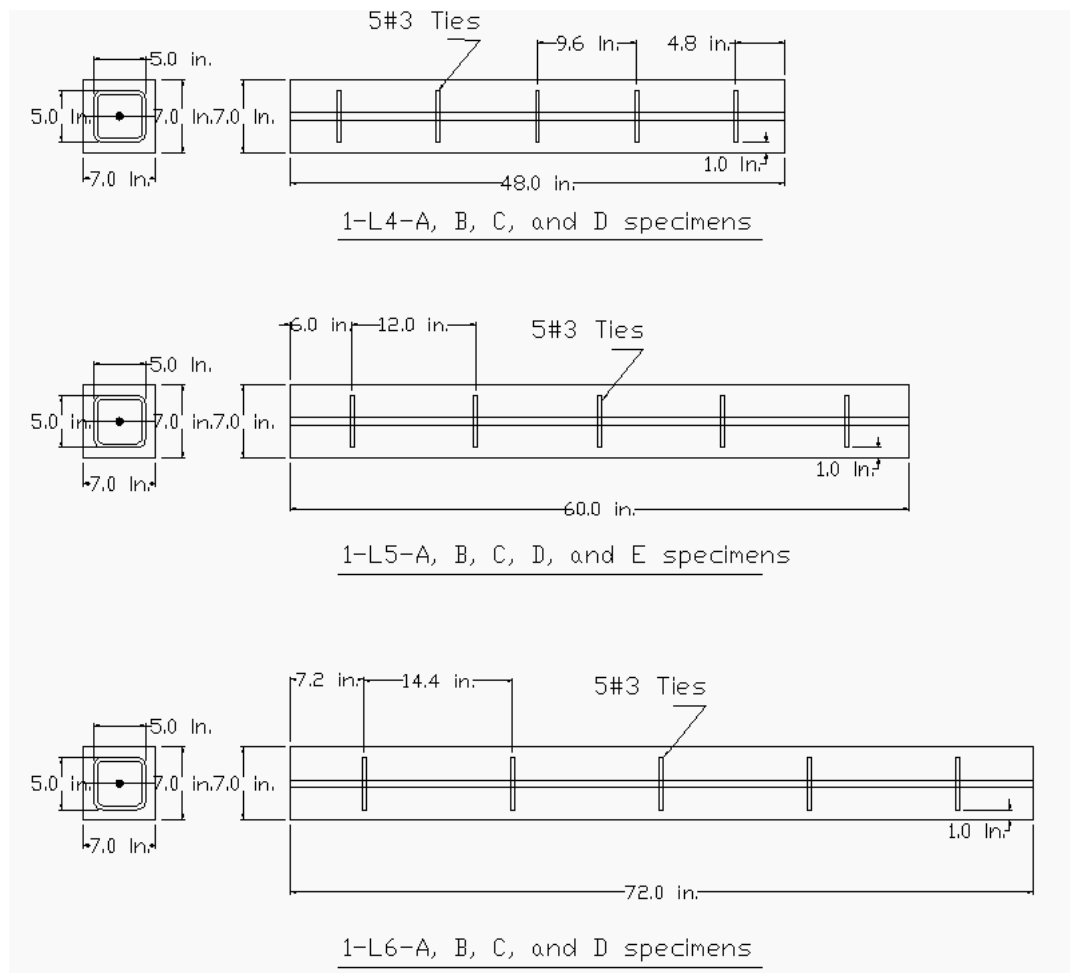
Figure 3.17: Set #1 Pullout specimens

The pullout test included four 4 ft specimens, five 5 ft. specimens, and four 6 ft specimens. Specimens' details and pullout test results are shown in Table 3.2

Table 3.2: Pullout test results (specimens set#1)

Specimen	Length (ft.)	Number of Ties	Length (ft.)	Reinforcement	Load (kips)	Stress at Rupture (ksi)
1-L4-A	4	5	4	#3 @ 9.6 in.	81.9	279
1-L4-B	4	5	4	#3 @ 9.6 in.	81.9	279
1-L4-C	4	5	4	#3 @ 9.6 in.	78.7	268
1-L4-D	4	5	4	#3 @ 9.6 in.	81.7	278
1-L5-A	5	5	5	#3 @ 12 in.	81.7	278
1-L5-B	5	5	5	#3 @ 12 in.	86.5	294
1-L5-C	5	5	5	#3 @ 12 in.	86.6	295
1-L5-D	5	5	5	#3 @ 12 in.	79.1	269
1-L5-E	5	5	5	#3 @ 12 in.	78.7	268
1-L6-A	6	5	6	#3 @ 14.4"	86.7	295
1-L6-B	6	5	6	#3 @ 14.4"	80.2	273.8
1-L6-C	6	5	6	#3 @ 14.4"	84.1	286
1-L6-D	6	5	6	#3 @ 14.4"	88.0	299

The results of ultimate pullout force compared to the required force for strand rupture according to ASTM A416 are presented in Figure 3.18
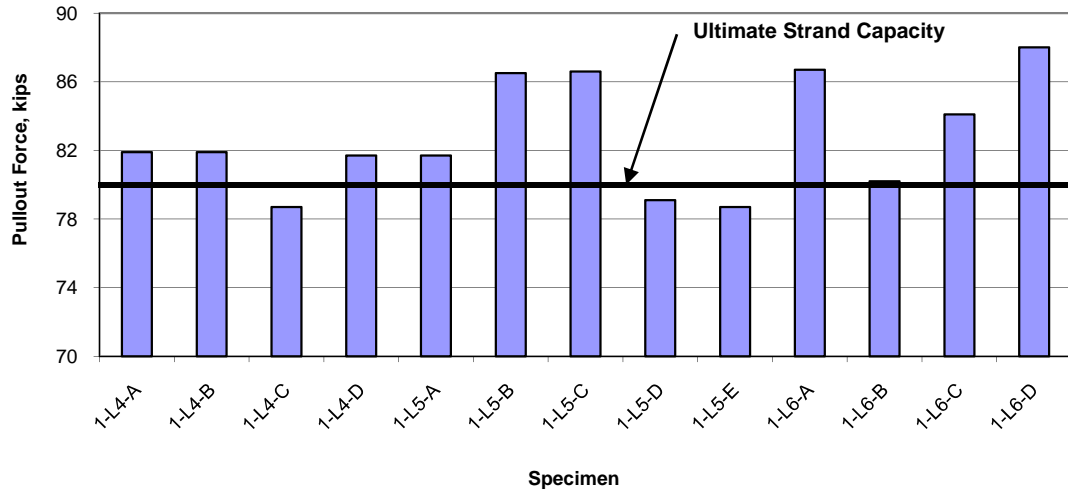
Figure 3.18: Strand rupture at pullout vs. ASTM A416 requirements

The following conclusions were achieved from results shown in Table 3.2:

1. The amount of reinforcement calculated using the shear-friction principal is adequate for the full development of 0.7 in. prestressing strands.

2. The value of co-efficient of friction considered in calculating the confinement effect (μ=1.4) is valid for pretensioned strands friction (with monolithically cast concrete).

3. Gripping technique #3 is essential to prevent any premature rupture of strands.

4. The amount of reinforcement used to confine the prestressing strands directly affects its development length. This is clearly concluded when the same number of ties developed the strand in concrete specimens with different lengths.

Strands pullout tests reported in Table 3.3 had similar mode of failure. Progressive rupture of the seven wires was initiated upon reaching the strand ultimate stress, followed by a sudden thrust of the gripping device from the load cell upon full strand rupture, as shown in Figure 3.19. Tested specimens are shown in Figure 3.20.

Figure 3.19: Strand rupture @ stress ≥ 270 ksi

Figure 3.20: Specimens set#1 strand rupture

3.3.3.2   Pretensioned Specimens Set#2

Second set of pretensioned specimens were designed to conduct pullout test. Four 4 ft. specimens were poured. Transverse reinforcement of 3#3 ties was used. All specimens were designed to fail by strand gradual or abrupt slippage. Similar concrete mix, as shown in Table 3.2 was used in strand pouring. Strands were released at concrete strength of 6 ksi, and pullout tests were conducted when concrete strength reached to 8 ksi. The main objective of this set of testing was to check how conservative are set#1 specimen. Specimens' details are shown in Figure 3.21, and test results are shown in Table 3.3.
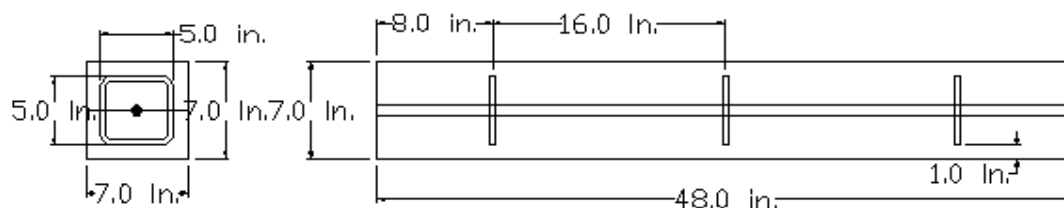
1-L5-A, B, C, D, and E specimens

Figure 3.21: Set#2 pullout specimens

Table 3.3: Pullout test results (specimens set #2)

Specimen	Number of Ties	Ultimate Load (kips)	Stress at failure (ksi)	Type of Failure
2-L4-A	3	81.5	277.2	Rupture durig gradual slippage
2-L4-B	3	74.9	255.4	Gradual slippage
2-L4-C	3	72.6	246.9	Gradual slippage
2-L4-D	3	73.1	248.6	Gradual slippage

Gradual slippage was achieved on the 4 tested specimens. In specimen 2-L4-A, the maximum load achieved was higher than the strand ultimate capacity. Thus, the gradual slippage was associated with rupture of the strand. While the maximum loads achieved at other strands slippage was less than strand ultimate strength. Thus, the test was halted without strand rupture, as no more load was resisted by the strand. The gradual slippage of strands at pullout load less than its ultimate capacity indicates that the amount of confining steel is insufficient to develop the strand. Hence, the amount of confining steel

calculated by the presented shear friction principal is necessary for 0.7 in. strands development. Figure 3.22 shows a comparison between the pullout force at strand slippage and the strand ultimate capacity as required by ASTM A416.
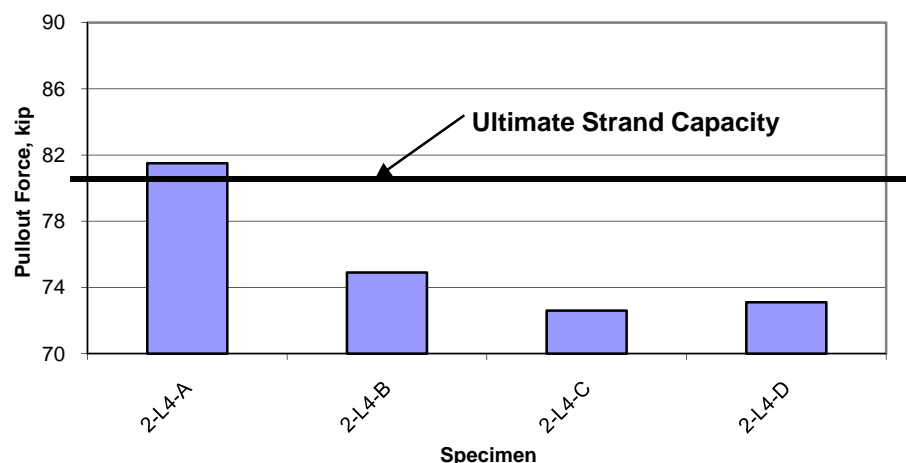
Figure 3.22: Pullout test results vs. strand ultimate strength (according to ASTM A416)

3.3.3.3   Non-Pretensioned Specimens Pullout Test

A set of non-pretensioned specimens were fabricated for pullout tests, as shown in Figure 3.23. The target of performing the pullout test on non-pretensioned specimens was to investigate the effect of strand wedging "Hoyer" effect on the strand-concrete bond. A set of four 7 in* 7in prismatic specimens, with 4 ft length, and 5 #3 ties were tested. All 4 tests were halted due to gradual strand slippage at a load value less than the strand ultimate strength. The pullout test results are shown in Table 3.4. The average pullout force for the tested specimens were 70.5 kips. This pullout force is less than the ultimate strength of the 0.7 in. strands, as shown in Figure 3.24.
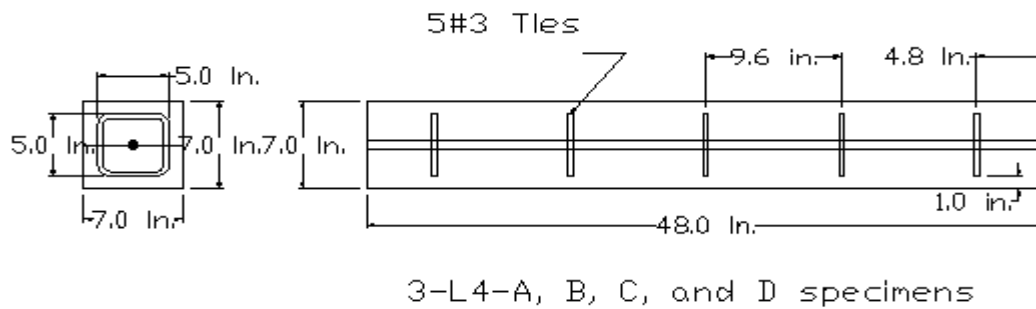
Figure 3.23: Set#3 pullout specimens

Table 3.4: Pullout test results (non-prestressed specimens)

Specimen	Number of Ties	Ultimate Load (kips)	Stress at failure (ksi)	Type of Failure
3-L4-A	5	73.1	248.6	Gradual slippage
3-L4-B	5	68.4	232.7	Gradual slippage
3-L4-C	5	72.8	247.6	Gradual slippage
3-L4-D	5	67.6	229.9	Gradual slippage
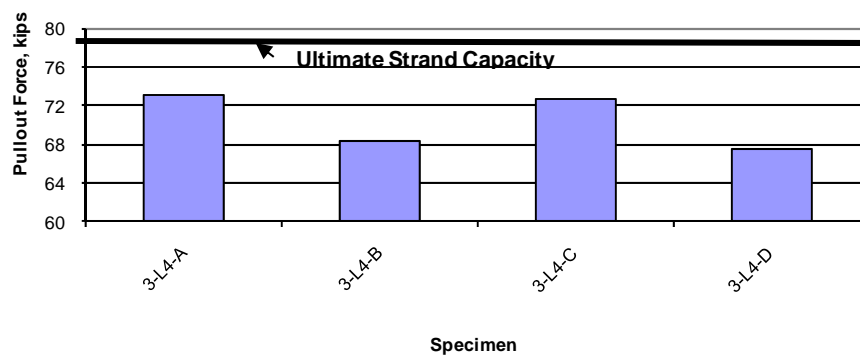
Figure 3.24: Pullout test results of non-prestressed specimens vs. strand ultimate strength

3.3.4 Statistical Analysis for Pullout Test Results

Table 3.5 presents a statistical analysis for the pullout test results of different sets of specimens.

Table 3.5: Statistical analysis of pullout test results

Specimen	Number of Ties	Ult. Load (kips)	Ult. Stress (kips)	Failure Mode
1-L4-A	5 # 3	81.9	279	Rupture
1-L4-B	5 # 3	81.9	279	Rupture
1-L4-C	5 # 3	78.7	268	Rupture
1-L4-D	5 # 3	81.7	278	Rupture
1-L5-A	5 # 3	81.7	278	Rupture
1-L5-B	5 # 3	86.5	294	Rupture
1-L5-C	5 # 3	86.6	295	Rupture
1-L5-D	5 # 3	79.1	269	Rupture
1-L5-E	5 # 3	78.7	268	Rupture
1-L6-A	5 # 3	86.7	295	Rupture
1-L6-B	5 # 3	80.2	273.8	Rupture
1-L6-C	5 # 3	84.1	286	Rupture
1-L6-D	5 # 3	88.0	299	Rupture
	Mean Value	82.8	281.7	
	Standard dev.	3.3	11.0	
	C.O.V.	**0.039**		
2-L4-A	3#3	81.5	277.2	Slip + Rupture
2-L4-B	3#3	74.9	255.4	Gradual Slip.
2-L4-C	3#3	72.6	246.9	Gradual Slip.
2-L4-D	3#3	73.1	248.6	Gradual Slip.
	Mean Value	75.5	257	
	Standard dev.	4.1	13.9	
	C.O.V.	**0.054**		
3-L4-A	5#3	73.1	248.6	Gradual Slip.
3-L4-B	5#3	68.4	232.7	Gradual Slip.
3-L4-C	5#3	72.8	247.6	Gradual Slip.
3-L4-D	5#3	67.6	229.9	Gradual Slip.
	Mean Value	70.5	239.7	
	Standard dev.	2.9	9.8	
	C.O.V.	**0.041**		

3.3.5   Comparison of Different Pullout Test Results

The pullout tests included in this research program included two similar sets of 4 ft specimens confined with 5 #3 ties. First set was fabricated using a pretensioned 0.7 in. strand. The pullout test results of this set are shown in Figure 3.18 (Specimens 1-L4-A, 1-L4-B, 1-L4-C, and 1-L4-D). The second set was fabricated using a non-prestressed 0.7 in. strand. The pullout test results of this set are shown in Figure 3.24 (Specimens 3-L4-A, 3-L4-B, 3-L4-C, and 3-L4-D). While the non-prestressed specimens failed due to gradual strand slippage at an average pullout force of 70.5 kips, the pretensioned specimens-using similar confinement- failed due to strand rupture at an average pullout force of 81.05 kips. The comparison of the two pullout tests is shown in Figure 3.25
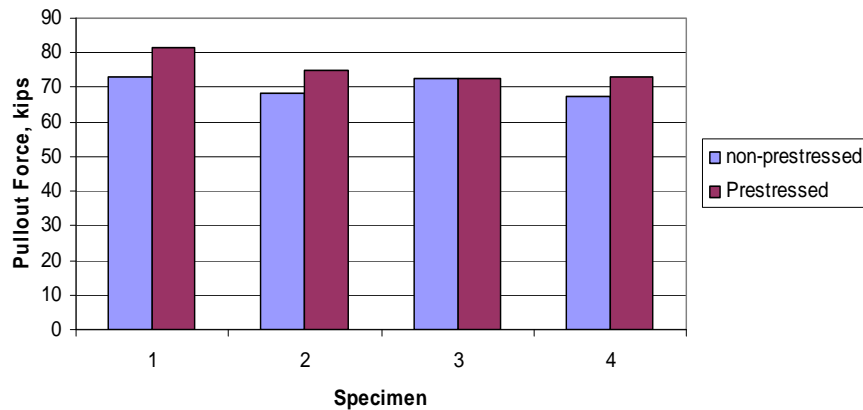
Figure 3.25: Pullout force of prestressed vs. non-prestressed specimens (at failure)

According to test results shown in Figure 3.24, the following conclusions were achieved:

1.   Prestressed specimens pullout tests are required for development length testing. while the prestressed specimens failed in rupture at an average load of 81.05 kips, indicating full strand development, similar specimens,

fabricated with non-prestressed strands, failed by gradual slippage, indicating bond failure.

2. The value of friction co-efficient of 1.4 used for confinement calculation is fulfilled for prestressed specimens, which simulates the practice in precast/prestressed concrete industry.

3.4 Transfer Length

3.4.1 Specimen Fabrication

Four 8 ft. specimens were used for transfer length calculations. The specimens had a square section of 7 in side. The confinement used was #3 bars placed at 3, 6, 9, and 12 in. spacing respectively. Specimen preparation for transfer length measurement started by stripping the form sides 24 hour after the concrete was poured. DEMEC discs was placed at the level of the centroid of the prestressing strand. The first disc was placed 2 in. from the end of the specimen. Subsequent discs were placed at intervals of 4 in. along the specimen two sides. A fast setting epoxy was used to bond the DEMEC discs to the concrete surface. Once the 8 lines of DEMEC discs were bonded to the specimens (2 lines * 4 specimens), readings were performed and recorded by using the DEMEC gauge, as shown in Figure 3.26. Details of transfer length specimens is shown in Figure 3.27

Figure 3.26: Performing a measurement using a DEMEC gauge
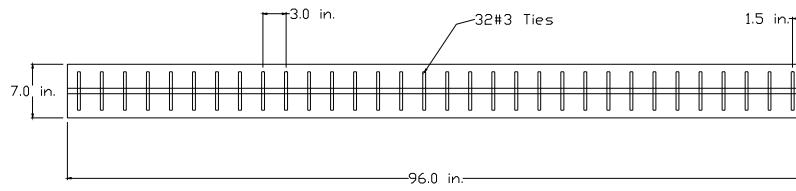
Specimen 1-L8-3
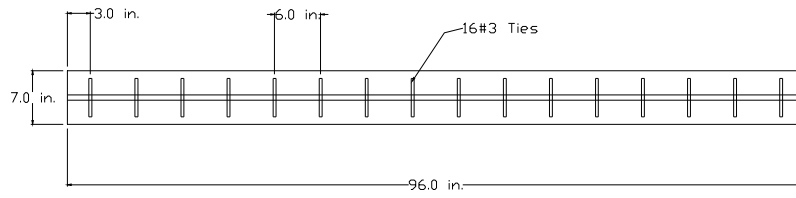
Specimen 1-L8-6
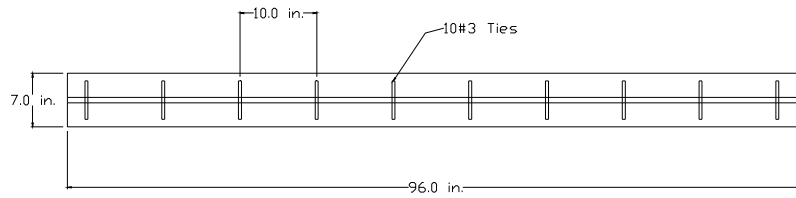
Specimen 1-L8-9
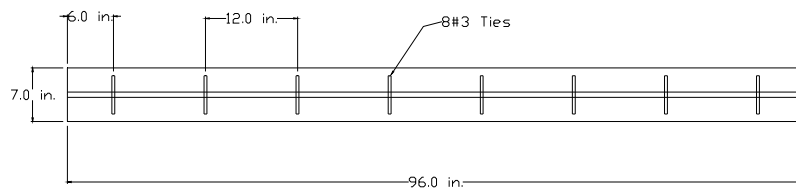
Specimen 1-L8-12

Figure 3.27: Transfer length specimens

3.4.2 Application of Prestress and Surface Strain Measurement

Once all the DEMEC measurement were taken and recorded. Prestressing strands are released. A flame-cutting process was used to cut the strands between consequetive specimens in the prestressing bed. DEMEC measurements were immediately taken after the strands were released. DEMEC measurements were taken and recorded at ages of 1, 3, 7, 14, and 28 days to calculate the surface strain. Hence, the transfer length of 0.7 in. prestressing strand at different ages. Specimens used in transfer length measurement and their confinement details are shown in Table 3.6

Table 3.6: Transfer length specimens details

Specimen	Length	Confinement	Number of Ties
1-L8-3	8 ft.	#3 @ 3 in.	32
1-L8-6	8 ft.	#3 @ 6 in.	16
1-L8-9	8 ft.	#3 @ 9 in.	10
1-L8-12	8 ft.	#3 @ 12 in.	8

3.4.3 Construction of Surface Compressive Strain Profile

Each of the specimens shown in Table 3.6 has DEMEC discs bonded to its two sides. For every specimen side, there is a live end and a dead end. This resulted in 4 transfer length estimations per specimens (2 live-end readings and 2 dead-end readings). The compressive strain for each measured 8 in. in. interval was calculated by multiplying the DEMEC gauge factor by the difference between the 1) The reading recorded at the time interval under investigation, and 2) The DEMEC gauge reading prior to the strand release of this specimen.

The transfer length was calculated by the 95% Average Maximum Strain (AMS) method, as noted by Girgis and Tuan (2005). Once the strain profile for the transfer zone was drawn, the strain values that lay in the strain profile plateau were identified, and the value of the average maximum strain was calculated using the arithmetic mean of these values. According to the 95% AMS method, the value of the transfer length at any time is identified by the distance of the point where the compressive strain profile intersects the horizontal line representing the 95% of the average maximum strain. The results of the four specimens are explained as follows:

- **Specimen 1-L8-3**

Specimen 1-L8-3 had a length of 8 ft, and confined by #3 bars at 3 in. spacing. The strain profile for specimen 1-L8-3 was measured by DEMEC gauge at different ages as shown in Figure 3.28, and Figure 3.29
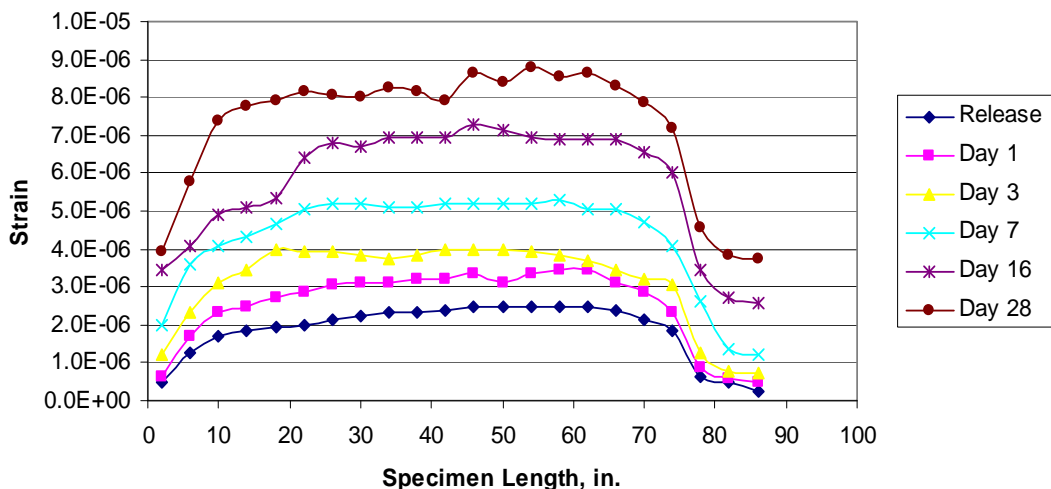
Figure 3.28: Strain profile for specimen 1-L8-3 side (1)
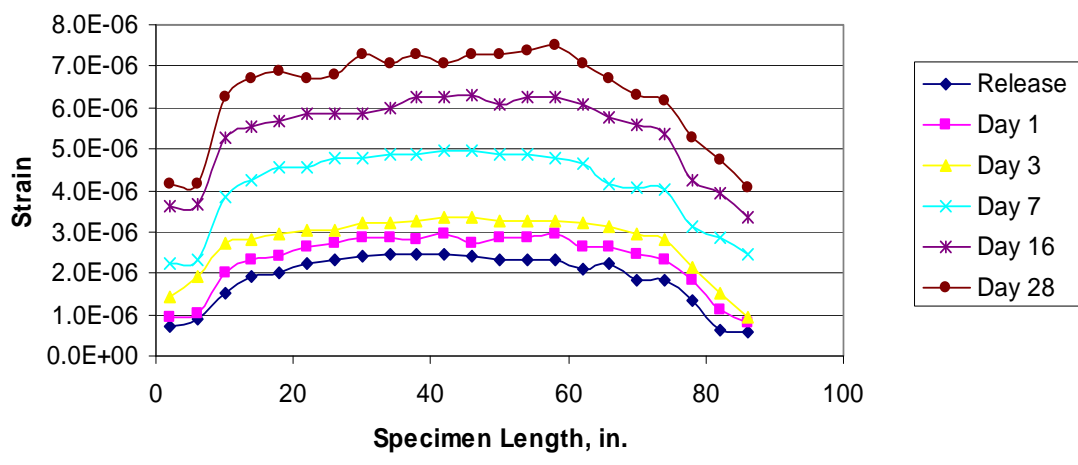
Figure 3.29: Strain profile for specimen 1-L8-3 side (2)

- **Specimen 1-L8-6**

Specimen 1-L8-6 had a length of 8 ft, and confined by #3 bars at 6 in. spacing. The strain

profile for specimen 1-L8-6 was measured by DEMEC gauge at different ages as shown

in Figure 3.30, and Figure 3.31
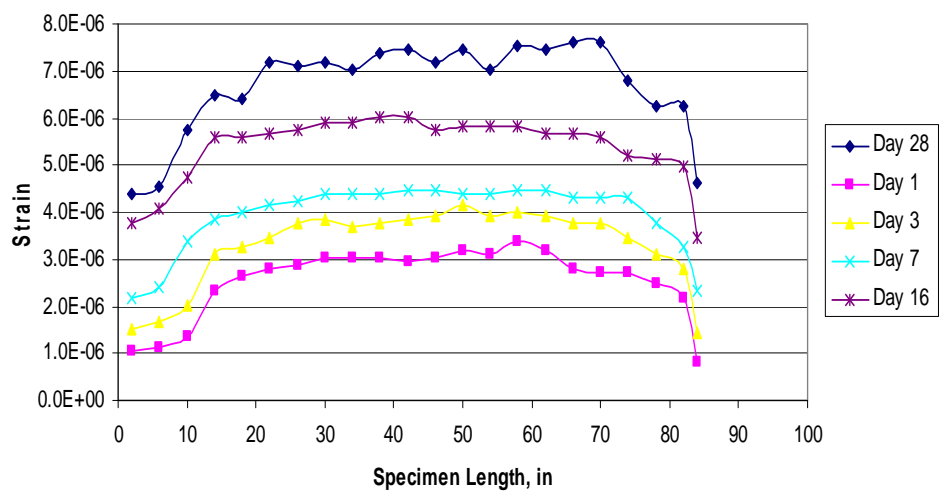
Figure 3.30: Strain profile for specimen 1-L8-6 side (1)
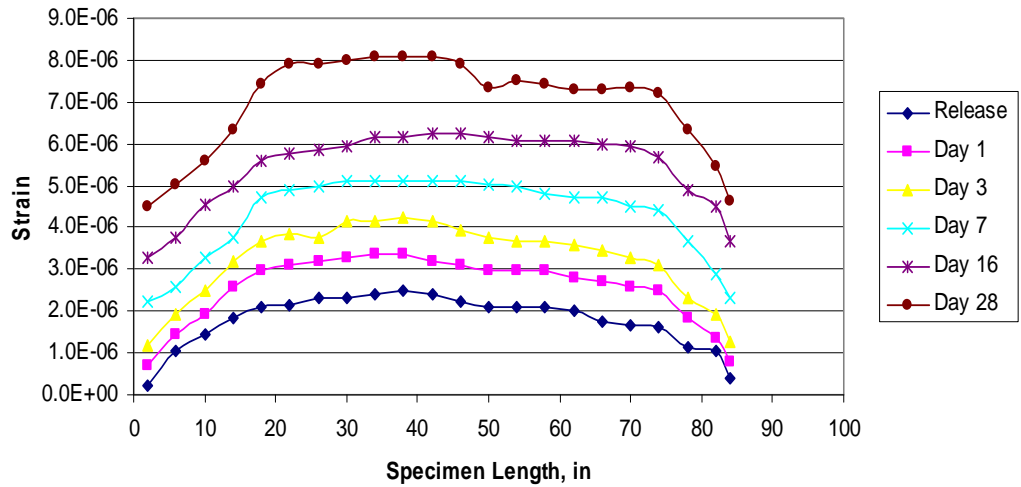
Figure 3.31: Strain profile for specimen 1-L8-6 side (2)

- Specimen 1-L8-9

Specimen 1-L8-9 had a length of 8 ft, and confined by #3 bars at 9 in. spacing. The strain

profile for specimen 1-L8-9 was measured by DEMEC gauge at different ages as shown

in Figure 3.32, and Figure 3.33
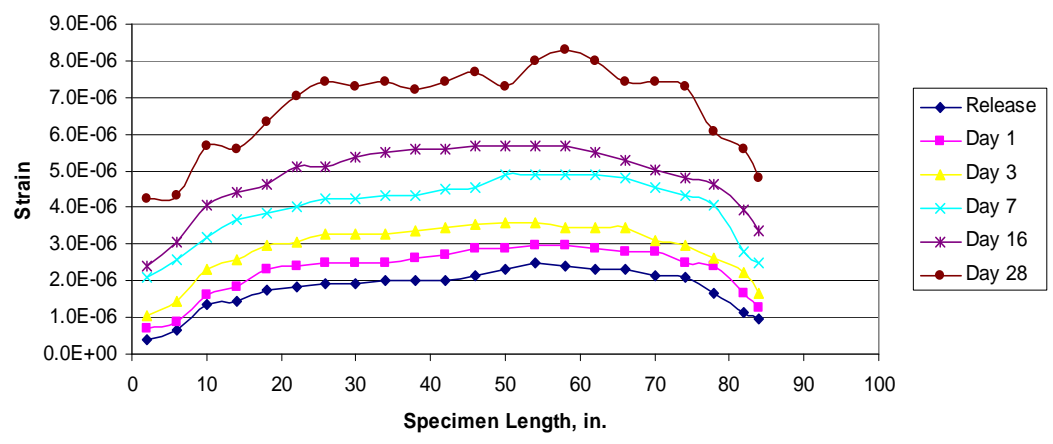
Figure 3.32: Strain profile for specimen 1-L8-9 side (1)
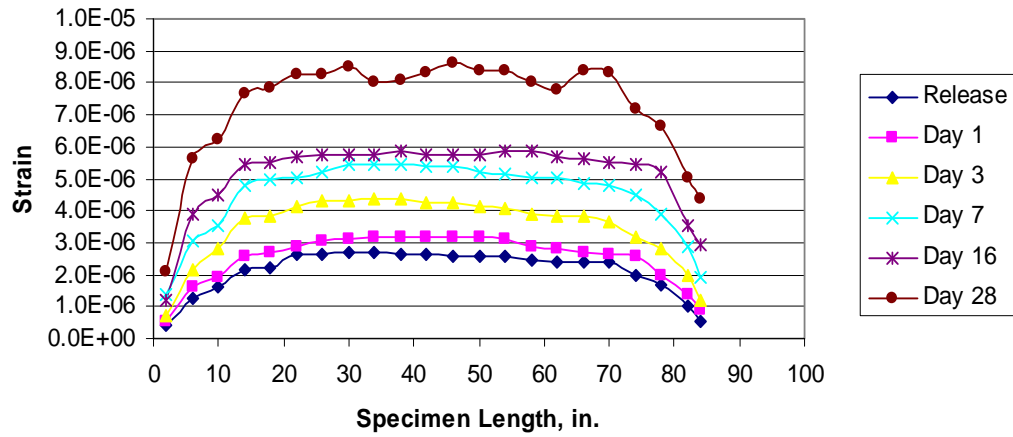
Figure 3.33: Strain profile for specimen 1-L8-9 side (2)

- Specimen 1-L8-12

Specimen 1-L8-12 had a length of 8 ft, and confined by #3 bars at 12 in. spacing. The strain profile for specimen 1-L8-12 was measured by DEMEC gauge at different ages as shown in Figure 3.34, and Figure 3.35
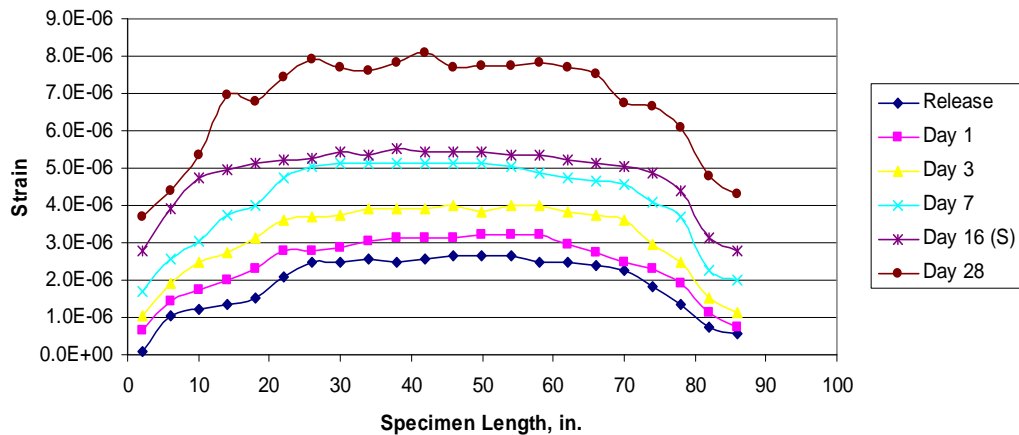
Figure 3.34: Strain profile for specimen 1-L8-12 side (1)
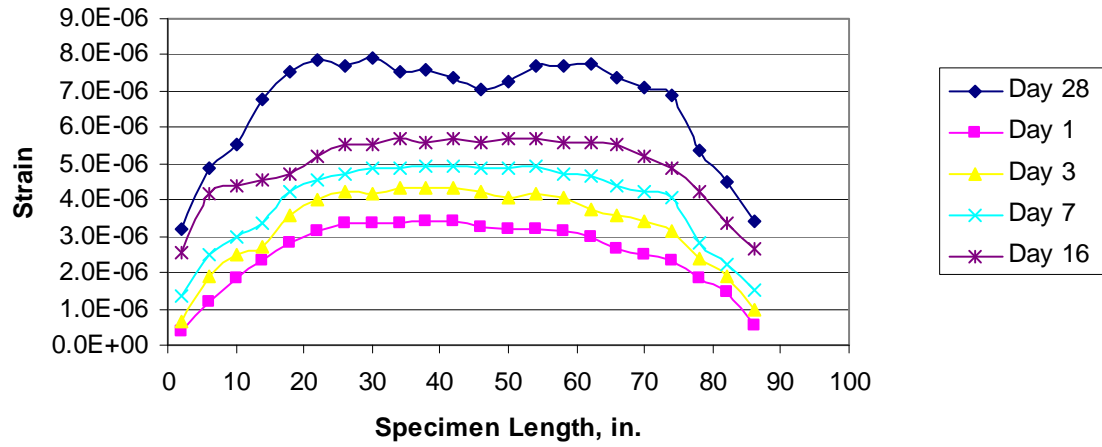
Figure 3.35: Strain profile for specimen 1-L8-12 side (2)

3.4.4 Transfer Length Measurement Results

Each of the afore-mentioned specimens had 4 transfer zone readings. The live-end transfer length for different specimens at age of 28-day is shown in Table 3.7.

Table 3.7: Live-end transfer length of specimens

Specimens	Side 1	Side 2
1-L8-3	29	28
1-L8-6	30	30
1-L8-9	31	32
1-L8-12	34	34
Average	**31**	**31**

Similarly, the transfer length for the specimens dead-end at age of 28-day is shown in Table 3.8

Table 3.8: Dead-end transfer length of specimens

Specimens	Side 1	Side 2
1-L8-3	28	28
1-L8-6	29	30
1-L8-9	31	30
1-L8-12	34	34
Average	**30.5**	**30.5**

The measured transfer length values well compares to the transfer length measured for the NU900 girder tested by Reiser (2007). This NU girder had 19 DEMEC discs placed every 4 in., starting 1 in. from the girder ends. The resulting transfer length was 35 in., as shown in Figure 3.36
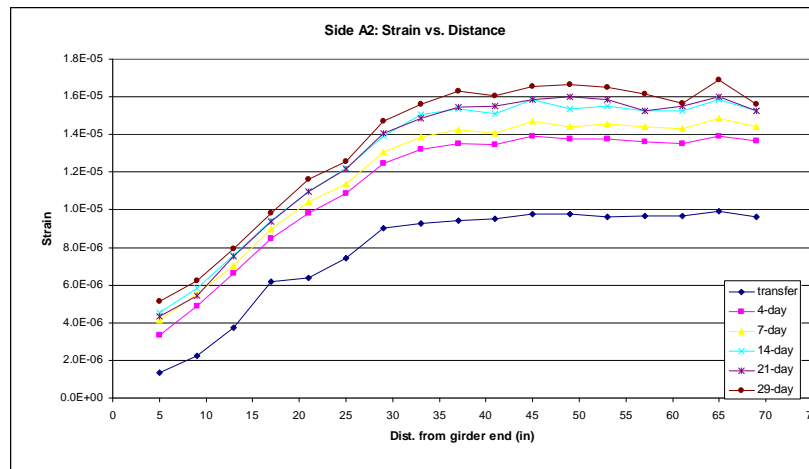
Figure 3.36: Transfer length measurement for NU900 fabricated with 0.7 in. prestressing strands (Reiser, 2007)

The dead end vs. live end transfer length for specimens is shown in Figure 3.37, and Figure 3.38. The dead end transfer length measures equal or less than the live end, since the prestressing force is applied in a more direct manner on the live end. The faster application of force on live end results in a larger transfer length.
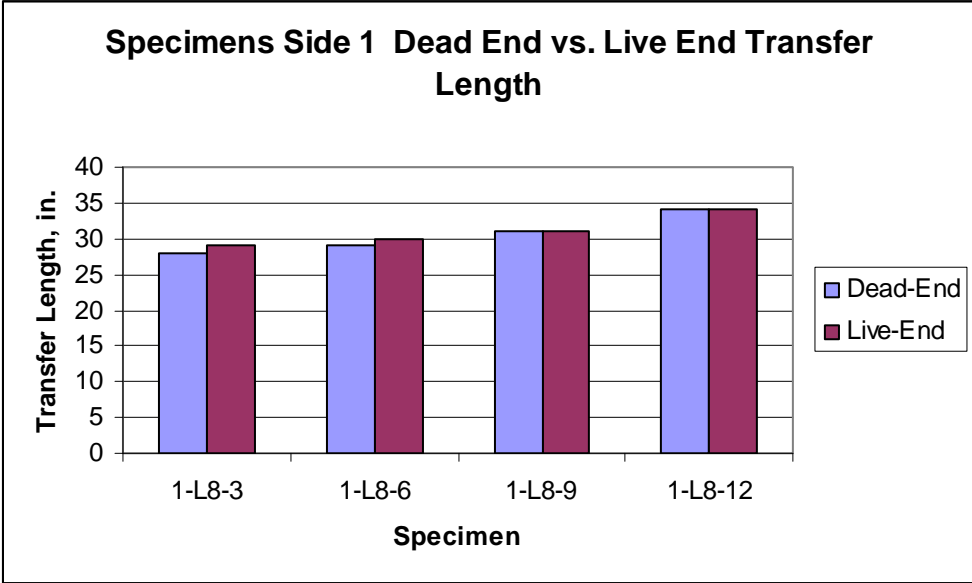
Figure 3.37: Specimens dead end vs. live end transfer length (side 1)

Figure 3.38: Specimens dead end vs. live end transfer length (side 2)

3.4.5   Transfer Length Conclusions

The following conclusions were made based on the results of transfer length testing:

1. Measured transfer length for pretensioned prisms compared well with the full scale testing done and reported by Reiser (2007).

2. The value of the transfer length measured on different days showed a slight increase in transfer length value along the time.

3. The transfer length values measured for different levels of confinement were less than the AASHTO LRFD specification estimated value (transfer length = 60 d_b)

4. Transfer length measured at the specimen dead end was slightly less than the live end transfer length. As previously mentioned, this is mainly due to the faster prestressing transfer that happens at the live end, which results in longer transfer length.

Chapter 4

Developing High-Strength Concrete for Precast/Prestressed Bridge Girders

4.1 Introduction

UHPC is a new class of concrete that has been developed in France in the 1990's. When compared with other types of concrete, UHPC shows superior material properties as high early strength, higher tensile and compressive strength, durability, and higher resistance to shrinkage, creep, and hard environmental conditions.

Standards and specifications for UHPC are set by different scientific societies in Europe and Japan. The Japan Society of Civil Engineers (JSCE*) Recommendations for design and construction of Ultra-High Strength Fiber Reinforced Concrete Structures (draft)* (2006) defines the UHPC as a type of cementitious composite reinforced by fibers with characteristic values in excess of 150 N/mm^2 (21.7 ksi) in compressive strength, 5 N/mm^2 (0.73 ksi) in tensile strength, and 4 N/mm^2 (0.58 ksi) in first cracking strength. The UHPC matrix should be composed of aggregates; whose maximum particle size is less than 2.5 mm, cement and pozzolans, and water-to-powder ratio is less than 0.24. UHPC contains random reinforcing steel fibers of more than 2% (by volume), whose tensile strength exceeds 2 x 10^3 N/mm^2 (290 ksi), and ranges from 10 to 20 mm in length and 0.1 to 0.25 mm in diameter. The Association Francaise de Genie Civil (AFGC) *Interim Recommendations for Ultra-High Performance Fibre-Reinforced Concrete (2002)* defines the UHPC as a material with a cement matrix and a characteristic compressive

strength in excess of 150 MPa (21.7 ksi), and containing steel fibers in order to achieve ductile behavior.

According to the AFGC, the following are the main differences between UHPC and other types of concrete:

- Higher compressive strength.

- Incorporation of random steel fibers in the mix, which ensures the non-brittle mix behavior, and alters the conventional requirement for passive and/or active reinforcement.

- High binder content and special selection of aggregates.

Different UHPC proprietary mixes are available in the international markets with standard characteristics. Example of the proprietary mixes are BSI "Beton Special Industrial" (Special Industrial Concrete) developed be Eiffage, Cemtec by LCPC, and different kinds of Ductal concrete resulting from a joint research by Bouygues, Lafarge, and Rhodia. Ductal concrete marketed by Lafarge and Bouygues is the only proprietary UHPC mix available in the US market. Therefore, the mix constituents and material properties of Ductal are used to represent proprietary UHPC mix constituents and properties throughout this report.

4.2 UHPC Mix Constituents

The UHPC mix constituents are proportioned to achieve an optimized packing order by reducing the voids ratio of the granular mixture. The largest granular material available in UHPC mix is fine sand, with a particle size ranging from 150 to 600 μm. Cement

particles have the second largest size in the mix, with a nominal size of 15 μm, and quartz flour with a nominal size of 10 μm. Silica fume (micro silica) is the smallest particle within the UHPC mix, with a diameter of 1 μm, sufficient to fill the voids among the mix constituents.

Random steel fibers are added to the UHPC mix to ensure its ductile behavior and increase the tensile strength of the mix. Fibers are the largest constituent, with a nominal diameter of 0.008 in. and a length of 0.5 in. Its average modulus of elasticity is 29,800 ksi, and the average ultimate strength is 474 ksi. A typical UHPC mix composition is shown in Table 4.1

Table 4.1: UHPC mix composition (Publication No. FHWA-HRT-06-103)

Material	Amount (lb/yd^3)	Percent by weight
Portland Cement	1200	28.5
Fine Sand	1720	40.8
Silica Fume	390	9.3
Ground Quartz	355	8.4
Super-plasticizer	51.8	1.2
Accelerator	50.5	1.2
Steel Fibers	263	6.2

4.3 UHPC Material Properties

The material properties of UHPC proprietary mix were studied through different research programs around the world. Markesat (2002) studied the application of UHPC in

protective structures. Acker (2004) explained the reasons behind the low shrinkage and creep of UHPC. Zakariasen and Perry (2004) introduced the design, prototyping, and manufacturing of panels and boxes using UHPC. Graybeal (2007) introduced a study of the compression behavior of the UHPC. The contribution of steel fibers to the performance of the UHPC mix was extensively considered, due to the high cost of fibers. Steel fibers have a material cost of $400 per cubic yard. This represents 40% of the final material cost of UHPC mix. Relevant studies considering random steel fiber are shown in the following section:

4.3.1 Permeability of Cracked Concrete by Rapoport et al.

Rapaport et al. (2002) conducted a research to investigate the permeability of UHPC mixes as compared to standard mixes. The researchers intentionally induced cracks of up to 500 microns (0.02 in.) using splitting tension test (Brazilian test) in specimens made of standard concrete mixes and UHPC mixes with 0.5 to 1.0 percent (by volume) of steel fiber reinforcement. Two major conclusions were drawn from this research. First, the steel fibers transformed the wider cracks to a larger number of small width cracks, which reduces the permeability of concrete. This positive behavior of steel fibers was noticed in sections having original cracks larger than 100 microns. Second, the steel fibers had no positive impact on reducing the permeability of concrete with initial cracks below 100 microns.

4.3.2 Strand Development by Steinberg and Lubbers

Steinberg and Lubbers (2003) completed a study at Ohio State University of the force transfer behavior of prestressing strands into UHPC and regular concrete mixes. In this

research, standard and oversized 0.5 inch diameter 270 ksi low relaxation prestressing strands where embedded in concrete blocks made by regular and UHPC mixes. Embedment lengths of 12, 18, and 24 inches were tested, and pullout tests were done for all specimens. Tests resulted in strand rupture without any significant slippage. This indicated that the development length of this type of prestressing strands in UHPC is less than 12 inches

4.3.3 Fiber Orientation Effect on Mechanical Properties by Stiel et al.

The effect of fiber orientation on the mechanical properties of UHPC was investigated by Stiel et al (2004). The researchers used a patented UHPC mix marketed under the name CARDIFRC®. The material properties of this UHPC mix is similar to Ductal. The mix constituents are similar, with the exception of using two steel fiber lengths and a total fiber volumetric percentage of 6%.

This research program focused on the effect of UHPC flow direction during casting on the compressive and flexural behavior of the concrete. It was noticed that random steel fibers tend to align with the direction of mix flow. Thus, the tensile and compressive behaviors of UHPC were investigated when loaded parallel to and perpendicular to the direction of flow. Cubes of 100 mm side dimensions were used as specimens for compression tests, and 100 mm x 100 mm prisms with 500 mm length were used to test for flexure using three-point loading flexure tests. The results of cube compression testing indicated that the orientation of fibers had no significant effect on the final compressive strength of the mix. However, the three-point loading flexure tests showed

that the flexural strength of the UHPC prisms was decreased to less than 35% of its value, when fibers were aligned perpendicular to the direction of the flexure tensile forces. In addition, the post-cracking toughness behavior associated with UHPC was not displayed by the prisms. These research findings pointed to the importance of following the correct placement techniques of UHPC mix, according to the expected structural loading directions that will be carried by the member.

4.3.4 HPC and UHPC Static and Fatigue Behavior in Bending by LaPPa et al.

Researchers at Delft University of Technology, Netherlands, (Lappa et al, 2007) conducted research to evaluate the bending behavior of high and ultra-high strength concrete mixes. The research included the selection of different HPC and UHPC mixes, with different strengths and fiber content. 750 mm (2.5 ft) span beams were tested in flexure, loaded at third points for static bending tests, followed by a number of fatigue bending tests. The results of the fatigue testing showed that the higher workability that existed in the case of self-compacting concrete, improves the homogeneity of the fiber distribution and alignment within the mix. This increases the consistency of the concrete behavior under fatigue loading.

4.4 Relevant Girder Testing Research Programs

4.4.1 AAHTO Type II Girders by Tawfiq

The Florida Department of Transportation (FDOT) sponsored a research to investigate the shear capacity performance of HSC bridge girders. In this research program, Tawfiq (1995, 1996) studied the shear capacity of AASHTO Type II girders. Six girders were

precast with concrete strength of 8, 10, and 12 ksi. The flexure reinforcement included 16 strands at the bottom flange and 2 at the top flange. Tested girder had a composite deck of 8 in. x 42 in. Shear reinforcement included two #4 stirrups spaced every 6 in. for the first 4 ft., two #4 stirrups every 8 in. for the next 4 ft, and single #4 stirrups at 8 in. and 12 in. spacing. The average shear capacity exhibited by the girder were 270 kips. .

4.4.2 AASHTO Type II Girders by Hartman and Graybeal

The ongoing research at Federal Highway Administration's Turner-Fairbank Highway Research Center (TFHRC) in Mclean, Virginia, is studying the advantages of using UHPC in highway bridges. The current research at the TFHRC focuses on Ductal as the only patented UHPC mix in the United States. The economic feasibility of fabricating UHPC bridge girders was checked. Then, the behavior of girders under shear and flexure loading is investigated through a series of testing. The last phase of the research includes analytical work to optimize the design of bridge girder/deck combination (Graybeal et al. 2004).

4.4.2.1 UHPC Girder Flexure Testing

AASHTO type II girder was fabricated using UHPC to be tested in flexure at the FHWA TFHRC. The cross-section of the AASHTO girder is 36 inch deep, 12 inch wide top flange, and 18 inch bottom flange. The girder web is 15 inch deep and 6 inch thick. The total length of the girder was 80 ft, and prestressed by twenty-four half-inch diameter low-relaxation strands at the bottom flange, and two similar strands at the top. The cross-section of the girder is shown in Figure 4.1
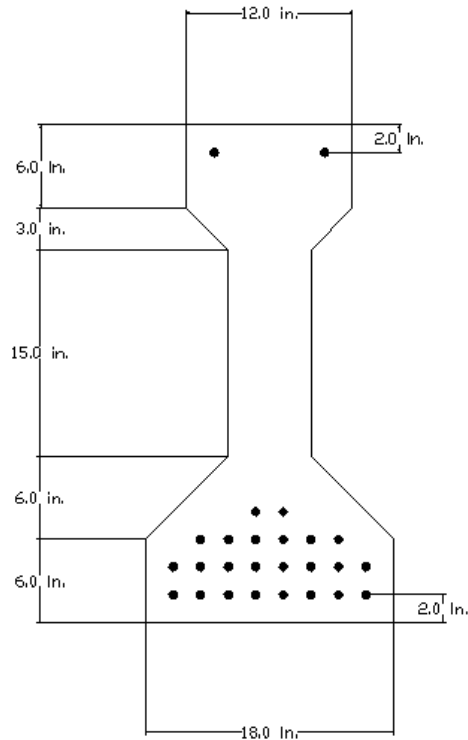
Figure 4.1: AASHTO Type II Girder (Publication No. FHWA-HRT-06-115)

The girder was supported by rollers at a distance of 9 inch from the girder both ends allowing the girder free rotation and axial displacement. The girder was loaded symmetrically by a two-point load each located 3 ft from the girder mid-span. The load vs. deflection is plotted for the girder. The deflection response shows that the girder started to soften at an applied load between 310 and 355 KN (70 and 80 kips), corresponding to a deflection of 75 mm (3 inches). The girder showed additional capacity, where a peak-load of 790 KN (178 kip) was reached at a deflection of 470 mm (18.5 inches). The girder was split into two smaller girders of spans 28 ft and 24 ft to be used in shear testing. Figure 4.2 shows the girder directly after the flexure failure.

Figure 4.2: Girder failure (Publication No. FHWA-HRT-06-115)

4.4.2.2 UHPC Girder Shear Testing

Three UHPC AASHTO Type II girders were tested to investigate their shear behavior. Tested girders had overall spans of 28 ft, 24 ft, and 14 ft. The girders were denoted as 28S, 24S, and 14 S respectively. The following represents the girders testing results:

Girder 28S: The girder 28S was a part of the 80 ft span AASHTO Type II girder tested in flexure, with an overall span of 28 ft. and a shear span of 6.5 ft. This results in a shear span-to-depth ratio of 2.17. During the test, the girder began to soften at a load of 1,110 KN (250 kips). Additional shear capacity was displayed by the shear girder, where a peak load of 2,220 KN (500 kips) were achieved. At this load, the shear load carried by the girder was 1,710 KN (384 kips).

Girder 24S: The second shear test was completed using the girder 24S, which represents the other part of the 80 ft. AASHTO Type II girder tested in flexure. This girder had an overall span of 24 ft and a shear span of 2.29 m (7.5 ft). This results in a shear span-to-

depth ratio of 2.5. During the test, the girder started to soften at a load between 1,330 and 1,780 KN (300 and 400 kips). However, a significant load capacity reserve was displayed, where a peak load of 3,250 KN (731 kips) was reached. This load resulted in a shear force of 2,230 KN (502 kips).

Girder 14S: The third shear test was completed using the girder 14S. The girder had an overall span of 14 ft and a shear span of 6 ft. This resulted in a shear span-to-depth ratio of 2.0. The girder began to show a softening behavior at a load between 2,000 and 2,220 KN (450 and 500 kips). The girder displayed a significant shear capacity beyond this point, and peak-load of 3,410 KN (766 kips) was achieved.. The shear load at this load was 1,950 KN (438 kips). The prediction of the shear behavior of the tested UHPC girders was attempted by using standard structural design procedures. However, the current design codes under-estimated the correct values of the girders shear capacity. This is attributed to the existence of random steel fiber reinforcement which added extra strength to the girder beyond cracking.

4.4.3 Shear Capacity of UHPC I-Shape Girders by Hegger

Hegger et al. (2004) completed several tests investigating the shear capacity of UHPC I-shape prestressed beams. The tested I-beams were precast using UHPC proprietary mix, with 2.5% (by volume) random steel fiber content, and no mild steel for shear reinforcement. The beam had 11.5 in. (292 mm) wide bottom flange, 8.7 in. (221 mm) wide top flange, 2.8 in. (71 mm) wide web, and overall length of 11.5 ft (3.5 m). The bottom flange was reinforced with eight 7-wire strands, 0.6 in. (15.2 mm) prestressing

strands. According to their research findings, the average ultimate shear capacity of these beams was 61.4 kips (273 kN). The average tensile stress across the shear failure plane was approximately 2 ksi (14 MPa). Given the small size of the tested I-beams, the research findings were very similar to the results of testing AASHTO Type II girders, reported by Graybeal et al (2004).

4.4.4 UHPC Girder Optimization

The flexure and shear tests results of the AASHTO Type II girders indicated that the UHPC behavior could be effectively used in the design and construction of highway bridge girders. However, the AASHTO Type II section did not display any significant advantage as a cross-section. Thus, optimization of bridge girders cross-section was required for exploiting the advantages of UHPC in bridge construction. Park et al. (2003) developed an optimized PI-shape girder/deck combination for a 21 to 30 m span range. Developed girder/deck combination has no mild steel reinforcement. The deck is 75 mm thick and 2.4 m wide, the girder webs thickness ranges from 64 to 76 mm thick. Pi-girder bridge is constructed at the TFHRC for full-scale testing, as shown in Figure 4.3.

Figure 4.3: Pi-girder bridge at TFHRC

Four optimized girders were produced and transported to the TFHRC. Two girders were used to construct a one lane highway bridge for testing purpose; the other two girders are to be destructively tested. Graybeal and Hartmann (2005) highlighted the advantages of the optimized UHPC girder during construction, a short time frame with two 54000 kg capacity cranes were used in the to place two girders in one hour.

Based on the Turner-Fairbank Pi-girders testing (Figure 4.4), the 3 inch thick deck did not satisfy the lateral test requirement for a service loading of 16 kips and an impact factor of 33% (Keierleber et al., 2007).

Figure 4.4: Pi-girder testing at TFHRC (Keierleber et al.)

The office of bridges and structures at the Iowa DOT analyzed several alternatives to solve the afore-mentioned problem. Finite element analysis for the optimized section, done by the Iowa DOT and checked by the Iowa State University, resulted in introducing

an alternative Pi-girder section with 4 inch thickness and later post tensioning, using either 5/8 inch high strength rod or 0.6 inch diameter prestressing strands.

4.5 Development of Economic High Strength Concrete Mixes

4.5.1 HSC Mix by Ma and Schneider

Ma and Schneider (2002) conducted a research program investigating the effect of optimizing the mix powder content on the concrete strength and flowing ability. In their research, the cement was stepwise replaced by fine particles of quartz flour with similar volume. A percentage of cement was replaced by quartz flour up to 30% without decreasing the mix compressive strength. Moreover, the cement replacement resulted in a more flowable mix, where the slump increased from 510 mm (20 inches) to 620 mm (24.4 inches). These results indicated that the low water-to-powder ratio in the HSC mixes lead to the existence of un-hydrated cement particles which lie in the matrix as fine aggregates. The replacement of the un-hydrated cement particles did not affect the mix strength. In addition, the finer quartz flour particle reduced the voids in the mix and resulted in a higher flowing ability.

4.5.2 Developing Cost-Efficient Non-Proprietary HSC Mixes by Kleymann et al.

Researchers at the University of Nebraska-Lincoln (Kleymann et al., 2006) conducted a recent study to produce cost-efficient non-proprietary HSC mixes using local materials available in the State of Nebraska. The research focused on developing user-friendly mixing and quality control procedures which could be introduced to the precast/prestress concrete industry. In their study, fiber reinforcement of UHPC was eliminated and class

C fly ash was utilized in mix design. In order to achieve appropriate flowing ability for the designed mixes, a high energy Hobart food mixer was used in mixing small quantities of HSC, as shown in Figure 4.5.

Figure 4.5: Hobart food mixer – University of Nebraska Lab

Several mixes were checked to achieve the required strength with the appropriate flowing ability. An average cost of $360 per cubic yard was achieved as a result, which is approximately one third the cost of the proprietary mixes. Developed mixes are shown in Appendix B. The compressive strength of the different UHPC non-proprietary mixes vs. time is shown in Figure 4.6.

Compressive Strength vs. Time
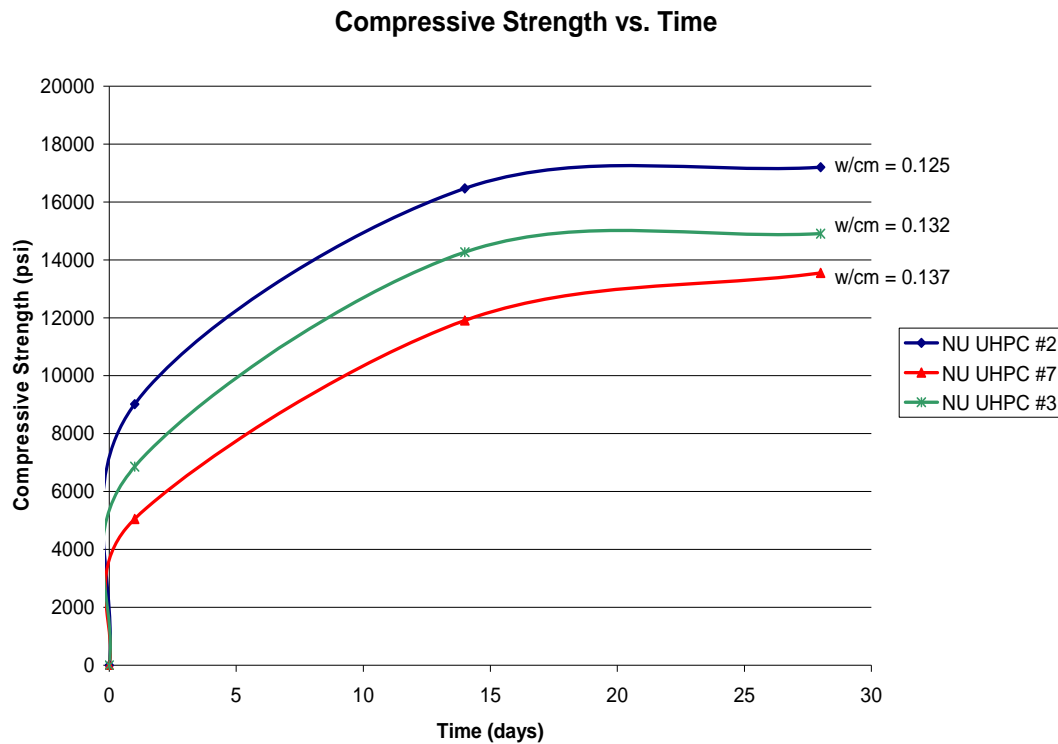
Figure 4.6: Compressive strength of developed HSC mixes (Kleymann et al., 2006)

4.5.3 Self-Consolidating Concrete Mixes for Bridges by Nowak et al.

Nowak et al. (2007) conducted an experimental research at the University of Nebraska-Lincoln to develop a practical guide for cast-in-place applications of self-consolidating concrete for bridges. The scope of the project was to develop SCC mixes using mix constituents as currently applied in precast yards in the State of Nebraska, in addition to specific SCC additives. The specific objectives of the project were:

1. Develop practical procedures for testing fresh SCC on site to determine its key properties such as filling ability, passing ability, and resistance to segregation.

2. Investigate the impact of the delivery time on the properties of fresh SCC. This investigation determines whether or not the developed SCC mixes can be used given the distance from the construction site to the ready mix plant.

As a result of the research project, SCC mixes were developed for on-site bridge applications. Mix constituents included 1PF cement, 47B sand and gravel, with a maximum aggregate size of 0.5 in., and HRWR. The reduced aggregate size helped to increase resistance to segregation and reduced the chances of voids formation. It was found that for on-site assessment of SCC mix quality, it is sufficient to perform the J-ring and slump flow tests, with visual stability index (VSI) tests. The analysis of the delivery time effect on SCC properties showed that a retarder should be used for on-site applications, and if needed, an additional amount of HRWR could be used.

Laboratory tests showed that it is possible for the mix to maintain SCC properties for up to 70 minutes. An additional dosage of HRWR could be used prior to concrete placement to recover SCC properties for mixing times greater than 70 minutes. On-site pilot tests showed that the SCC mix remains pumpable even in high temperatures.

4.5.4 Non-Proprietary HSC Mixes by Hawkins and Kuchma

Hawkins and Kuchma (2007) conducted a research at the University of Illinois at Urbana-Champaign to develop recommendations to extend the applicability of shear design provisions of the AASHTO code to concrete with compressive strength above 10 ksi. Throughout the research, non-proprietary HSC mixes were developed for testing

purpose. The HSC mixes were developed at Wiss, Janney, Elstner Associates, Inc. (WJE) using aggregate supplies from the precaster, Prestress Engineering Cooperation (PEC), and traprock aggregate available from Wisconsin. Water-to-powder ratio used was below 0.28. After several trial mixes, a concrete of compressive strength of 17.8 ksi was achieved. Detailed research findings and mixes material properties can be found in the National Cooperative Highway Research Program report no. 579. Developed mixes are shown in Appendix B.

4.6 Development of Economic Self-Consolidating HSC Mix

The high shear capacity resulted from the testing of UHPC girders at the FHWA Turner Fairbank Highway Research Center resulted in increasing interest of using UHPC in the precast/prestressed concrete industry. The interest in using UHPC by state highway agencies is impeded by the high initial cost of the proprietary UHPC mixes, which is $1000 per cubic yard, including $400 per cubic yard for the random steel fibers.

In the following sections, the development of an economical non-proprietary high strength concrete mixes is discussed. The performance of AASHTO Type II girders fabricated with the developed mix and grade 80 WWR as shear reinforcement was tested and reported in Chapter 5. Based on the research findings, the use of WWR as shear reinforcement of prestressed girders fabricated with the developed HSC mix was structurally and economically compared to the results of the FHWA girder testing program results.

4.6.1 Development of HSC Mixes

The HSC mixes were developed for precast/prestressed concrete industry. As a requirement of this industry, the following mix properties were specified:

1. Mixing time should not exceed 20 minutes. This is to follow the common practice at precast yards in the State of Nebraska, and avoid the formation of cold joints.

2. Self-consolidating concrete (SCC) flowing ability should be achieved. No specific standard is set for this definition. However, according to the current practice, an average spread diameter ranging from 22 in. to 30 in. is considered acceptable.

3. Minimum 24-hour compressive strength of 10 ksi, for early release of prestressing strands.

4. Minimum compressive strength of 15 ksi at 28 days.

5. A maximum material cost of $250 per cubic yard.

6. Local aggregates available at the State of Nebraska should be used in the mix constituents.

The HSC mixes were designed in a specific way to meet the afore-mentioned requirements. First, Type III Portland cement was used to achieve high early strength. Second, Two supplementary cementitious materials were used in the mix development. Mixes with more than one supplementary cementitious material are called ternary mixes. These mixes are characterized by higher strength and durability. Third, the random steel fibers were eliminated to reduce the mix material cost. Despite of the disadvantage of eliminating fibers, it was an economical requirement to reduce the material cost. Finally, the water-to-powder ratio was kept below 0.2 to achieve the required strength. This low

ratio is compensated by adding high range water reducers (HRWR) to maintain sufficient flowing ability.

The methodology followed in HSC mixes development included the following steps:

1. Developing user-friendly mixing procedures to produce HSC mixes.

2. Optimize the mix proportions to achieve the required 24-hour and 28-day compressive strength, without altering the mixing time and/or mix flowing ability.

3. Material properties of the developed mixes were tested in the lab. Results of material properties testing were compared to their estimated values using current AASHTO LRFD specifications

4.6.2 Developing of User-Friendly Mixing Procedures

The conventional concrete mixer (drum mixer) was replaced by a vertical shaft high energy paddle mixer. The paddle mixer, shown in Figure 4.7, has a 5.5 horsepower motor, a drum capacity of 27 ft^3, and a batch output of 17 ft^3**.** During the experimental investigation, a batch size of 3 ft^3 was tried. Mixing procedures were adjusted, so that the produced mix meets the SCC requirements in a total mixing time less than 20 minutes.

Figure 4.7: High energy paddle mixer – University of Nebraska Lab

Based on Kleymann et al. (2006) research findings, the following mixing procedures were specified:

1. Dry blend all the mix granular material. This includes the cement, silica fume, class c fly ash, and fine sand.

2. Place preblended granular material in a separate container.

3. Add all water and ½ HRWR amount to the mixer.

4. The preblended granular material is gradually added to the mixer.

5. The remaining amount of HRWR is gradually added to the mix over a period of 1 minute.

6. Continue mixing until sufficient mix workability is achieved.

Four trial mixes were produced to try and modify the afore-mentioned mixing procedures. Limited success was achieved due to the inability to adjust the pace of adding the preblended granular material to the water and HRWR available in the mixer (step 4).

Alternative two-step mixing procedures were successfully achieved based on technical advice from Lafarge, Canada and Chryso, Inc., USA, and experimental iterations in the University of Nebraska. These procedures were as follows:

1. Granular constituents are pre-blended. Pre-blending procedures ranges from 2 to 3 minutes.

2. The total amount of water and HRWR is added to the blended constituents. Mixing continues till sufficient flowing ability is achieved. This procedure ranges from 10 to 15 minutes.

4.6.3 Optimizing Mix Proportions

Seven trial mixes were produced using the afore-mentioned mixing procedures to select mix constituents that achieve the required strength and flowing ability. The 7 mixes were produced in batches of 3 cubic feet. The mix flowing ability was tested in accordance with ASTM C1611, and mix compressive strength was tested in accordance with ASTM C39. Mixes achieving targeted flowing ability and strength requirements were selected for further material testing. Mixes 5 through 11 are shown in Table 4.2.

Table 4.2: Material constituents of mixes 5 through 11

Material (lbs/yd^3)	Mix 5	Mix 6	Mix 7	Mix 8	Mix 9	Mix 10	Mix 11
#10 sand			2193	1457	1449	1449	1449
47 B sand							
¼ in. limestone				620	616	616	616
Cement III	950.5*	1227	1040	1040	1040	960	1120
C fly ash	340.2	363	320	320	240	320	240
Silica fume	279.9	369	240	240	320	320	240
HRWR	39.6	117	72.5	68	80	78	75
Water	270	294.3	243	240	225	248	240
Mix weight, lbs	3950.2	4128.3	4109	3985	3970	3991	4059
W/C ratio	0.199	0.192	0.191	0.186	0.181	0.195	0.189
Cost $	200	333	232.4	227.9	265.4	259.5	240.0

The following conclusions were drawn from the testing results of the produced mixes:

1. Mixes 5 and 6 average spread diameter was less than 22 in. after 35 minutes of mixing. The low mix workability did not allow for compressive strength testing. For the sake of research, cylinders were poured and placed in the moisture room. Upon cylinders stripping after 24 hours, a significant rough surface and voids were visualized on the cylinder ends and outside surface, and no strength results were reported for the 2 mixes.

2. Mixes 7 through 11 satisfied the slump flow test. The achieved average spread diameters ranged from 23 in. to 25 in. Cylinders were tested at age of 1, 3, 7, 14, and 28 days. Cylinders were end ground before being tested. The load increment in the test ranged from 500 to 600 lbs/sec. The compressive strength test results are shown in Figure 4.8
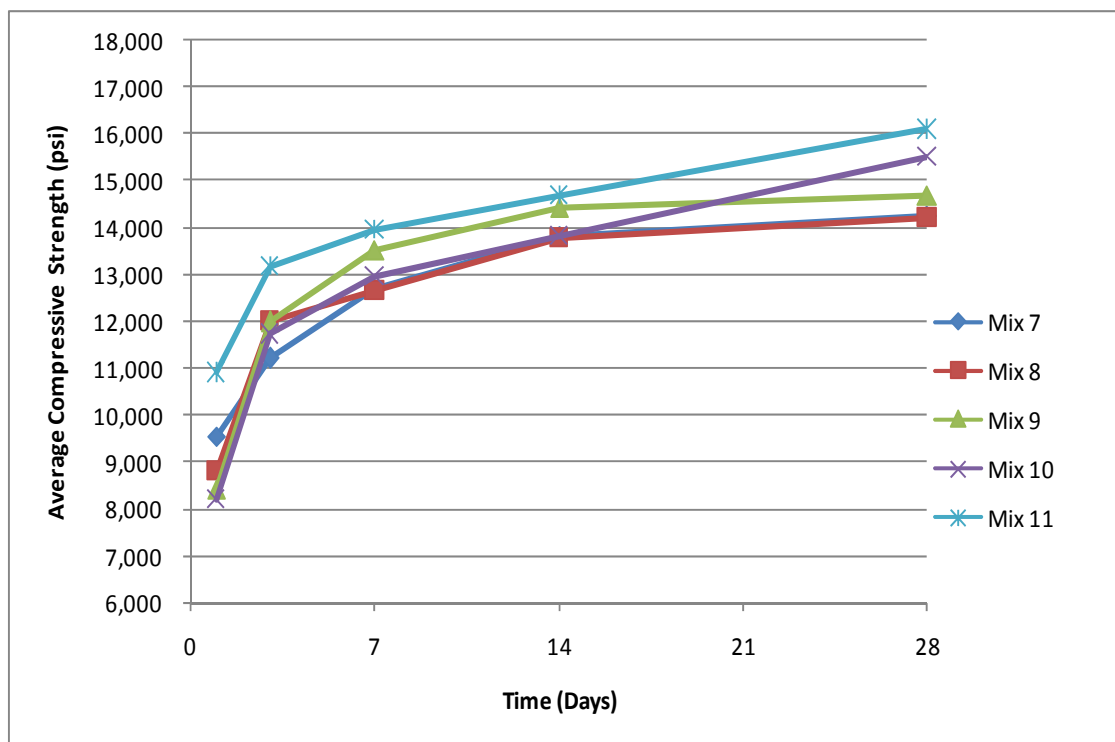
Figure 4.8: Compressive strength test results of mixes 5 through 11

Based on the results, mixes 10 and 11 achieved the required flowing ability and final compressive strength greater than 15 ksi. However, due to economical reasons, mix 10 was eliminated, and mix 11 was considered for further material testing.

4.6.4   Minimizing Material Cost

A different research philosophy was followed during trial mixes 12 through 19. The main objective of these trial mixes was to reduce the material cost, without altering the mix flowing ability and compressive strength. This was done as follows:

1. Mix 12 proportions were based on non-proprietary HSC mix reported by Georgia Institute of technology. The lower cementitious and supplementary cementitious materials used in this mix resulted in a lower material cost. Mix 12 was produced using Type I/II Portland cement, to replicate the original mix produced at Georgia Institute of technology.

2. Mix 13 was produced using similar material constituents as Mix 12. However, type III Portland cement was used to replace type I/II cement, to produce HSC mix with early high strength. Mix 13 showed that similar flowing ability could be achieved using different types of cement.

3. Mixes 14 through 19 were produced using the same cementitious and supplementary cementitious materials, while reducing the amount of HRWR to minimize the final material cost of the mix. The reduction of HRWR amount was accompanied by using additional amount of water and/or introducing higher

portions of larger aggregates, to help achieving required flowing ability with a lower water-to-powder ratio. Mixes 14 through 19 are shown in Table 4.3.

Table 4.3: Material constituents of mixes 13 through 19

Material (lbs/yd³)	Mix 13	Mix 14	Mix 15	Mix 16	Mix 17	Mix 18	Mix 19
#10 sand	2434	2434	2434	852	2434	726	863
C33				852		726	863
½" BRS				730	616	622	742
Cement III	1050	1050	1050	1050	1050	1050	1050
C fly ash	150	150	150	150	150	150	150
Silica fume	150	150	150	150	150	150	150
HRWR	55	41	27	23	27	27	38
Water	261	230	284	284	284	278	235
Mix weight, lbs	3950.2	4128.3	4109	3985	3970	3991	4059
W/C ratio	0.23	0.2	0.23	0.23	0.23	0.19	0.21
Cost $	160	145	130	127	130	165	144

Specimens for compressive strength tests at ages of 1 and 3 days were prepared from mixes 13 through 19. Specimens prepared for compressive strength testing were moisture cured at 72°F and 95% humidity. Due to time limitations, a compressive strength range of 10 to 12 ksi at age of 3 days was set to consider the mix for further material property testing. The predefined strength range of 10 to 12 ksi was determined based on the strength gain of concrete mixes versus time and the correlation between accelerated and

moisture cured specimens results. Theoretically, the achievement of a strength range of 10 to 12 ksi under moisture curing conditions at age of 3 days will result in a minimum strength of 10 ksi at age of 1 day and 15 ksi at age of 28 days using accelerated curing. The strength results of mixes 14 through 19 at ages of 1 and 3 days are shown at Figure 4.9
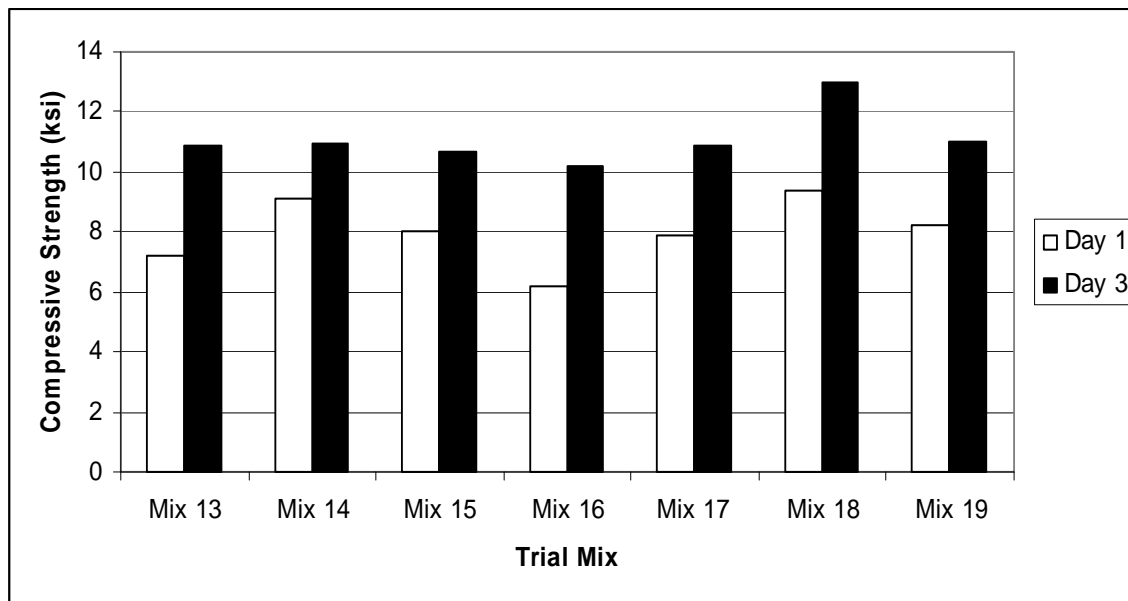
Figure 4.9: Compressive strength of mixes 13 through 19 (day 1 and day 3 results)

Based on the flowing ability, compressive strength, and material cost of the 19 trial mixes, five mix designs were selected for further material properties testing. Selected mixes-denoted as HSC mixes 1 through 5- were produced in batches of 5 cubic feet. The mix constituents of selected HSC mixes is shown in Table 4.4. Concrete specimens were prepared for further material testing in accordance with ASTM C192. In addition to the flowing ability and compressive strength, the following material tests were conducted on the produced HSC mixes:

1. Static modulus of elasticity, according to ASTM C469.

2. Split cylinder cracking strength, according to ASTM C496.

3. Modulus of Rupture, according to ASTM C78

Table 4.4: Selected HSC mixes

Type	HSC #1	HSC #2	HSC #3	HSC #4	HSC #5
Cement, lbs	1050	1040	1050	1120	1050
C fly ash, lbs	300	130	300	240	300
Silica fume, lbs	150	130	150	240	150
#10 Sand, lbs	2255	2428	1580	2255	1580
Limestone, lbs	0	0	672	0	672
Water, lbs	225	260	240	240	234
HRWR, lbs	61.9	35.4	61.9	70.8	72
Cost, \$/yd^3	**204**	**141**	**180**	**218**	**191**

4.7 Material Properties of Developed HSC Mixes

4.7.1 Compressive Strength (f_c') (ASTM C39)

Tested cylindrical specimens were heat cured using a temperature of 130°F, according to the PCI concrete quality control manual provisions to accelerate the strength gain at early ages. Due to the high compressive strength expected, cylinders were end ground and load

was directly applied to the cylinder ends, without using steel caps or neoprene pads. Cylinders end grinding process is shown in Figure 4.10.
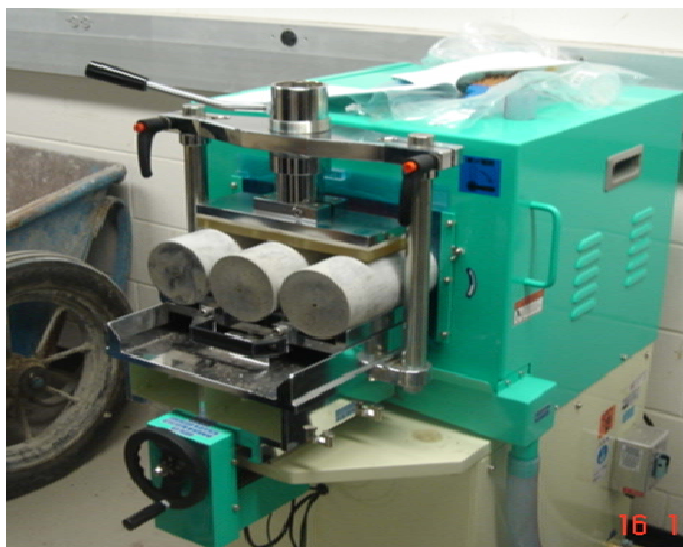
Figure 4.10: End grinding of cylinders

A 400,000 lbs capacity Forney compression testing machine was used to test concrete cylinders in compression at the designated ages. The results of compression testing of HSC mixes at different ages is shown in Figure 4.11
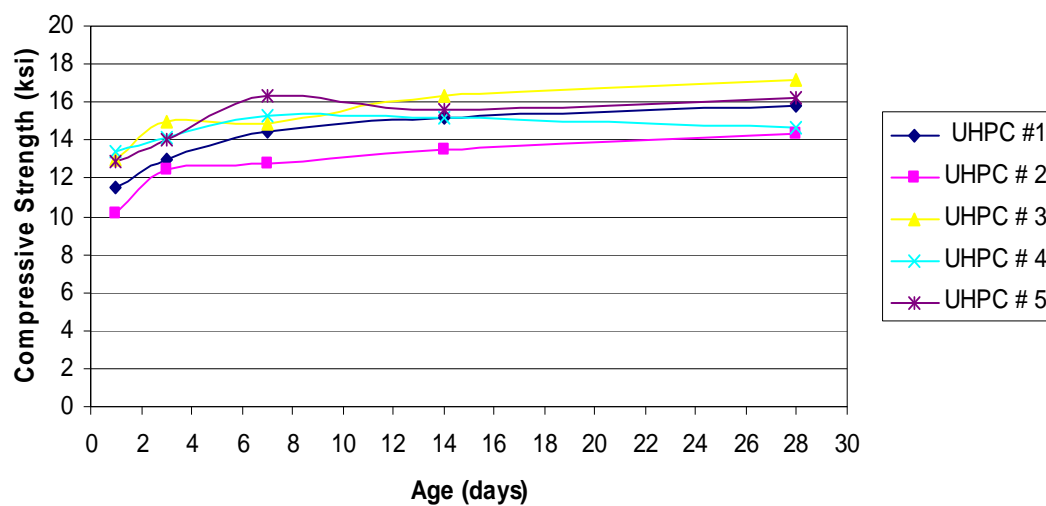
Figure 4.11: Compressive strength of HSC mixes

The minimum 24-hour strength achieved was 11 ksi. The accelerated (heat) curing of concrete specimens, in addition to the use of Type III cement, resulted in a significant increase in concrete strength at early age. Average compressive strength for moisture-cured specimens was 20% less than heat-cured specimens at age of 24 hours. The results of the two curing techniques leveled off, when specimens was tested at age of 28 days. The relation between moisture and heat-cured specimens are shown in Figure 4.12.
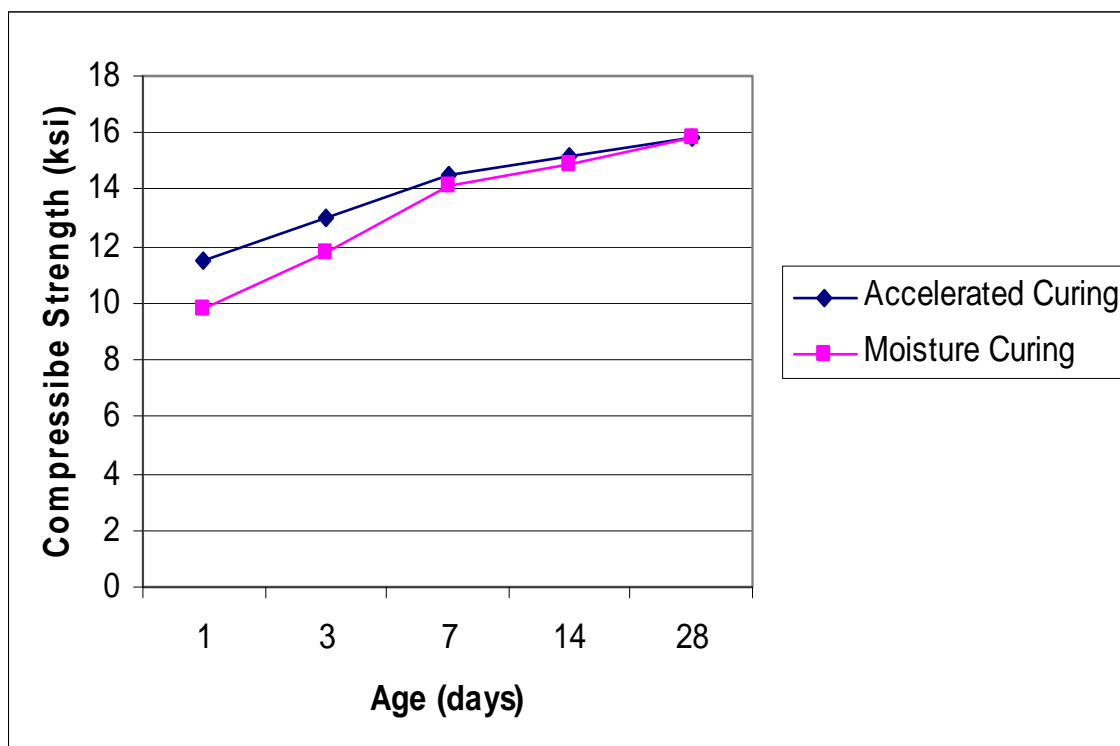
Figure 4.12: Moist-cured vs. heat-cured compressive strength results

4.7.2   Modulus of Elasticity (MOE) (ASTM C469)

The static modulus of elasticity of concrete is defined as the ratio between the normal stress acting on the concrete section and the corresponding strain. The MOE is essential to calculate the deflection of bridge girders under service loads and the estimation of prestressing losses. While it is easy to test specimens for their compressive strength

through lab testing, the MOE measurement is laborious and time consuming. The AASHTO LRFD specifications for highway bridges presents an empirical formula that calculates the modulus of elasticity of concrete based on the square root of concrete compressive strength. AASHTO LRFD equation is written as:

$$E_c = 33,000 \, k_1 w_c^{1.5} \sqrt{f_c'} \qquad (4.1)$$

The MOE testing of the HSC was performed using 6 in. x 12 in. cylinders, as shown in Figure 4.13

Figure 4.13: Capped 6x12 in. cylinder fitted with electronic combined compress-o-meter and extensometer

Specimens were tested for MOE measurement at age of 28-day. The MOE was measured as the average MOE of three specimens. The test results shown in Figure 4.14 showed that the AASHTO LRFD current equation over-predicts the MOE values. This non-conservative result should be considered for further research, as lower MOE values

results in higher prestressing losses and higher deflection. Similar research findings were introduced by Mokhtarzadeh and French (2001).
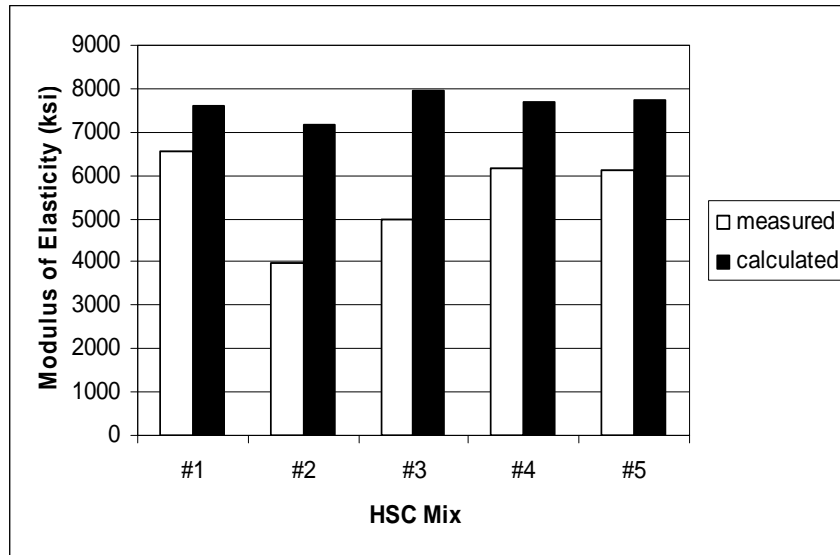
Figure 4.14: Modulus of elasticity of HSC mixes

4.7.3   Split Cylinder Cracking Strength (ASTM C496)

The split cylinder cracking strength was measured at age of 28 days using 6 in. x 12 in. cylinders. The test results represent an estimate for the tensile capacity of the HSC. Test setup is shown in Figure 4.15.

Figure 4.15: Split cylinder cracking strength test set-up
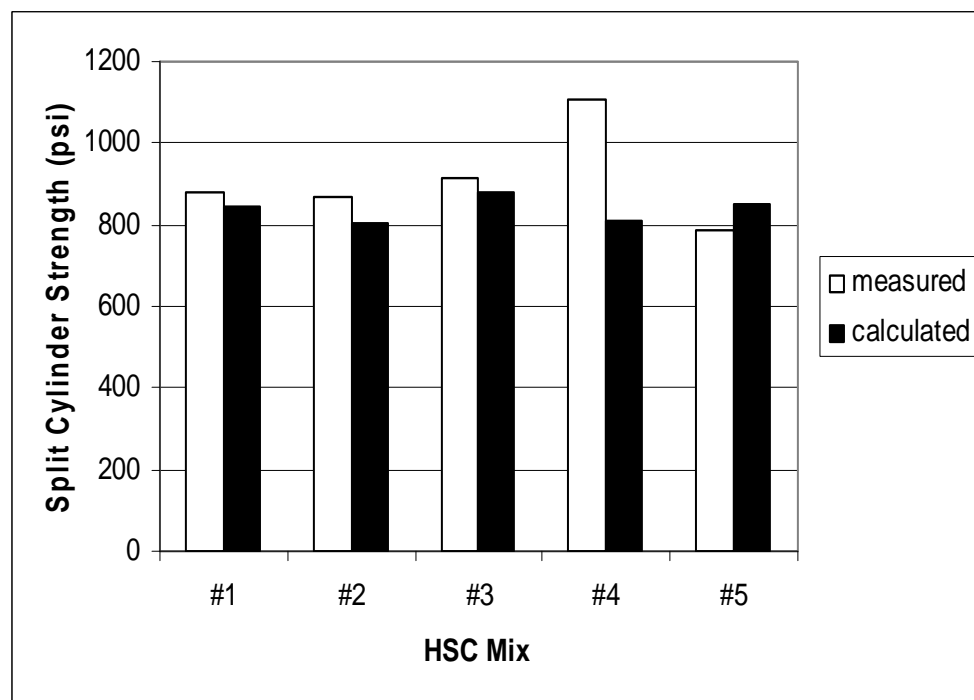
Figure 4.17: Modulus of rupture test setup

MOR, also known as flexural tensile strength, measured by this study was higher than the estimated value presented by AASHTO LRFD equation ($f_r = 0.24\sqrt{f_c^{'}}$), as shown in Figure 4.18. The underestimation of MOR values is conservative because the actual shear capacity will be greater than predicted. Similar findings were presented by Khan et al. (1996), Mokhtarzadeh and French (2001), Hueste et al. (2004)
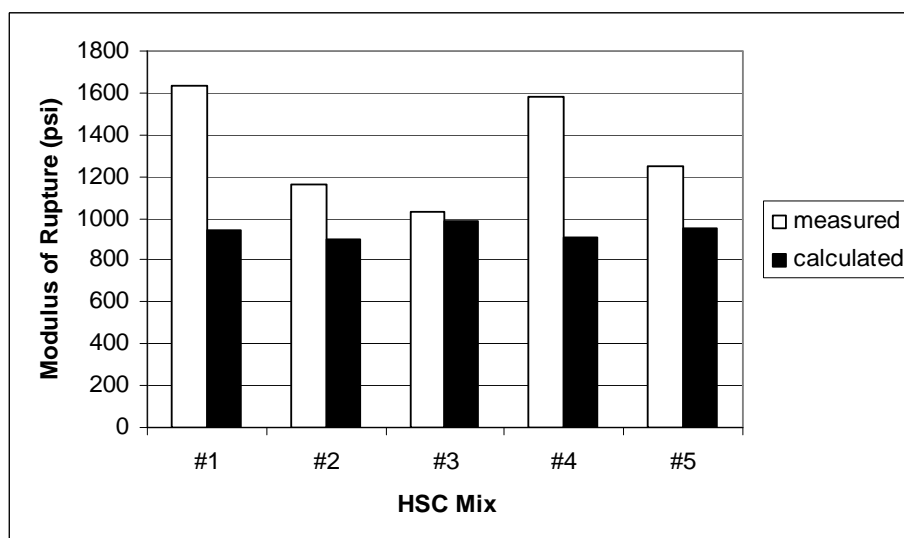
Figure 4.18: Modulus of rupture test results

Chapter 5

The Use of Welded Wire Fabric as Shear Reinforcement of

Precast/Prestressed I-Girders

5.1 Introduction

WWR is increasingly used in the precast/prestressed concrete industry because of its ease in construction, time and money savings due to reduced labor, as shown in Figure 5.1. The fabrication of welded wire fabric into different structural shapes is easily accomplished using two basic equipments, a bending machine and a cutting device. According to ASTM A497, welded deformed wire reinforcement for concrete should have a minimum tensile strength of 80 ksi, minimum yield strength of 70 ksi, and weld shear strength of 35 ksi. The WWR is manufactured from cold-worked steel wires, welded in orthogonal mesh. The cold working process results in higher yield strength. However, it significantly decreases the ductility of the WWR (Mirza et al, 1981).

Figure 5.1: Placing a WWR shear cage in a girder (WRI Manual of Standard Practice, 2006)

WWR is manufactured according to the following variables:

1. Longitudinal wire spacing.

2. Longitudinal wire size.

3. Width.

4. Side and end of overhangs.

5. Transverse wire size.

6. Transverse wire spacing.

7. Length.

The latest welded wire machinery can be used to produce WWR with diameters up to 0.75 in. diameter, which is currently used in fabricating highway median barriers as shown in Figure 5.2

Figure 5.2: WWR used in fabricating highway median barriers (WRI Manual of Standard Practice, 2006)

5.2 Background and Previous Work

The adequacy of the anchorage of smooth WWR was studied by Leonhardt and Walter (1965). Mansour et al. (1986) studied the anchorage of deformed WWR. It was found that one or two cross wires are required to furnish the necessary anchorage of the stirrups at the open end. Taylor and El-Hammasi (1980) tested 15 full size beams with three different WWR arrangements. The test results indicated that the shear cracks were better controlled by a closer distribution of both longitudinal and horizontal wires.

Robertson et al (1987) reported that the WWR could be effectively used in shear reinforcement, due to their capability of controlling the width of diagonal cracks. They reported that the development of the ultimate strength of the wire is highly dependent on the quality of the weld. Xuan et al. (1988) studied the effectiveness of WWR in shear reinforcement of prestressed concrete T-beams. The research results indicated that deformed WWR increased the shear capacity of the beams, through improved distribution of diagonal cracks. Pincheira et al. (1989) studied the effectiveness of WWR in shear reinforcement of prestressed T-beams under static and cyclic loading. The research concluded that WWR increased the beams shear capacity under static loading. However, the performance of WWR under cyclic loading was over-estimated by the ACI building code. Hence, minimum web reinforcement is required for beams subjected to cyclic loading.

The effect of using WWR as shear reinforcement on the flexure capacity of beams was studied by Lin and Perng (1998). In their experimental program, the flexure behavior of

beams with WWR as shear reinforcement was investigated, and compared to beams with conventional stirrups. The results showed that the flexural strength of beams with WWR exhibited higher strength than those with conventional shear reinforcement.

Amorn et al. (2007) conducted a testing program to study the fatigue of deformed WWR. Their research reported on testing WWR, supplied by three different producers to account for variability among WWR producers. WWR were tested in air only, using 5 million load cycles. Based on the results of this program, full monotonic axial stress-strain relationships are presented, and a conservative stress range formula for WWR is presented. This formula is adopted in the 2007 interim AASHTO LRFD Bridge Design Specifications.

In this experimental investigation, the WWR is used as shear reinforcement of precast/prestressed girders fabricated using one of the developed HSC mixes. Two AASHTO Type II girders were fabricated, and tested until failure. The performance of the tested girders, the ultimate shear capacity achieved, and the total material cost is compared to similar girders fabricated with Ductal, and tested at the FHWA labs in McLean, Virginia.

5.3 Test Specimens

Two AASHTO type II prestressed girders were tested in this research program. The 36 in deep girders were 18.5 ft long. The flexure reinforcement of the girder included twenty-four 0.6 in. diameter, 270 ksi low relation prestressing strands, tensioned at 202.5 ksi in

the bottom flange. The compression reinforcement contained 2#6 and 2#9 grade 60 bars. In addition, two partially 0.6 in. prestressing strands were used in the top flange, tensioned at 102 ksi, to control tension cracks upon strand release. The girder end zone was reinforced by four 0.75 in. coil rods, placed at 2 in spacing along the girder axis. Bottom flange prestressing strands were confined by D11 WWR at 6 in spacing to control bursting cracks developed upon strands release. A steel bearing plate was placed at each end of the girder. The steel plate was 16.5 in wide and 8.0 in long, and 2.5 in thick. The Bearing plate was connected to the girder through four ends welded 0.5 in. x 5 in studs. The section reinforcement is shown in Figure 5.3
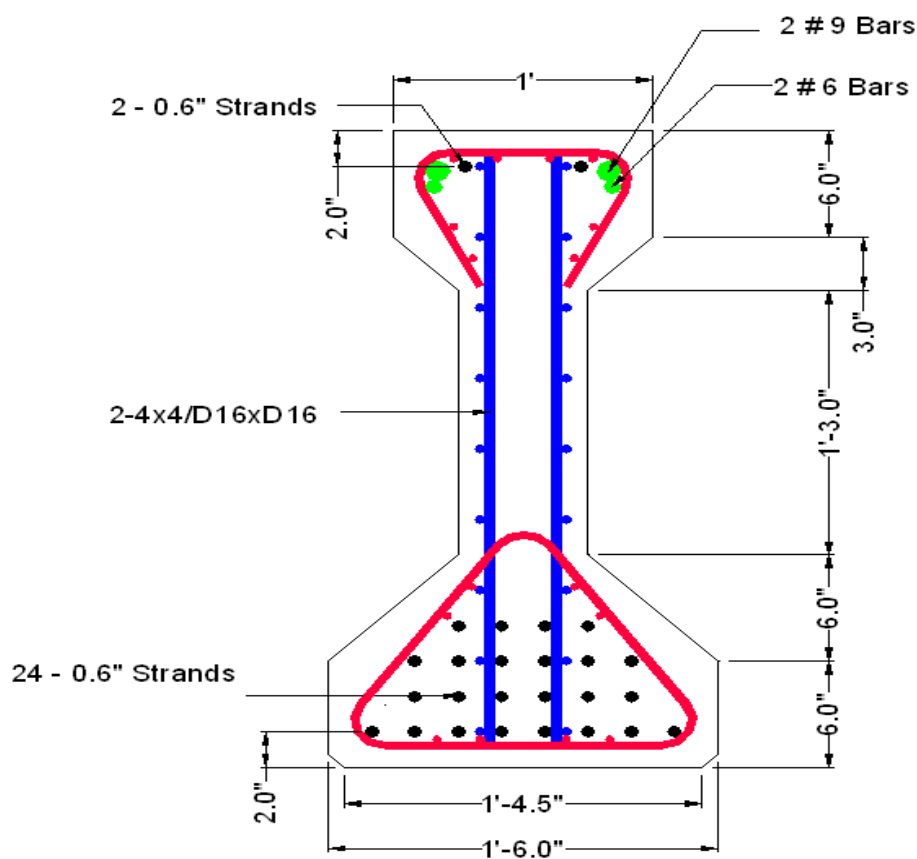
Figure 5.3: AASHTO Type II test specimen flexure reinforcement

5.4 Girders Fabrication

The girders were designed and fabricated in a specific way to satisfy the research purpose. First, developed HSC mix with no random steel fibers was used in girder fabrication. Second, conventional mild steel used for shear reinforcement is replaced with two grade 80 4 x4 – D 16 x D16 WWR meshes, as shown in Figure 5.4.
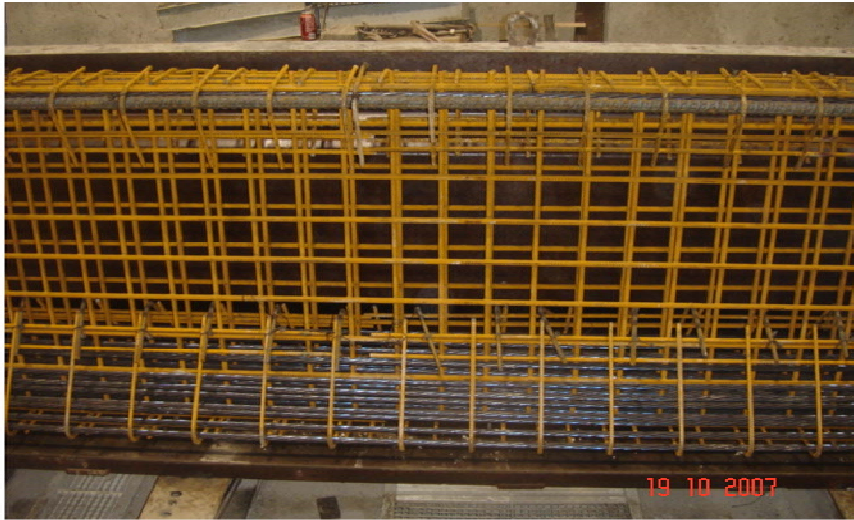
Figure 5.4: WWR used in AASHTO type II girder fabrication

The two AASHTO Type II girders were fabricated using HSC mix # 4. The concrete mix for the first girder-denoted as girder A- was mixed in a high energy paddle mixer according to the HSC mixing procedures specified in Chapter 4. The mix was held in a ready-mix delivery truck, which conveyed the concrete to the prestressing bed. Mix flowing ability was checked prior to pouring the concrete. The average spread diameter was 29 in, as shown in Figure 5.5. The high flowing ability resulted in quick progress of the concrete placement. After filling the form, the top of the girder was covered by insulating tarp to retard the water losses.
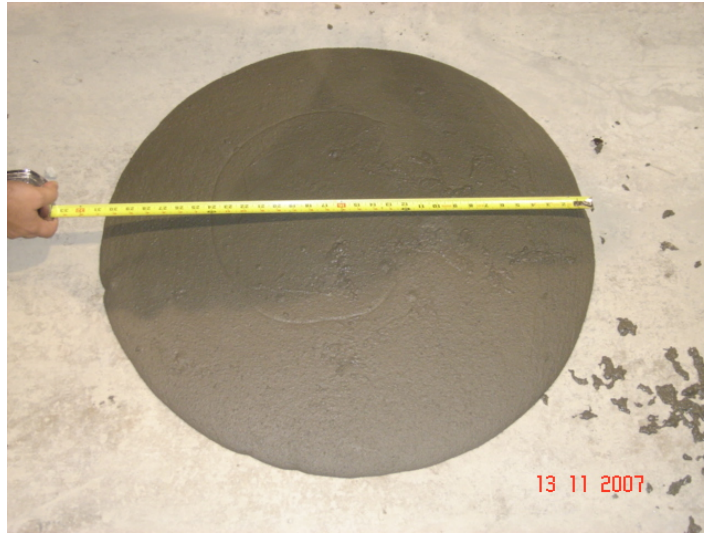
Figure 5.5: Slump flow test for HSC concrete used in pouring I-girders

For research purpose, alternative mixing procedures were followed to produce HSC mix #4 for the second girder-denoted as girder B. This included the following steps:

1. Cementitious and supplementary cementitious materials were mixed, with all the water and HRWR content of the mix. The duration of this procedure was 5 minutes.

2. Fine sand was added, and mixing continued for additional 10 minutes.

The HSC mix produced didn't attain the required flowing ability. Additional quantity of HRWR was added to the HSC mix. The average spread diameter of the mix was 26 in. Due to leakage problems, girder B top flange was not poured, after all the HSC mix was placed in the forms. The incomplete girder was covered by insulated tarp.

Accelerated heat curing was applied to accelerate the strength gain of concrete. The concrete temperature was kept as $130^{o}F$ ($55^{0}C$). Specimens for compressive strength testing were poured and cured alongside of the two girders. Compressive strength testing

was used to determine the time of strands release, and actual compressive strength at girder testing. The average 24-hour compressive strength of tested cylinders was above 13 ksi for both girders specimens, concrete test results are shown in Figure 5.6. The design strength of concrete at release was 8 ksi. Forms were stripped and strands were released after 24 hour of girders fabrication. For research purpose, it was decided to use a different HSC mix to pour girder B top flange, as shown in Figure 5.7. The main purpose was to investigate the performance of different HSC mixes. HSC mix # 3 was selected, as an economical mix, to pour girder B top flange. Diaphragms were poured at the girder ends to ensure the development of prestressing strands at the point of loading. The diaphragm total depth was 36 in. The diaphragms extended to a distance of 1 ft along the beam directions. Conventional concrete mix of 5 ksi was used in pouring the diaphragms.
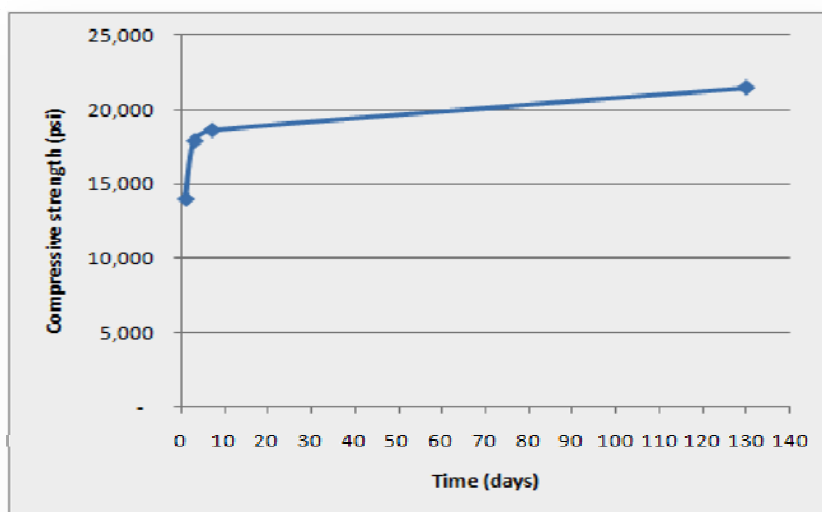
Figure 5.6: Compressive strength of HSC used in pouring AASHTO type-II girders

Figure 5.7: Pouring girder B top flange – University of Nebraska Lab

5.5 Test Setup

Girders A and B were designed to fail in shear. The two 18.5 ft long AASHTO Type II girders were tested in shear through a similar test set-up. Loads were vertically applied to the top flanges through two hollow hydraulically actuated jacks. A manually controlled, variable speed pump was used to operate the actuated jacks. The jacks were acting simultaneously on two load cells, which applied the load on a small steel beam. The load point-bearing assembly was a steel plate grouted to the top flange. The girder was supported on roller bearings at 3 inch from the ends. The girder test set-up is shown in Figure 5.8

Figure 5.8: Shear test setup – girder A

The girder was instrumented with linear variable differential transformer (LVDT) at the bottom extreme fibers at a distance of 6.25 ft from the girder end. The LVDT location was aligned vertically with the point of load application. The LVDT was used to measure the vertical deflection. Resulting load deflection curve was used to determine the point where the non-linear in-elastic behavior of the tested girder started.

5.6 Shear Test Results

5.6.1 Girder A Test Results

The first shear test was completed on Girder A. The girder shear span was 6 ft, resulting in a shear span-to-depth ratio of 2.0. Figure 5.9 shows the load-deflection response of the

girder section at point loading, from initial load application till peak load of 746 kips was reached. The peak load deflection was 0.97 in.
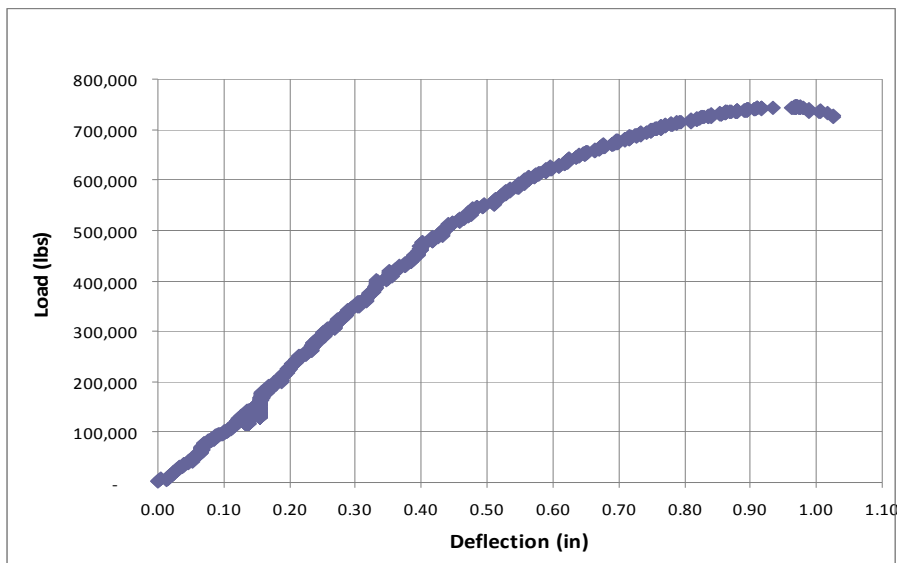
Figure 5.9: Load-deflection curve for girder A

The load-deflection response of the girder shows that the elastic (linear) behavior of the girder was altered at a load of 480 kips. Despite of the girder softening behavior, additional load-carrying capacity was displayed. The reserve shear capacity was due, in part, to the WWR used as shear reinforcement. The WWR improvement to the cracking pattern resulted in a better post-cracking performance of the web concrete. The girder shear capacity, at a peak load of 746 kips, was 497 kips.

5.6.2 Girder B Test Results

Girder B was tested for shear, using similar test set-up and shear span. Figure 5.10 shows the load-deflection response of the girder section at point loading, from initial load application till peak load of 649 kips was reached. The peak load deflection was 0.93 in
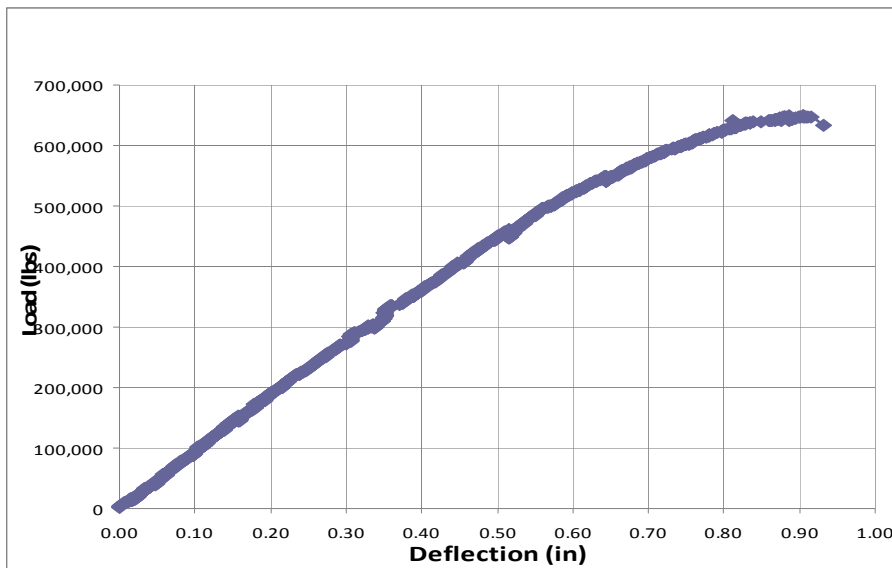
Figure 5.10: Load-deflection curve for girder B

The load-deflection response of the girder shows that the elastic (linear) behavior of the girder was altered at a load of 280 kips. Despite of the softening behavior of the girder, significant reserve load capacity was displayed. The girder failed in shear at an ultimate load of 649 kips. The girder shear capacity at the peak load was 433 kips.

5.7 Failure Mechanism

Despite of the different ultimate capacity of the girders, the two tested girders failed in shear, through similar failure mechanism. The first diagonal shear cracks were initiated within the girders shear span. Additional diagonal cracks were formed with flatter angle as the load increased. Cracks widened as the ultimate capacity of the girder was approached. At a total load of 600 kips (shear load of 400 kips) significant compression cracking and spalling of concrete were apparent at the top flange, below the loading point.

In addition, extensive concrete spalling existed at the girder web. At a total load of 700 kips, WWR mesh started to separate from the concrete, and the diaphragms had a wide vertical crack. The upper part of the diaphragm was totally separated from the girder top flange. Audible wide cracks started to appear at the bottom flange when the girder reached its ultimate capacity (Refer to Figure 5.11, and 5.12).

Figure 5.11: Shear cracks at failure of AASHTO Type II girders

Figure 5.12: Diaphragm failure at ultimate capacity

Girder B lower shear capacity was expected. This is attributed to the following reasons:

1. The concrete compressive strength of girder B was lower than A. Thus, the girder concrete contribution to shear capacity was less.

2. The lower concrete strength resulted in a lower strand-concrete bond. This initiated the strand slippage at lower levels of loading. Shear cracks was significant and resulted in girder failure at lower ultimate load value.

5.8 Analytical Investigation

5.8.1 Theoretical Capacity of Tested Specimens

The shear capacity of precast/prestressed concrete girders results from the contribution of concrete, transverse web reinforcement, and prestressing strands. According to the AASHTO LRFD (5.8.3.3-1)

$$V_n = V_c + V_s + V_p \qquad (5.1)$$

The critical section for shear design for these 2 girders was directly below the acting load, at a distance = 6 ft. from the support centerline. At this section, a shear force equal to two thirds of the acting point load, in addition to maximum bending moments were applied. Due to the absence of any harped strands in the tested girder, the value of prestressing steel contribution to the girder shear capacity (V_p) was zero. The concrete and WWR contributions were calculated as follows:

5.8.1.1 Concrete Contribution to Shear Capacity, V_c

According to AASHTO LRFD (5.8.3.3-3), the concrete contribution to the shear capacity is calculated as:

$$V_c = 0.0316\beta\sqrt{f_c'}\,b_v d_v \qquad (5.2)$$

In order to calculate β, the quantities $\dfrac{V}{f_c'}, \varepsilon_x$ were determined as follows:

$$\frac{V}{f_c'} = \frac{V_u - \phi V_p}{\phi b_v d_v f_c'} \qquad (5.3)$$

$$\varepsilon_x = \frac{\dfrac{M_u}{d_v} + 0.5N_u + (V_u - V_p) - A_{ps} f_{po}}{2(E_s A_s + E_p A_{ps})} \le 0.001 \qquad (5.4)$$

The analytical investigation was used to model for experimental behavior of the AASHTO Type II girders loaded till failure. Thus, strength reduction factor was set equal to 1. For concrete compressive strength of 15 ksi (103 MPa), values of $\dfrac{V}{f_c'}, \varepsilon_x$ were calculated as follows:

$$\frac{V}{f_c'} = \frac{500 - 0}{1.0 * 6 * 28.35 * 15} = 0.195$$

$$\varepsilon_x = \frac{\dfrac{3000 \times 12}{28.35} + 0.5x0 + (500 - 0) - 5.208x0.7x270}{2 * (29{,}000 * 0 + 28{,}500 * 24 * 0.217)} = 0.00264 > 0.001$$

Thus $\varepsilon_x = 0.001$

From AASHTO LRFD Table 5.8.3.4.2-1, values of β, and θ are 1.79 and 36.1° respectively. The concrete contribution to shear capacity is calculated from equation 5.2 as follows:

$$V_c = 0.0316 * 1.79 * \sqrt{15} * 6 * 28.35 = 37.3 kips$$

5.8.1.2 WWR Contribution to Shear Capacity, V_s

According to AASHTO LRFD (C5.8.3.3-4), the WWR contribution to shear capacity is calculated as:

$$V_s = \frac{A_v f_y d_v (\cot\theta + \cot\alpha)\sin\alpha}{s} \qquad (5.5)$$

For 2 WWR meshes of 4 x 4 - D16 x D16, Av = 1.92 in^2, the ultimate shear capacity of WWR was calculated as follows:

For vertical WWR:

$$V_s = \frac{A_v f_y d_v (\cot\theta)}{S} = \frac{0.96 * 80 * 28.35 * \cot 35.7}{12} = 252.5 kips$$

For horizontal WWR:

$$V_s = \frac{A_v f_y d_v \cos\alpha}{S} = \frac{0.96 * 80 * 28.35}{12} = 181.44 kips$$

Based on equation (5.1), the ultimate shear capacity of tested specimens was:

$$V_n = 37.30 + 252.5 + 181.44 = 471.2 \text{ kips}$$

5.8.2 Economical Analysis of Using WWR in Shear Reinforcement

The fabrication of AASHTO type II girders, used in this research project, with WWR as shear reinforcement allowed for the elimination of random steel fibers from the material constituents of the HSC mix. The cost of developed HSC mix and WWR content in these two girders is compared with the UHPC proprietary mix used to fabricate a similar girder, as follows:

5.8.2.1 HSC Mix Material Cost

The cost of HSC mix constituents is calculated based on the cost of materials in the State of Nebraska. This includes $95 per ton for type III Portland cement, $600 per ton for silica fume, $15 per ton for class c fly ash, $10 per ton for fine sand, $15 per ton for limestone and $10 per gallon for HRWR.

The 18.5 ft long AASHTO type II girder, with a cross-section area of 369 in^2 required 1.76 yd^3 of HSC for its fabrication. Based on the afore-mentioned material prices and the mix design of HSC #4 used in specimens fabrication, the material cost of the non-proprietary concrete mix used in girder fabrication was $405.

5.8.2.2 WWR Cost

Due to the elimination of random steel fibers, two meshes of grade 80 4 x 4- D16 x D16 WWR was used for girder shear reinforcement. Additional top stirrups (D11 @ 6 in spacing) were used to confine the partially reinforced strands and compression reinforcement, and bottom stirrups of same size and distribution were used to contain the

24 strands at the bottom flange. Total WWR weight was 560 lbs. The weight of WWR per unit volume of the HSC was 318 lbs. Based on WWR cost of $0.5/lbs, total cost of WWR used in girder reinforcement was $280. Based on the afore-mentioned cost analysis, the cost per cubic yard of HSC using WWR for shear reinforcement was $389.

5.9 Comparison of WWR and Random Steel Fibers

5.9.1 Shear Capacity

The primary goal of the two full-scale shear tests was to determine the shear capacity of the precast, prestressed AASHTO type II girders reinforced with WWR for shear. The experimental investigation resulted in ultimate shear capacity of 497 kips for girder A, and 433 kips for girder B. The shear capacity calculated for the girders using AASHTO LRFD design equations was 5% higher than the lab results. On the other hand, there are no design equations included in the US codes that can estimate the shear capacity of fiber-reinforced UHPC. The Association Francaise de genie civil presents empirical formulas that can be used in estimating the shear capacity of concrete sections, with random fiber reinforcement. The design approach is analogous to prestressed concrete applications with regular shear reinforcement. Based on this analogy, the shear capacity of fiber-reinforced UHPC girders is calculated by superposition of concrete and random steel fiber capacities.

5.9.2 Economical Comparison

The cost analysis of the AAHSTO type II girders fabricated using HSC mix #4 and WWR as shear reinforcement, indicated that the total material cost for girder fabrication

was $389 per cubic yard, compared to $1000 per cubic yard for proprietary UHPC mixes. This is equivalent to 61% saving in material cost. In addition to material cost saving, the incorporation of random steel fibers in UHPC mixes requires an additional step, which is more laborious and time consuming.

Chapter 6

Conclusions

Based on the results of the analytical and experimental investigations performed, the following conclusions are made:

1. The shear friction theory can be successfully used to estimate the level of confinement required for prestressing strands to comply with the current AASHTO LRFD specifications of transfer and development length. A simplified equation was developed to calculate the required area of confining reinforcement as a function of the amount of prestressing, concrete strength, and strand distribution. The accuracy of the developed equation was validated using theoretical and experimental data.

2. Pullout testing of prestressed specimens results in more accurate and consistent values for development length compared to those of non-prestressed specimens. This is attributed to the wedging effect of prestressing strands when released. Pullout testing of non-prestressed strands is not recommended as it results in premature strand slippage. For proper pullout testing of prestressed specimens, special grip inserts need to be used to minimize stress concentrations at gripping locations and eliminate premature failure of strands.

3. The transfer length of 0.7 in. strands is conservatively estimated by current AASHTO LRFD specifications. Experimental data indicated that the transfer length of 0.7 in strands is approximately 35 in. as compared to 42 in. calculated by AASHTO LRFD specifications. Test results also indicated that the level of confinement has a slight effect on the measured transfer length. The more the confinement, the shorter the transfer length.

4. The development of economical high strength concrete mixes that satisfy the needs of the precast prestressed industry is attainable. These requirements include:

   - Final specified compressive strength of 15 ksi

   - Specified compressive strength at release of 10 ksi

   - Self consolidating with an average spread of 26 in.

   - Maximum mixing time of 20 minutes.

   - Material cost is less than $200 per cubic yard.

   - No special pouring or curing conditions are required.

5. The modulus of elasticity of the developed HSC mixes is over-estimated by AASHTO LRFD specifications, while the tensile strength of the same mixes is under-estimated by the same specifications.

6. Grade 80 WWR is an economical alternative to random steel fibers for shear reinforcement of UHPC girders. Experimental results have shown that precast prestressed bridge I-girders reinforced with WWR have higher capacity than those reinforced by random steel fibers and tested by FHWA. In addition, the use of WWR results in much lower material cost and more predictable design strength.

List of Symbols

L_t **:** Transfer length.

L_d : Development length.

f_{si} : Initial prestressing value.

f_{se} : Effective prestressing value.

f_{pu} : Ultimate prestressing value.

f_{ps} : Maximum prestressing (at member ultimate capacity).

d_b : Prestressing strand diameter.

A_{ps} : Area of prestressing strands.

$f_c^{'}$: 28-day concrete compressive strength.

$f_{ci}^{'}$: 24-hour concrete compressive strength.

U_t, B : Empirical bond coefficients.

λ **:** Constant term (function in strand strain).

ε_{ps} **:** Strain in prestressing strands at ultimate load, (microstrain).

A_{ps} **:** Total area of prestressing strands.

F_{ts} **:** Force due to transverse steel acting on strands in vertical direction.

μ **:** Co-efficient of shear friction.

A_{ts} **:** Area of transverse steel.

f_{tsy} **:** Yield strength of confining steel.

$P_{bearing}$ **:** Bearing pressure.

n_{ps} : Number of prestressing strands in one row.

d_{ps} : Prestressing strands diameter**.**

References

1. AASHTO, LRFD Bridge Design Specifications for Highway Bridges, Third Edition, American Association of State Highway and Transportation Officials, Washington, DC, 2006

2. Abdalla, O.A., Ramirez, J.A., and Lee, R.H., "Strand Debonding in Pretensioned Beams – Precast Prestressed Concrete Bridge with Debonded Strands – Simply Supported Tests," Part 2, Final Report FHWA/INDOT/JHRP-92, 1993, 228 pp.

3. ACI Committee 318, "Building Code Requirements for Structural Concrete (ACI 318-02) and Commentary (318R-02)," American Concrete Institute, Farmington Hills, Mich., 2002, 443 pp.

4. Acker, P., "Why Does Ultra High performance Concrete Exhibits Such Low Shrinkage and Such Low Creep?" ACI Special Publications, 220, 141-154, 2004

5. Amorn, W., Bowers, J., Girgis, A., and Tadros, M.K., "Fatigue of Deformed Welded-Wire Reinforcement," PCI Journal, Jan.-Feb., 2007

6. ASTM A497, "Standard Specification for Steel Welded Wire Reinforcement, Deformed, for Concrete" *Annual Book of ASTM Standards*, American Society for Testing and Materials, 2005

7. ASTM C1611, "Standard Test Method for Slump Flow of Self-Consolidating Concrete," *Annual Book of ASTM Standards*, American Society of Testing and Materials, 2005.

8. ASTM C192, "Standard Practice for Making and Curing Concrete Test Specimens in the Laboratory," *Annual Book of ASTM Standards*, American Society for Testing and Materials, 1995

9. ASTM C39, "Standard Test Method for Compressive Strength of Cylindrical Concrete Specimens," *Annual Book of ASTM Standards*, American Society for Testing and Materilas, 2005.

10. ASTM C469, "Standard Test Method for Static Modulus of Elasticity and Poisson's Ratio of Concrete in Compression," *Annual Book of ASTM Standards*, American Society for Testing and Materials, 2001.

11. ASTM C496, "Standard Test Method for Splitting Tensile Strength of Cylindrical Concrete Specimens," *Annual Book of ASTM Standards*, American Society for Testing and Materials, 2004.

12. ASTM C78, "Standard Test Method for Flexural Strength of Concrete (Using Simple Beam with Third-Point Loading," *Annual Book of ASTM Standards*, American Society for Testing and Materials, 2002.

13. Ban, S., Muguruma, H., and Morita, S., "Study on Bond Characteristics of 7-Wire Strand at Prestress Transfer," Technical Report No. 67, Engineering Research Institute, Kyoto University, Kyoto, Japan, 1960.

14. Barnes, R.W., Burns, N.H., and Kreger, M.E., "Development Length of 0.6-Inch Prestressing Strand in Standard I-Shaped Pretensioned Concrete Beams," Report No. FHWA/TX-02/1388-1, Dec. 1999.

15. Barnes, R.W., and Burns, N.H., "Anchorage Behavior of 15.2 mm (0.6 in.) Prestressing Strand in High Strength Concrete," PCI/FHWA/FIB International Symposium on High Performance Concrete, Orlando, Florida, Sep. 25-27, 2000, pp. 484 – 493.

16. Buckner, C.D., "An Analysis of Transfer and Development Lengths for Pretensioned Concrete Structures", Report No. FHWA-RD-94-049, Federal Highway Administration, Washington D.C., December 1995.

17. Castrodale, R.W., Kreger, M.E., and Burns, N.H., "A Study of Pretensioned High-Strength Concrete Girders in Composite Highway Bridges – Laboratory Tests," Research Report 381-3, Center for Transportation Research, University of Texas at Austin, Texas, 1988.

18. CEB-FIP model code, Comite Euro-Internationale du Beton (CEB) Bulletin d'information 213/214. London: Thomas Telford, 1990

19. Cooke, D.E., Shing, P.B., and Frangopol, D.M., "Colorado Study on Transfer and Development of Prestressing Strands in High Performance Concrete Box Girders," University of Colorado Research Series No. CU/SR-97/4, April 1998, pp. 168.

20. Cousins, T.E., Johnston, D.W., and Zia, P., "Transfer and Development Length of Epoxy-Coated and Uncoated Prestressing Strands," PCI Journal, Vol. 35, No. 3, Jul.-Aug. 1990, pp 92-106.

21. Deatherage, J.H., Burdette, E.G., and Chew, C.K., "Development Length and Lateral Spacing Requirements of Prestressing Strand for Prestressed Concrete Bridge Girders," PCI Journal, Vol. 39, No. 1, Jan.-Feb. 1994, pp. 70-83.

22. Einea, A., Yehia, S., and Tadros, M.K., "Lap Splices in Confined Concrete" ACI Structural Journal, Vol. 96, No. 6, Nov.-Dec. 1999, pp. 947-958.

23. FHWA, "Memorandum" Federal Highway Administration, Washington D.C., Oct. 26, 1988.

24. FHWA, "Memorandum" Federal Highway Administration, Washington D.C., May 8, 1996.

25. Girgis, A.M., and Tuan, C.Y., "Bond Strength and Transfer Length of Pretensioned Bridge Girders Cast with Self-Consolidating Concrete" PCI Journal, 72-87, Nov-Dec., 2005.

26. Graybeal, B.A., "Compressive Behavior of Ultra-High Performance Fiber-Reinforced Concrete" ACI Material Journal, 104, 146-152, 2004

27. Graybeal, B.A., and Hartmann, J.L., "Construction of an Optimized UHPC Vehicle Bridge" ACI Special Publication, 228, 1109-1118, 2005

28. Graybeal, B.A., Hartmann J., and Perry, V, "Ultra-High Performance Concrete for Highway Bridges". Proceedings of the Federation International du Beton Symposium, Avignon, France, 2004

29. Gross, S.P., and Burns, N.H., "Transfer and Development Length of 15.2 MM (0.6 in.) Diameter Prestressing Strand in High Performance Concrete: Results of the Hoblitzell-Buckner Beam Tests", Report No. FHWA/TX-97/580-2, June 1995.

30. Guyon, Y., Prestressed Concrete, John Wiley and Sons, New York, N.Y., 1953.

31. Hanson, N.W., and Kaar, P.H., "Flexural Bond Tests of Pretensioned Prestressed Beams," ACI Journal, Vol. 55, No. 7, 1959, pp. 783-803.

32. Hegger, J., Tuchlinski, D., Kommer, B., "Bond Anchorage Behavior and Shear Capacity of Ultra-High Performance Concrete Beams" *Proceedings* of the International Symposium on Ultra High Performance Concrete, Kassel, Germany, September 13-15, 2004, pp. 351-360.

33. Holmberg, A., and Lindgren, S., "Anchorage and Prestress Transmission," Document D1, National Swedish Institute for Building Research, Stockholm, Sweden, 1970.

34. Hueste, M.B., Chompreda, P., Trejo, D., Cline, D.B., Keating. P.B., "Mechanical Properties of High-Strength Concrete for Prestressed Members," ACI Structural Journal, Vol. 101, No. 4, July-Aug. 2004, pp. 457-465

35. Janney, J.R., "Nature of Bond in Pretensioned Prestressed Concrete," ACI Journal, Vol. 50, No. 8, 1954, 717-736.

36. Jukarev, Y.V., "Investigation of Development of Prestressing Strands and Deformed Bars", MS Thesis, University of Nebraska-Lincoln, Omaha, 2004.

37. Kaar, P.H., LaFraugh, R.W., and Mass, M.A., "Influence of Concrete Strength on Strand Transfer Length," PCI Journal, Vol. 8, No. 5, October 1963, pp. 47-67.

38. Keierleber, B., Bierwagen, D., Fanous, F., Phares, B., and Couture, I., " Design of Buchanan County, Iowa, Bridge Using Ultra High Performance Concrete and PI Girder", Proceedings of the 2007 Mid-Continent Transportation Research Symposium, Ames, Iowa, August, 2007

39. Kahn, L.F., Dill, J.C., and Reutlinger C.G., "Transfer and Development Length of 15-mm Strand in High Performance Concrete Girders", Journal of Structural Engineering, Vol. 128, No. 7, Jul. 2002, pp. 913-921.

40. Khan, A.A., Cook W.D., and Mitchell D., "Tensile Strength of Low, Medium, and High-Strength Concretes at Early Ages," ACI Material Journal, Vol. 93, No. 5, Sep.-Oct. 1996, pp. 487-493.

41. Kleymann, M., Girgis, A.M., and Tadros, M.K., "Development of User-Friendly and Cost-Effective Ultra-High Performance Concrete" *Proceedings* of the Concrete Bridge Conference, Reno, Nevada, 2006.

42. Kose, M.M., "Prediction of Transfer Length of Prestressing Strands using Neural Networks," ACI Structural Journal, Vol. 104, No. 2, Mar.-Apr. 2007, pp. 162-169.

43. Kose, M.M., and Burkett W.R., "Evaluation of Code Requirement for 0.6 in. (15 mm) Prestressing Strand," ACI Structural Journal, Vol. 102, No.3, May-Jun. 2005, pp. 422-428.

44. Lane, S.N., "A New Development Length Equation for Pre-tensioned Strands in Bridge Beams and Piles", Report No. FHWA-RD-98-116, Federal Highway Administration, McLean, VA, December 1998, 123 pp.

45. Lappa, E.S., "High Strength Fibre Reinforced Concrete, Static and Fatigue Behavior in Bending" Doctoral Dissertation, Delft University of Technology, June. 2007.

46. Leonhardt, F., and Walther, R., "Welded Wire Mesh as Stirrup Reinforcement-Shear Tests on T-Beams and Anchorage Tests," DieBautechnik (Berlin), V. 42, Oct. 1965.

47. Lin, C., Perng, S., "Flexural Behavior of Concrete Beams with Welded Wire Fabric as Shear Reinforcement," *ACI Structural Journal*, Vol. 95, N0. 5, Sep.-Oct., 1998

48. Logan, D.R., "Acceptance Criteria for Bond Quality of Strand for Pretensioned Prestressed Concrete Applications," PCI Journal, Vol. 42, No. 2, 1997, pp. 52-90.

49. Ma, J., and Schneider, H., "Properties of Ultra-High-Performance Concrete," Lacer No.7, Leipzig University, Germany, 2002

50. Malvar, L.J., "Bond of Reinforcement under Controlled Confinement," ACI Material Journal, Vol. 89, No. 6, Nov.-Dec., 1992.

51. Mansour, M.A., Lee C.K., and Lee, S.L., "Deformed Wire Fabric as Shear Reinforcement in Concrete Beams" ACI Structural Journal, Vol. 84, No. 3, Sep.-Oct. 1987, pp. 392-399

52. Mirza, S. A., and MacGregor, J.G., "Strength and Ductility of Concrete Slabs Reinforced with Welded Wire Fabric," ACI Journal, Vol. 78, No. 5, Sep.–Oct. 1981, pp. 374-381

53. Mitchell, D., Cook, W.D., Khan, A.A., and Tham, T., "Influence of High Strength Concrete on Transfer and Development Length of Pretensioning Strand," PCI Journal, Vol. 38, No. 3, May-Jun. 1993, pp. 52-66.

54. Mokhtarzadeh, A., and French, C., "Mechanical Properties of High-Strength Concrete with Consideration for Precast Applications," ACI Materials Journal, Vol. 97, No. 2, March-April 2000, pp. 136-148

55. Moustafa, S., "Pullout Strength of Strand Lifting Loops," Technical Bulletin 74-B5, Tacoma, Washington, Concrete Technology Associates, 1974

56. NCHRP Report No. 579, "Application of LRFD Bridge Design Specifications to High-Strength Structural Concrete: Shear Provisions" National Cooperative Highway Research Program, (2007)

57. Nowak, A., Morcous, G., and Tuan, C.Y., "Development of a Guide for Cast-in-Place Applications of Self-Consolidating Concrete," NDOR Project Number, SPR-1(07) 594, Nov., 2007.

58. Oh, B.H., and Kim, E.S., "Realistic Evaluation of Transfer Length in Pretensioned, Prestressed Concrete Members," ACI Structural Journal, Vol. 97, No. 6, Nov.-Dec. 2000, pp. 821-830.

59. Orangum, C.O., Jirsa, J.O., and Breen, J.E., "A Reevaluation of Test Data on Development Length and Splices," Journal of the American Concrete Institute, Proceedings, Vol. 74, No.3, pg. 114-122, Detroit, Michigan, March 1977

60. Orangum, C.O., Jirsa, J.O., and Breen, J.E., "The strength of Anchor Bars: A Reevaluation of Test Data on Development Length and Splices," Center for Highway Research, Report 154-3F, Austin, Texas, January 1975.

61. Ozyildirim, C., and Gomez, J.P., "High Performance Concrete in a Bridge in Richlands, Virginia," Virginia Transportation Research Council, Charlottesville, Virginia, 1999.

62. Park, H., Chuang, E., and Ulm, F.-J. (2003). Model Based Optimization of Ultra-High Performance Concrete Highway Bridge Girders. (MIT-CEE Report R03-01), Massachusetts Institute of Technology. Boston, Massachusetts.

63. Pincheira, J.A., Rizkalla, S.H., Attiogbe, E.K., "Performance of Welded Wire Fabric as Shear Reinforcement under Cyclic Loading," *ACI Structural Journal*, V. 86, No. 6, Nov.-Dec., 1989, pp. 728-735.

64. Ramirez, J.A., and Russell, B.W., "Transfer, Development, and Splice Length for Strand/Reinforcement in High-Strength Concrete", NCHRP Report 12-60, July 2007.

64. Rapoport, J., Aldea, C.M., Shah, S.P., and Karr, A., "Permeability of Cracked Steel Fiber-Reinforced Concrete," ASCE Journal of Materials in Civil Engineering, Vol. 14, No. 4, Jul-Aug. 2002, pp. 355-358.

65. Reutlinger, C.G., "Direct Pullout Capacity and Transfer Length of 0.6-inch Diameter Prestressing Strand in HPC", *MS Thesis*, Georgia Institute of Technology, Atlanta, 1999.

66. Reiser, N.P, "Innovative Reinforced/Prestressed Concrete Bridge Superstructure Systems" A Thesis, University of Nebraska-Lincoln, Nebraska, 2007

67. Robertson, I.N., and Durani, A.J., "Shear Strength of Prestressed Concrete T-Beams with Welded Wire Fabric as Shear Reinforcement," Journal of Prestressed Concrete Institute, V. 32, No. 2, Mar.-Apr.1987, pp. 46-59

68. Rose, D.R., and Russell, B.W., "Investigation of Standardized Tests to Measure the Bond Performance of Prestressing Strand," PCI Journal, Vol. 42, no. 4, 1997, pp. 56-80

69. Russell, B.W., and Burns, N.H., "Static and Fatigue Behavior of Pretensioned Composite Bridge Girders Made with High Strength Concrete," PCI Journal, Vol. 38, No. 3, May-June, 1993, pp. 118-128,

70. Russell, B.W., and Burns, N.A., "Design Guidelines for Transfer, Development, and Bonding of Large Diameter Seven-Wire Strands in Pretensioned Concrete Girders," Research Report No. 1210-5F, Center for Transportation Research, University of Texas at Austin, Austin, TX, 1997, 286 pp.

71. Russell, B.W., and Burns, N.H., "Measured Transfer Lengths of 0.5 in and 0.6 in Strands in Pretensioned Concrete," PCI Journal V.41, N.5, Sep.-Oct. 1996, pp. 44-63.

72. Salmons, R.J., and McCrate, T.E., "Bond of Untensioned Prestress Strand", Study Number 72-2, Missouri State Highway Department, August 1973.

73. Shahawy, M.A., "A Critical Evaluation of the AASHTO Provisions for Strand Development Length of Prestressed Concrete Members", PCI Journal, No. 4, Jul.-Aug., 2001, pp. 94-117.

74. Shahawy, M.A., and Batchelor, B., "Bond and Shear Behavior of Prestressed AASHTO Type II Beams," Progress Report No. 1, Structural Research Center, Florida Department of Transportation, 1991.

75. Shahawy, M.A., and Issa, M., "Effect of Pile Embedment on the Development Length of Prestressing Strands," PCI Journal, Vol. 37, No. 6, Nov.-Dec., 1992, pp. 44-59.

76. Shahawy, M.A., Issa, M., and Batchelor, B., "Strand Transfer Lengths in Full Scale AASHTO Prestressed Concrete Girders," PCI Journal, Vol. 37, No. 3, May-Jun. 1992, pp. 84-96.

77. Steinberg, E., and Lubbers, A., "Bond of Prestressing Strands in UHPC," Proceedings, 2003 International Symposium on High Performance Concrete, Orlando, Florida, Oct. 2003, 15 pp.

78. Stiel, T.B., Karihaloo, B., and Fehling, E., "Effect of Casting Direction on the Mechanical properties of CARDIFRC®," Proceedings of the International Symposium on Ultra-High Performance Concrete, Kassel, Germany, September 13-15, 2004, pp. 481-493

79. Tawfiq, K., "Cracking and Shear Capacity of High Strength Concrete Bridge Girders," FL/DOT/RMC/612(1) – 4269, Jan. 1995, 145 pp.

80. Tawfiq, K., "Cracking and Shear Capacity of High Strength Concrete Bridge Girders under Fatigue Loading," FL/DOT/RMC/612-7896, Nov. 1996, 127 pp.

81. Taylor, M.A., and El-Hammasi, S., "Web Cracking Behavior of Beams using Welded Wire Fabric as Shear Reinforcement" ACI Journal, Vol. 77, No. 2, Jan.-Feb 1980, pp. 12-17

82. Tepfers, R., "Lapped Tensile Reinforcement Splices," ASCE, Vol. 108, No. ST1, Jan. 1982.

83. The Association Francaise de Genie Civil (AFGC) *Interim Recommendations for Ultra-High Performance Fibre-Reinforced Concrete*, 2002

84. The Japan Society of Civil Engineers (JSCE), *Recommendations for Design and Construction of Ultra High Fiber Reinforced Concrete Structures (draft),* JSCE Guideline for Concrete No. 9, 2006.

85. Untrauer, R.E., and Henry, R.L., " Influence of Normal Pressure on Bond Strength," Journal of the American Concrete Institute, Proceedings Vol. 62, No. 5, Detroit, Michigan, May 1965.

86. Welded Reinforcement Institute, Manual of Standard Practice-Structural Welded Wire Reinforcement, WWR-500, Updated 8th Edition, 2006

87. Xuan, X., Rizkalla, S., Maruyama, K., "Effectiveness of Welded Wire Fabric as Shear Reinforcement in Pretensioned Prestressed Concrete T-Beams," *ACI Structural Journal*, Vol. 85, No. 6 , July-Aug., 1998, pp. 429-436

88. Zakariasen, D., and Perry V., "Ultra-High Performance Concrete with Ductility: Design, Prototyping, and Manufacturing of Panels and Boxes, ACI Special Publications, 224, 71-88, 2004

89. Zia, P., and Mostafa T., "Development Length of Prestressing Strands", PCI Journal, Vol. 22, No. 5, Sep.-Oct. 1977, pp. 54-65.

90. Zia, P., Leming, M.L., and Ahmad, S.H., "High Performance Concretes. A State-of-the-Art-Report," Strategic Highway Research Program, SHRP-C/FR-91-103, 1991.

APPENDIX A: Design of I-girder Bridge using NU900 girders fabricated with HSC and 0.7 in. strands vs. 8 ksi concrete and 0.6 in. strands

- Moment values for different spans for NU900 placed at 12 ft. spacing
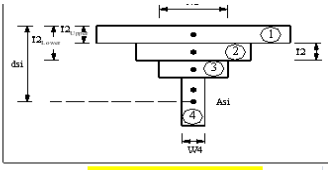
	Service III			Strength I		
	Moment +ive		Moment -	Moment +ive		Moment -
Span	0.4L	0.5L	Support	0.4L	0.5L	Support
70 ft	2725	2715	1774	4774	4730	3541
75 ft	3033	2929	1973	5273	5228	3925
80 ft	3385	3376	2195	5853	5804	4357
85 ft	3752	3743	2421	6456	6407	4794
90 ft	4107	4127	2645	7083	7030	5222
95 ft	4535	4527	2874	7734	7679	5658
100 ft	4950	4945	3120	8406	8297	6127
105 ft	5382	5378	3370	9106	9047	6605
110 ft	5630	5826	3625	9828	9768	7083

- Details of loading at span = 105 ft.

NU900
60 - 0.7 in. strands
Initial concrete strength = 12 ksi
Final concrete strength = 15 ksi
Deck strength = 5 ksi
4 girders at 12 ft. spacing
5.33 overhang at both sides
0.025 ksi wearing surface
7.5 in. structural thickness deck
8.0 in. total thickness deck
48.3 in. width haunch
1 in. thickness haunch

				Service III			Strength I		
				Moment +ive		Moment -	Moment +ive		Moment -
Span	Moment	Type	Section	0.4L	0.5L	Support	0.4L	0.5L	Support
105 ft	Self weigt	simple	non-comp	893	931		1116	1163	
	Haunch+Deck	simple	non-comp	1554	1620		1942	2025	
	Wearing surface	continous	composite	234	210	-398	351	314	-598
	Barriers	continous	composite	128	114	-218	161	144	-273
	L.L + Impact	continous	composite	1614	1585	-1578	3531	3467	-3450
				4423	4460	-2194	7101	7113	-4321

Critical Sections:
1) Positive Moment @ 0.4L
Service III   4423 kip.ft
Strength I   7101 kip.ft
2) Negative Moment @ Support
Strength I   -4321 kip.ft
Using NU900 and 60-0.6 in. strands for span of 105 ft.
Using 6 girders @ 8 ft. +3.33 ft (overhang at each end)
Spacing   8 ft.

				Service III			Strength I		
				Moment +ive		Moment -	Moment +ive		Moment -
Span	Moment	Type	Section	0.4L	0.5L	Support	0.4L	0.5L	Support
105 ft	Self weigt	simple	non-comp	893	931		1116	1163	
	Haunch+Deck	simple	non-comp	1058	1103		1323	1379	
	Wearing surface	continous	composite	156	140	-265	107	96	-399
	Barriers	continous	composite	39	35	-145	234	209	-182
	L.L + Impact	continous	composite	1245	1233	-1197	2726	2699	-2618
				3391	3442	-1607	5506	5546	-3199

0.7 in strands + HPC concrete
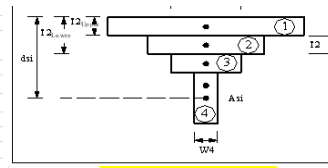
- **Flexure capacity (+ive moment) at mid-span**
-

			a	8.764
Sum of forces				0.00
			Design	P/C AASHTO
			ANSWER:	
			φ	1.00
			φMₙ kip-in	157234
			kip*ft	13102.9

mtadros:
sum of steel and concrete forces

Av. β₁ : 0.793

Units in kips and inches

f'c	Width, W	Thick., T	Depth, d꜀	β₁	T_upper	T_lower	Revised T	Beta1calcuation			Area	Force	Mₙ k-in.		
5.000	96.000	7.500	3.750	0.800	0.000	7.500	7.500	2880	3600		720.000	-3060.00	-11475.00		
5.000	48.250	1.000	8.000	0.800	7.500	8.500	1.000	193	241.25		48.250	-205.06	-1640.50		
15.000	48.250	2.560	8.632	0.650	8.500	11.060	0.264	124.3563023	191.317388		12.754	-162.62	-1403.76		
15.000	27.090	1.750	11.060	0.650	11.060	12.810	0.000	0	0		0.000	0.00	0.00		
15.000	5.940	20.290	12.810	0.650	12.810	33.100	0.000	0	0		0.000	0.00	0.00		
15.000	22.160	5.500	33.100	0.650	33.100	38.600	0.000	0	0		0.000	0.00	0.00		
15.000	38.380	5.300	38.600	0.650	38.600	43.900	0.000	0	0		0.000	0.00	0.00		
								3197.356302	4032.56739						

Area A_si	Grade	Effective Prest.	Depth d_si	E_s	Q	fpy	R	K	ε_so	Δε	Total ε_s	Stress	Force	Moment	Modified stress	corresp. f'c
12.6	60	0	2.000	29000	0	60	100	1.096	0.0000	-0.0025	-0.0025	-60.00	-702.45	-1404.90	-55.75	5.00
9.4	60	0	5.500	29000	0	60	100	1.096	0.0000	-0.0015	-0.0015	-43.71	-370.94	-2040.16	-39.46	5.00
	60	0	6.500	29000	0	60	100	1.096	0.0000	-0.0012	-0.0012	-35.84	0.00	0.00	-31.59	5.00
	60	0	9.125	29000	0	60	100	1.096	0.0000	-0.0005	-0.0005	-15.18	0.00	0.00	-15.18	15.00
	60	0	11.750	29000	0	60	100	1.096	0.0000	0.0002	0.0002	5.48	0.00	0.00	5.48	15.00
	60	0	14.375	29000	0	60	100	1.096	0.0000	0.0009	0.0009	26.14	0.00	0.00	26.14	15.00
	60	0	17.000	29000	0	60	100	1.096	0.0000	0.0016	0.0016	46.80	0.00	0.00	46.80	15.00
	60	0	19.625	29000	0	60	100	1.096	0.0000	0.0023	0.0023	60.00	0.00	0.00	60.00	15.00
	60	0	22.250	29000	0	60	100	1.096	0.0000	0.0030	0.0030	60.00	0.00	0.00	60.00	15.00
	60	0	24.875	29000	0	60	100	1.096	0.0000	0.0038	0.0038	60.00	0.00	0.00	60.00	15.00
	60	0	27.500	29000	0	60	100	1.096	0.0000	0.0045	0.0045	60.00	0.00	0.00	60.00	15.00
	60	0	30.125	29000	0	60	100	1.096	0.0000	0.0052	0.0052	60.00	0.00	0.00	60.00	15.00
	60	0	32.750	29000	0	60	100	1.096	0.0000	0.0059	0.0059	60.00	0.00	0.00	60.00	15.00
	70	0	0.000	29000	0	70	100	1.06	0.0000	-0.0030	-0.0030	-70.00	0.00	0.00	-65.75	5.00
	120	0	5.125	29000	0.0217	81.00	4.224	1.01	0.0000	-0.0016	-0.0016	-45.71	0.00	0.00	-41.46	5.00
	150	0	5.125	29000	0.0217	120.00	4.224	1.01	0.0000	-0.0016	-0.0016	-46.47	0.00	0.00	-42.22	5.00
	270	28	1.500	28500	0.031	243	7.36	1.043	0.0010	-0.0016	-0.0016	-45.90	0.00	0.00	-41.65	5.00
	270	160	33.400	28500	0.031	243	7.36	1.043	0.0056	0.0000	0.0117	251.73	0.00	0.00	251.73	15.00
0	270	160	10.500	28500	0.031	243	7.36	1.043	0.0056	0.0000	0.0055	155.16	0.00	0.00	155.16	15.00
0.588	270	160	29.900	28500	0.031	243	7.36	1.043	0.0056	0.0051	0.0107	247.70	145.65	4354.95	247.70	15.00
0.588	270	160	31.900	28500	0.031	243	7.36	1.043	0.0056	0.0057	0.0113	250.24	147.14	4693.72	250.24	15.00
0.588	270	160	33.900	28500	0.031	243	7.36	1.043	0.0056	0.0062	0.0118	252.17	148.28	5026.60	252.17	15.00
1.764	270	160	35.900	28500	0.031	243	7.36	1.043	0.0056	0.0067	0.0124	253.69	447.50	16065.41	253.69	15.00
3.528	270	160	37.900	28500	0.031	243	7.36	1.043	0.0056	0.0073	0.0129	254.91	899.31	34083.76	254.91	15.00
5.292	270	160	39.900	28500	0.031	243	7.36	1.043	0.0056	0.0078	0.0134	255.92	1354.31	54036.94	255.92	15.00
5.292	270	160	41.900	28500	0.031	243	7.36	1.043	0.0056	0.0084	0.0140	256.78	1358.88	56937.20	256.78	15.00
	270	160	26.333	28500	0.031	243	7.36	1.043	0.0056	0.0000	0.0098	240.97	0.00	0.00	240.97	15.00

- **Flexure capacity (-ive moment) at support**
-

			a	8.265
Sum of forces				-6.00
			Design	P/C AASHTO
			ANSWER:	
			φ	1.00
			φMₙ kip-in	52239
			kip*ft	4353.2

Calculate

Av. β₁ : 0.650

Units in kips and inches

Concrete Layers		f'c	Width, W	Thick., T	Depth, d꜀	β₁	T_upper	T_lower	Revised T	Beta1calcuation			Area	Force
	1	15.000	38.400	5.300	2.650	0.650	0.000	5.300	5.300	1984.32	3052.8		203.520	-2594.8
	2	15.000	22.200	5.500	6.782	0.650	5.300	10.800	2.965	641.7601277	987.32327		65.822	-839.22
	3	15.000	5.940	20.290	10.800	0.650	10.800	31.090	0.000	0	0		0.000	0.00
	4	15.000	27.090	1.750	31.090	0.650	31.090	32.840	0.000	0	0		0.000	0.00
	5	15.000	48.200	2.560	32.840	0.650	32.840	35.400	0.000	0	0		0.000	0.00
	6	5.000	48.200	1.000	35.400	0.800	35.400	36.400	0.000	0	0		0.000	0.00
	7	5.000	96.000	7.500	36.400	0.800	36.400	43.900	0.000	0	0		0.000	0.00
										2626.080128	4040.1233			

Steel Layers		Area A_si	Grade	Effective Prest.	Depth d_si	E_s	Q	fpy	R	K	ε_so	Δε	Total ε_s	Stress	Force
Grade 60 Bars	1	9.4	60	0	38.400	29000	0	60	100	1.096	0.0000	0.0061	0.0061	60.00	564.00
	2	12.6	60	0	41.900	29000	0	60	100	1.096	0.0000	0.0069	0.0069	60.00	756.00
	3		60	0	6.500	29000	0	60	100	1.096	0.0000	0.0000	-0.0015	-42.53	0.00
	4		60	0	9.125	29000	0	60	100	1.096	0.0000	0.0000	-0.0008	-24.57	0.00
	5		60	0	11.750	29000	0	60	100	1.096	0.0000	0.0000	-0.0002	-6.60	0.00
	6		60	0	14.375	29000	0	60	100	1.096	0.0000	0.0000	0.0004	11.36	0.00
	7		60	0	17.000	29000	0	60	100	1.096	0.0000	0.0000	0.0010	29.32	0.00
	8		60	0	19.625	29000	0	60	100	1.096	0.0000	0.0000	0.0016	47.28	0.00
	9		60	0	22.250	29000	0	60	100	1.096	0.0000	0.0000	0.0022	60.00	0.00
	10		60	0	24.875	29000	0	60	100	1.096	0.0000	0.0000	0.0029	60.00	0.00
	11		60	0	27.500	29000	0	60	100	1.096	0.0000	0.0000	0.0035	60.00	0.00
	12		60	0	30.125	29000	0	60	100	1.096	0.0000	0.0000	0.0041	60.00	0.00
	13		60	0	32.750	29000	0	60	100	1.096	0.0000	0.0000	0.0047	60.00	0.00
Grade 70 Plate	1		70	0	0.000	29000	0	70	100	1.06	0.0000	0.0000	-0.0030	-70.00	0.00
Gr. 120 Rods	1		120	0	5.125	29000	0.0217	81.00	4.224	1.01	0.0000	0.0000	-0.0018	-50.31	0.00
Gr. 150 Rods	1		150	0	5.125	29000	0.0217	120.00	4.224	1.01	0.0000	0.0000	-0.0018	-51.60	0.00
Gr 270	1		270	28	1.500	28500	0.031	243	7.36	1.043	0.0010	0.0000	-0.0017	-47.41	0.00
Gr 270	2		270	160	33.400	28500	0.031	243	7.36	1.043	0.0056	0.0000	0.0105	246.37	0.00
Gr 270	3	5.292	270	160	2.000	28500	0.031	243	7.36	1.043	0.0056	-0.0025	0.0031	87.94	532.87
Gr 270	4	5.292	270	160	4.000	28500	0.031	243	7.36	1.043	0.0056	-0.0021	0.0036	101.38	603.98
	5	3.528	270	160	6.000	28500	0.031	243	7.36	1.043	0.0056	-0.0016	0.0040	114.80	450.00
	6	1.764	270	160	8.000	28500	0.031	243	7.36	1.043	0.0056	-0.0011	0.0045	128.18	248.60
	7	0.588	270	160	10.000	28500	0.031	243	7.36	1.043	0.0056	-0.0006	0.0050	141.48	83.19
	8	0.588	270	160	12.000	28500	0.031	243	7.36	1.043	0.0056	-0.0002	0.0054	154.65	90.93
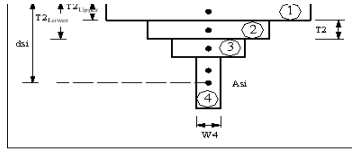
- **Service loads check (0.7 in. strands)**

Beam		
A	648.10	in^2
I	110262	in^4
y_b	16.1	in
h	35.4	in
V/S	3.00	in
A_{ps}	17.64	in^2
f_{pi}	202.5	ksi
E_s	28500	ksi
y_{pb}	5.00	in
span	105	

Deck		
Width	96	in
Thickness	7.5	in
Haunch width	48.2	in
Haunch thickness	1	in
V/Sd	0.50	

Materials		
H	70	%
f_{ci}	12.000	ksi
f'_c	15.000	ksi
f'_{cd}	5.000	ksi
t_i (release)	1	days
t (deck pour)	60	days
t_f (final)	20000	days

Service load moments		
Girder	11172	kip-in
Deck, haunch, diaphragms	20808	kip-in
SI dead ld.	2532	kip-in
LL	19020	kip-in

Prestress Loss Using 2005 LRFD Detailed Method

Formulas in this method use gross section properties to approximate net section properties. Otherwise the results are identical to those of NCHRP 18-07

Project Name	Residential Floor Beam	Date:	30-Jan-07
Designer:	Maher Tadros		

Loading	Prestress Loss Components (ksi)		f_{ps}	
			Change	Net
	(1) Initial prestress just before release			202.5
	(2) Elastic shortening due to initial prestress plus self weight		-31.145	
Prestress transfer, t_{egp} =	7.258 ksi			171.4
	(3) Shrinkage between release and deck place (Eq 5.9.5.4.2a-1) See list of equations below		-3.557	167.8
	(4) Creep between release and deck place (Eq 5.9.5.4.2b-1)		-15.085	152.7
	(5) Relaxation between release and deck place (assumption)		-1.200	151.5
Total long-term (initial to deck placemnt)$_{id}$			-19.842	151.5
	(6) Elastic due to deck weight Mdecketr-fin/Ibm-tr-fin°n		7.095	158.6
	(7) Elastic due to superimposed DL (on composite section) MADLecomp-fin/Icomp-fin°n		0.686	159.3
Deck + SIDL: Df_{cd} and Df_{pED}			7.781	159.3
	(8) Shrinkage of beam bet.deck place and final (Eq 5.9.5.4.3a-1) f		-0.788	158.5
	(9) Creep of beam bet.deck place and final, initial loads (Eq 5.9.5.4.3b-1)		-3.340	155.2
	(10) Creep of beam due to deck and SIDL (Eq 5.9.5.4.3b-1)		4.173	159.3
	(11) Relaxation between deck place and final (assumption)		-1.200	158.1
	(12) Shrinkage of deck (Eq 5.9.5.4.3d-1,2)		0.626	158.8
Total long-term (deck placemnt to final)$_{df}$			-0.529	158.8
	(13) Elastic due to LL n*MLLecomp_tr/Icomp_tr		5.153	
Total loss and effective prestress including gain due to LL,			-38.582	163.9

Only the two highlighted loss values are needed in concrete stress analysis, when transformed section properties are used

Extreme Fiber Stresses (using transformed/net section properties)						
Bottom Fibers			Top Fibers			
Cause	Initial	Final	Cause	Initial	Dead load	Full load
Pi (transf. section, release)	9.789	9.789	Pi (transf. section, release)	-1.237	-1.237	-1.237
Mg (transf., release)	-1.452	-1.452	Mg (transf., release)	1.933	1.933	1.933
Loss (net section, precast)		-1.107	Loss (net section, precast)		0.140	0.140
deck weight (transf., service)		-2.745	deck weight (transf., service)		3.605	3.605
SIDL (transf. composite)		-0.224	SIDL (transf. composite)		0.099	0.099
Loss (net, composite)		-0.028	Loss (net, composite)		-0.001	-0.001
LL (transf., composite)		-1.686	LL (transf., composite)			0.744
Net	8.337	2.546		0.695	4.538	5.283
ACI Code Limit	7.200	-0.918		-0.328	6.750	9.000
PCI Handbook Limit	8.400			-0.800		

0.6 in strands + HPC concrete

- **Flexure capacity (+ive moment) at mid-span**

	Sum of forces	0.00		Calculate
	Design	P/C AASHTO		
	ANSWER:			
	φ	1.00		
	φMₙ kip-in	121872	Av. β₁ :	0.800
	kip*ft	10156.0		
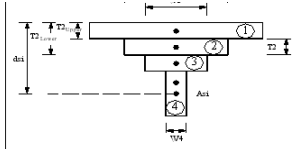
Units in kips and inches

f'c	Width, W	Thick., T	Depth, dₒ	β₁	T_upper	T_lower	Revised T	Beta1calcuation				Area	Force	Mₙ k-in.
5.000	96.000	7.500	3.208	0.800	0.000	7.500	6.416	2463.700792	3079.62599			615.925	-2617.68	-8397.38
5.000	48.250	1.000	7.500	0.800	7.500	8.500	0.000	0	0			0.000	0.00	0.00
15.000	48.250	2.560	8.500	0.650	8.500	11.060	0.000	0	0			0.000	0.00	0.00
15.000	27.090	1.750	11.060	0.650	11.060	12.810	0.000	0	0			0.000	0.00	0.00
15.000	5.940	20.290	12.810	0.650	12.810	33.100	0.000	0	0			0.000	0.00	0.00
15.000	22.160	5.500	33.100	0.650	33.100	38.600	0.000	0	0			0.000	0.00	0.00
15.000	38.380	5.300	38.600	0.650	38.600	43.900	0.000	0	0			0.000	0.00	0.00
								2463.700792	3079.62599					

Area Aₛᵢ	Grade	Effective Prest.	Depth dₛᵢ	Eₛ	Q	fpy	R	K	εₛₒ	Δε	Total εₛ	Stress	Force	Moment	Modified stress
12.6	60	0	2.000	29000	0	60	100	1.096	0.0000	-0.0023	-0.0023	-60.00	-702.45	-1404.90	-55.75
1.8	60	0	4.000	29000	0	60	100	1.096	0.0000	-0.0015	-0.0015	-43.61	-70.84	-283.38	-39.36
	60	0	6.500	29000	0	60	100	1.096	0.0000	0.0000	-0.0006	-16.49	0.00	0.00	-16.49
	60	0	9.125	29000	0	60	100	1.096	0.0000	0.0000	0.0004	11.99	0.00	0.00	11.99
	60	0	11.750	29000	0	60	100	1.096	0.0000	0.0000	0.0014	40.46	0.00	0.00	40.46
	60	0	14.375	29000	0	60	100	1.096	0.0000	0.0000	0.0024	60.00	0.00	0.00	60.00
	60	0	17.000	29000	0	60	100	1.096	0.0000	0.0000	0.0034	60.00	0.00	0.00	60.00
	60	0	19.625	29000	0	60	100	1.096	0.0000	0.0000	0.0043	60.00	0.00	0.00	60.00
	60	0	22.250	29000	0	60	100	1.096	0.0000	0.0000	0.0053	60.00	0.00	0.00	60.00
	60	0	24.875	29000	0	60	100	1.096	0.0000	0.0000	0.0063	60.00	0.00	0.00	60.00
	60	0	27.500	29000	0	60	100	1.096	0.0000	0.0000	0.0073	60.00	0.00	0.00	60.00
	60	0	30.125	29000	0	60	100	1.096	0.0000	0.0000	0.0083	60.00	0.00	0.00	60.00
	60	0	32.750	29000	0	60	100	1.096	0.0000	0.0000	0.0093	60.00	0.00	0.00	60.00
	70	0	0.000	29000	0	70	100	1.06	0.0000	0.0000	-0.0030	-70.00	0.00	0.00	-65.75
	120	0	5.125	29000	0.0217	81.00	4.224	1.01	0.0000	0.0000	-0.0011	-31.28	0.00	0.00	-27.03
	150	0	5.125	29000	0.0217	120.00	4.224	1.01	0.0000	0.0000	-0.0011	-31.38	0.00	0.00	-27.13
	270	28	1.500	28500	0.031	243	7.36	1.043	0.0010	0.0000	-0.0015	-41.51	0.00	0.00	-37.26
	270	160	33.400	28500	0.031	243	7.36	1.043	0.0056	0.0000	0.0151	258.27	0.00	0.00	258.27
0	270	160	10.500	28500	0.031	243	7.36	1.043	0.0056	0.0000	0.0065	184.02	0.00	0.00	184.02
0.434	270	160	29.900	28500	0.031	243	7.36	1.043	0.0056	0.0082	0.0138	256.50	111.32	3328.45	256.50
0.434	270	160	31.900	28500	0.031	243	7.36	1.043	0.0056	0.0089	0.0145	257.57	111.78	3565.89	257.57
0.434	270	160	33.900	28500	0.031	243	7.36	1.043	0.0056	0.0097	0.0153	258.50	112.19	3803.13	258.50
1.302	270	160	35.900	28500	0.031	243	7.36	1.043	0.0056	0.0104	0.0160	259.34	337.65	12121.81	259.34
2.604	270	160	37.900	28500	0.031	243	7.36	1.043	0.0056	0.0112	0.0168	260.12	677.35	25671.52	260.12
3.906	270	160	39.900	28500	0.031	243	7.36	1.043	0.0056	0.0119	0.0175	260.86	1018.93	40655.50	260.86
3.906	270	160	41.900	28500	0.031	243	7.36	1.043	0.0056	0.0127	0.0183	261.58	1021.75	42811.23	261.58
	270	160	26.333	28500	0.031	243	7.36	1.043	0.0056	0.0000	0.0125	253.95	0.00	0.00	253.95
	270	160	28.667	28500	0.031	243	7.36	1.043	0.0056	0.0000	0.0133	255.73	0.00	0.00	255.73

- **Flexure capacity (-ive moment) at support**

	a	6.333		Calculate
	Sum of forces	0.00		
	Design	P/C AASHTO		
	ANSWER:			
	φ	1.00		
	φMₙ kip-in	38604	Av. β₁ :	0.650
	kip*ft	3217.0		

Units in kips and inches

Concrete Layers		f'c	Width, W	Thick., T	Depth, dₒ	β₁	T_upper	T_lower	Revised T	Beta1calcuation			Area	Force	Mₛ k-in.
	1	15.000	38.400	5.300	2.650	0.650	0.000	5.300	5.300	1984.32	3052.8		203.520	-2594.88	-6876.43
	2	15.000	22.200	5.500	5.316	0.650	5.300	10.800	0.033	7.09872235	10.9211113		0.728	-9.28	-49.35
	3	15.000	5.940	20.290	10.800	0.650	10.800	31.090	0.000	0	0		0.000	0.00	0.00
	4	15.000	27.090	1.750	31.090	0.650	31.090	32.840	0.000	0	0		0.000	0.00	0.00
	5	15.000	48.200	2.560	32.840	0.650	32.840	35.400	0.000	0	0		0.000	0.00	0.00
	6	5.000	48.200	1.000	35.400	0.800	35.400	36.400	0.000	0	0		0.000	0.00	0.00
	7	5.000	96.000	7.500	36.400	0.800	36.400	43.900	0.000	0	0		0.000	0.00	0.00
										1991.418722	3063.72111				

Steel Layers		Area Aₛᵢ	Grade	Effective Prest.	Depth dₛᵢ	Eₛ	Q	fpy	R	K	εₛₒ	Δε	Total εₛ	Stress	Force	Moment	Modified stress
Grade 60 Bars	1	1.8	60	0	38.400	29000	0	60	100	1.096	0.0000	0.0110	0.0110	60.00	108.00	4147.20	60.00
	2	12.6	60	0	41.900	29000	0	60	100	1.096	0.0000	0.0123	0.0123	60.00	756.00	31676.40	60.00
	3		60	0	6.500	29000	0	60	100	1.096	0.0000	0.0000	-0.0006	-18.07	0.00	0.00	-18.07
	4		60	0	9.125	29000	0	60	100	1.096	0.0000	0.0000	0.0003	9.76	0.00	0.00	9.76
	5		60	0	11.750	29000	0	60	100	1.096	0.0000	0.0000	0.0013	37.60	0.00	0.00	37.60
	6		60	0	14.375	29000	0	60	100	1.096	0.0000	0.0000	0.0023	60.00	0.00	0.00	60.00
	7		60	0	17.000	29000	0	60	100	1.096	0.0000	0.0000	0.0032	60.00	0.00	0.00	60.00
	8		60	0	19.625	29000	0	60	100	1.096	0.0000	0.0000	0.0042	60.00	0.00	0.00	60.00
	9		60	0	22.250	29000	0	60	100	1.096	0.0000	0.0000	0.0051	60.00	0.00	0.00	60.00
	10		60	0	24.875	29000	0	60	100	1.096	0.0000	0.0000	0.0061	60.00	0.00	0.00	60.00
	11		60	0	27.500	29000	0	60	100	1.096	0.0000	0.0000	0.0071	60.00	0.00	0.00	60.00
	12		60	0	30.125	29000	0	60	100	1.096	0.0000	0.0000	0.0080	60.00	0.00	0.00	60.00
	13		60	0	32.750	29000	0	60	100	1.096	0.0000	0.0000	0.0090	60.00	0.00	0.00	60.00
Grade 70 Plate	1		70	0	0.000	29000	0	70	100	1.06	0.0000	0.0000	-0.0030	-70.00	0.00	0.00	-57.25
Gr. 120 Rods	1		120	0	5.125	29000	0.0217	81.00	4.224	1.01	0.0000	0.0000	-0.0011	-32.50	0.00	0.00	-19.75
Gr. 150 Rods	1		150	0	5.125	29000	0.0217	120.00	4.224	1.01	0.0000	0.0000	-0.0011	-32.62	0.00	0.00	-19.87
Gr 270	1		270	28	1.500	28500	0.031	243	7.36	1.043	0.0010	0.0000	-0.0015	-41.87	0.00	0.00	-29.12
Gr 270	2		270	160	33.400	28500	0.031	243	7.36	1.043	0.0056	0.0000	0.0148	257.93	0.00	0.00	257.93
Gr 270	3	3.906	270	160	2.000	28500	0.031	243	7.36	1.043	0.0056	-0.0023	0.0033	95.33	422.17	844.35	108.08
Gr 270	4	3.906	270	160	4.000	28500	0.031	243	7.36	1.043	0.0056	-0.0015	0.0041	116.14	503.43	2013.72	128.89
	5	2.604	270	160	6.000	28500	0.031	243	7.36	1.043	0.0056	-0.0008	0.0048	136.83	356.32	2137.90	136.83
	6	1.302	270	160	8.000	28500	0.031	243	7.36	1.043	0.0056	-0.0001	0.0055	157.24	204.73	1637.85	157.24
	7	0.434	270	160	10.000	28500	0.031	243	7.36	1.043	0.0056	0.0007	0.0063	176.99	76.81	768.13	176.99
	8	0.434	270	160	12.000	28500	0.031	243	7.36	1.043	0.0056	0.0014	0.0070	195.43	84.82	1017.79	195.43
	9	0.434	270	160	14.000	28500	0.031	243	7.36	1.043	0.0056	0.0021	0.0077	211.71	91.88	1286.35	211.71
	10		270	160	33.400	28500	0.031	243	7.36	1.043	0.0056	0.0000	0.0148	257.93	0.00	0.00	257.93
	11		270	160	26.333	28500	0.031	243	7.36	1.043	0.0056	0.0000	0.0122	253.40	0.00	0.00	253.40
	12		270	160	28.667	28500	0.031	243	7.36	1.043	0.0056	0.0000	0.0131	255.29	0.00	0.00	255.29
	13		270	160	31.000	28500	0.031	243	7.36	1.043	0.0056	0.0000	0.0139	256.73	0.00	0.00	256.73
	Sum of M										MAXIMUM	Δε :	0.0123		Moment (	0.00	38603.91 kip*in

- **Service loads check (0.7 in. strands)**

Beam		
A	648.10	in^2
I	110262	in^4
y_b	16.1	in
h	35.4	in
V/S	3.00	in
A_{ps}	13.02	in^2
f_{pi}	202.5	ksi
E_s	28500	ksi
y_{pb}	5.00	in
span	105	

Deck		
Width	96	in
Thickness	7.5	in
Haunch width	48.2	in
Haunch thickness	1	in
V/Sd	0.50	

Materials		
H	70	%
f_{ci}	12.000	ksi
f'_c	15.000	ksi
f'_{cd}	5.000	ksi
t_i (release)	1	days
t (deck pour)	60	days
t_f (final)	20000	days

Service load moments		
Girder	10716	kip-in
Deck, haunch, diaphragms	13680	kip-in
SI dead ld.	1680	kip-in
LL	14796	kip-in

Loading	Prestress Loss Components (ksi)		f_{ps}	
			Change	Net
	(1) Initial prestress just before release			202.5
	(2) Elastic shortening due to initial prestress plus self weight		-22.865	
Prestress transfer, f_{cgp} =	5.328 ksi			179.6
	(3) Shrinkage between release and deck place (Eq 5.9.5.4.2a-1) See list of equations below		-3.792	175.8
	(4) Creep between release and deck place (Eq 5.9.5.4.2b-1)		-11.807	164.0
	(5) Relaxation between release and deck place (assumption)		-1.200	162.8
Total long-term (initial to deck placemnt)$_{ld}$			-16.800	162.8
	(6) Elastic due to deck weight Mdecketr-fin/Ibm-tr-fin*n		4.813	167.6
	(7) Elastic due to superimposed DL (on composite section) MADLecomp-fin/Icomp-fin*n		0.469	168.1
Deck + SIDL: Df_{cd} and Df_{pED}			5.282	168.1
	(8) Shrinkage of beam bet.deck place and final (Eq 5.9.5.4.3a-1) f		-0.838	167.3
	(9) Creep of beam bet.deck place and final, initial loads (Eq 5.9.5.4.3b-1)		-2.610	164.7
	(10) Creep of beam due to deck and SIDL (Eq 5.9.5.4.3b-1)		2.939	167.6
	(11) Relaxation between deck place and final (assumption)		-1.200	166.4
	(12) Shrinkage of deck (Eq 5.9.5.4.3d-1,2)		0.666	167.1
Total long-term (deck placemnt to final)$_{df}$			-1.042	167.1
	(13) Elastic due to LL n*MLLecomp_tr/Icomp_tr		4.132	
Total loss and effective prestress including gain due to LL,			-31.293	171.2

Only the two highlighted loss values are needed in concrete stress analysis, when transformed section properties are used

Extreme Fiber Stresses (using transformed/net section properties)							
Bottom Fibers				Top Fibers			
Cause	Initial	Final		Cause	Initial	Dead load	Full load
Pi (transf. section, release)	7.488	7.488		Pi (transf. section, release)	-0.947	-0.947	-0.947
Mg (transf., release)	-1.433	-1.433		Mg (transf., release)	1.859	1.859	1.859
Loss (net section, precast)		-0.692		Loss (net section, precast)		0.087	0.087
deck weight (transf., service)		-1.851		deck weight (transf., service)		2.376	2.376
SIDL (transf. composite)		-0.153		SIDL (transf. composite)		0.066	0.066
Loss (net, composite)		-0.040		Loss (net, composite)		-0.002	-0.002
LL (transf., composite)		-1.348		LL (transf., composite)			0.577
Net	6.054	1.970			0.913	3.440	4.017
ACI Code Limit	7.200	-0.918			-0.328	6.750	9.000
PCI Handbook Limit	8.400				-0.800		

APPENDIX B: HSC Mixes

1- Mixes done by Kleymann et al. (2006)

Material	Mix #1	Mix #2	Mix #3	Mix #4	Mix #5	Mix #6
Fine Sand	1,758	1716	1730	1758	1663	1730
Cement I/II	1,227	1217	1207	1227	1208	1207
C fly Ash	363	360	372	363	343	372
Silica Fume	399	395	382	399	377	382
HRWR	81	107	86	194	106	86
Water	204	202	221	204	242	221
W/CM ratio	0.125	0.132	0.137	0.156	0.156	0.137
Cost/yd^3	$380	$441	$385	$652	$433	$385
Strength, ksi	18.2	17.6	15	15.8	16.4	13

2- NCHRP Report (Prof. Dan. Kuchma, at the University of Illinois at Urbana, Champaign).

Property	G1 & G2	G3 & G4	G5 & G6	G7 & G8	G9	G10
Type I Cement	-	-	1,050	-	-	1050
Type III Cement	750	1,030	-	1,030	700	-
Fly Ash	-	-	-	-	-	-
Silica Fume	-	125	150	125	-	150
Water	210	300	264	300	280	264
Sand	1,328	777	858	777	1,180	858
Coarse agg. (max. ¾ in.)	1,880	-	-	-	1,786	-
Coarse agg. (max. ½ in.)	-	1,820	-	1,820	-	-
Coarse agg. (max. 3/8 in.)	-	-	1,820	-	-	1,820
Retarder (100XR)	-	-	4 oz/100 lbs	20 oz/yard	-	4 oz/100 lbs
Super Plast. (MB 300FC)	-	As needed	15-18 0z/100 lbs	As needed	175 oz/yard	15-18 oz/100 lbs
Water-CM	0.28	0.24	0.25	0.24	0.40	0.25
Strength, ksi	12.6	16.3	17.8	13.3	9.6	10.6